united nations educational, scientific and cultural organization
international atomic energy agency
the abdus salam international centre for theoretical physics
40th anniversary 1964 2004

H4.SMR/1586-2

"7th Workshop on Three-Dimensional Modelling of Seismic Waves Generation and their Propagation"

25 October - 5 November 2004

Modelling of Seismic Input

G.F. Panza[1, 2]

[1] **Department of Earth Sciences University of Trieste**

[2] **ICTP SAND Group, Trieste**

strada costiera, 11 - 34014 trieste italy - tel. +39 040 2240111 fax +39 040 224163 - sci_info@ictp.trieste.it - www.ictp.trieste.it

Seventh workshop on ***Three-Dimensional Modeling of Seismic waves Generation, Propagation and their inversion*** - *ICTP 2004*

MODELLING OF SEISMIC INPUT

by

Giuliano F. Panza

the abdus salam international centre for theoretical physics

united nations educational, scientific and cultural organization

international atomic energy agency

UNIVERSITA' DEGLI STUDI DI TRIESTE

More effective prevention strategies would save not only tens of billions of dollars, but save tens of thousands of lives. Funds currently spent on intervention and relief could be devoted to enhancing equitable and sustainable development instead, which would further reduce the risk for war and disaster.

- Kofi Annan,1999

*Building a culture of prevention is not easy. While the **costs of prevention** have to be paid in the present, its **benefits** lie in a **distant future**. Moreover, the benefits are not tangible; they are the disasters that did **NOT** happen.*

\- Kofi Annan,1999

The realistic modelling of ground motion can now be done by making use of global observations from digital networks, application of modern theories for the forward and the inverse problems, and by use of widely available computers.

We do not have to wait for earthquakes to occur in likely focal regions and then to measure ground motion with an extremely dense set of recording instruments.

With the available geological, geophysical, seismological and seismotectonic data, we can compute these seismograms from theoretical considerations

(*Panza, Radulian and Trifu, Editors,* 2000).

A complete database for all sites and predicted focal mechanisms can be constructed immediately; no delay is necessary while we wait for experimental evidence and recordings.

This database is then, naturally, updated continuously by comparison with incoming new experimental data (*Costa et al., 1993, Panza et al., 1999, 2001*).

The seismic input modelling we developed capably addresses key aspects such as:

- the direct evaluation of resulting maps in terms of design parameters, without requiring the adaptation of probabilistic maps to design ground motions;
- the effect of crustal properties on attenuation;

- the derivation of ground motion parameters from synthetic time histories, instead of using overly simplified attenuation functions;
- the generalization of design parameters to locations where there is little seismic history.

The example of Italy

The seismo-tectonic model, proposed by GNDT

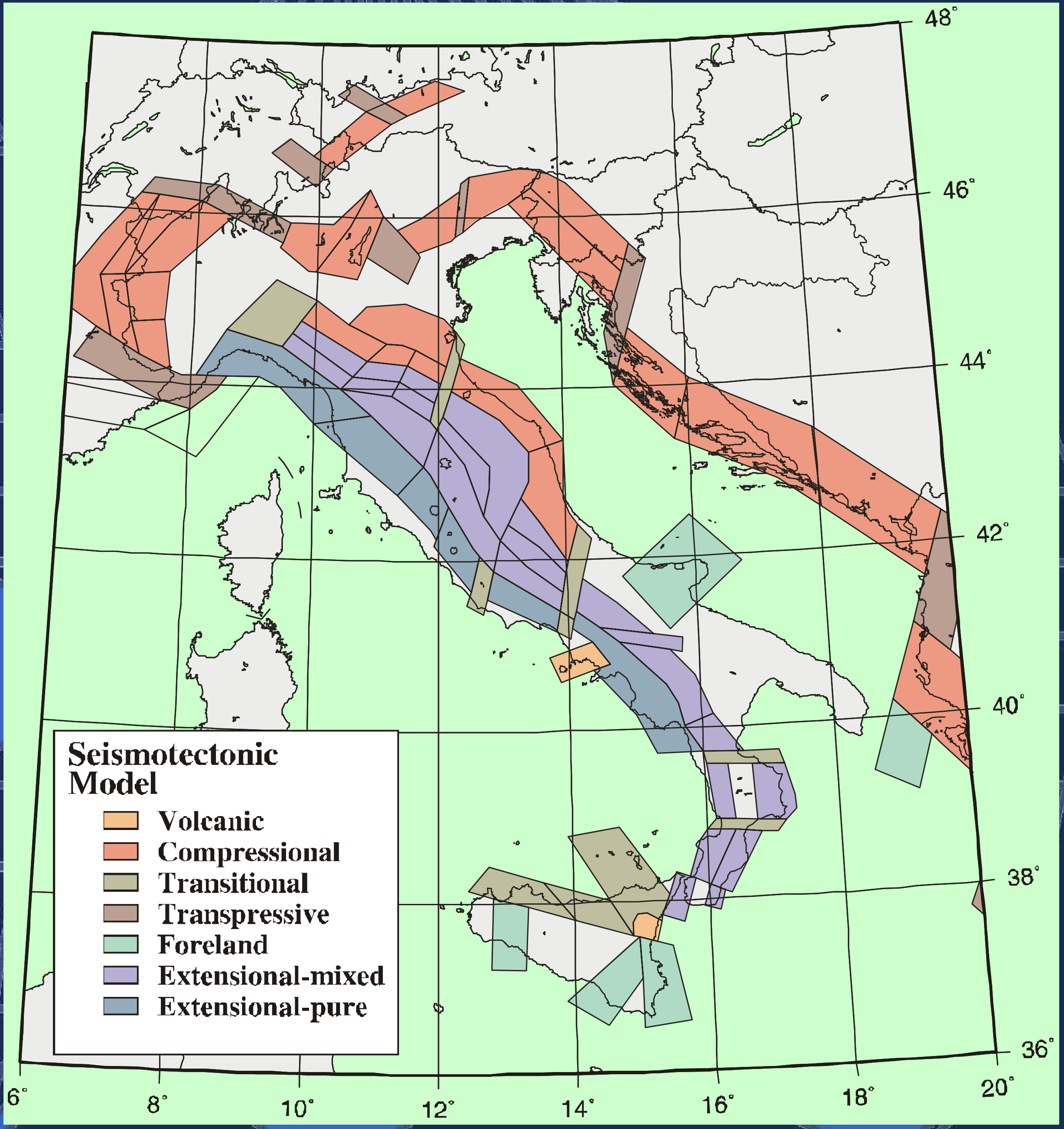

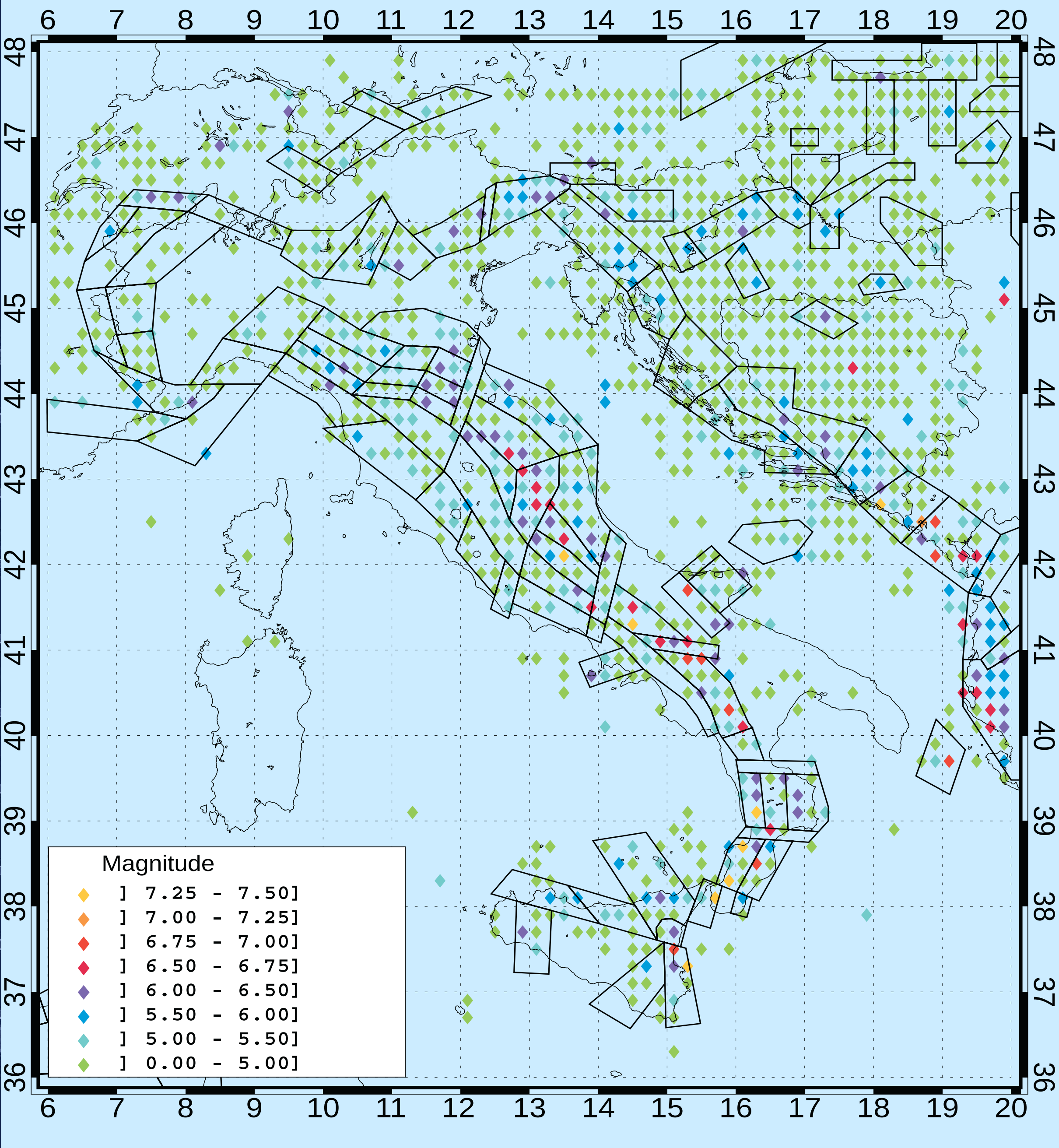

Observed maximum magnitudes in the period 1000-1992 (symbols), and sketch of the seismotectonic model (polygons)

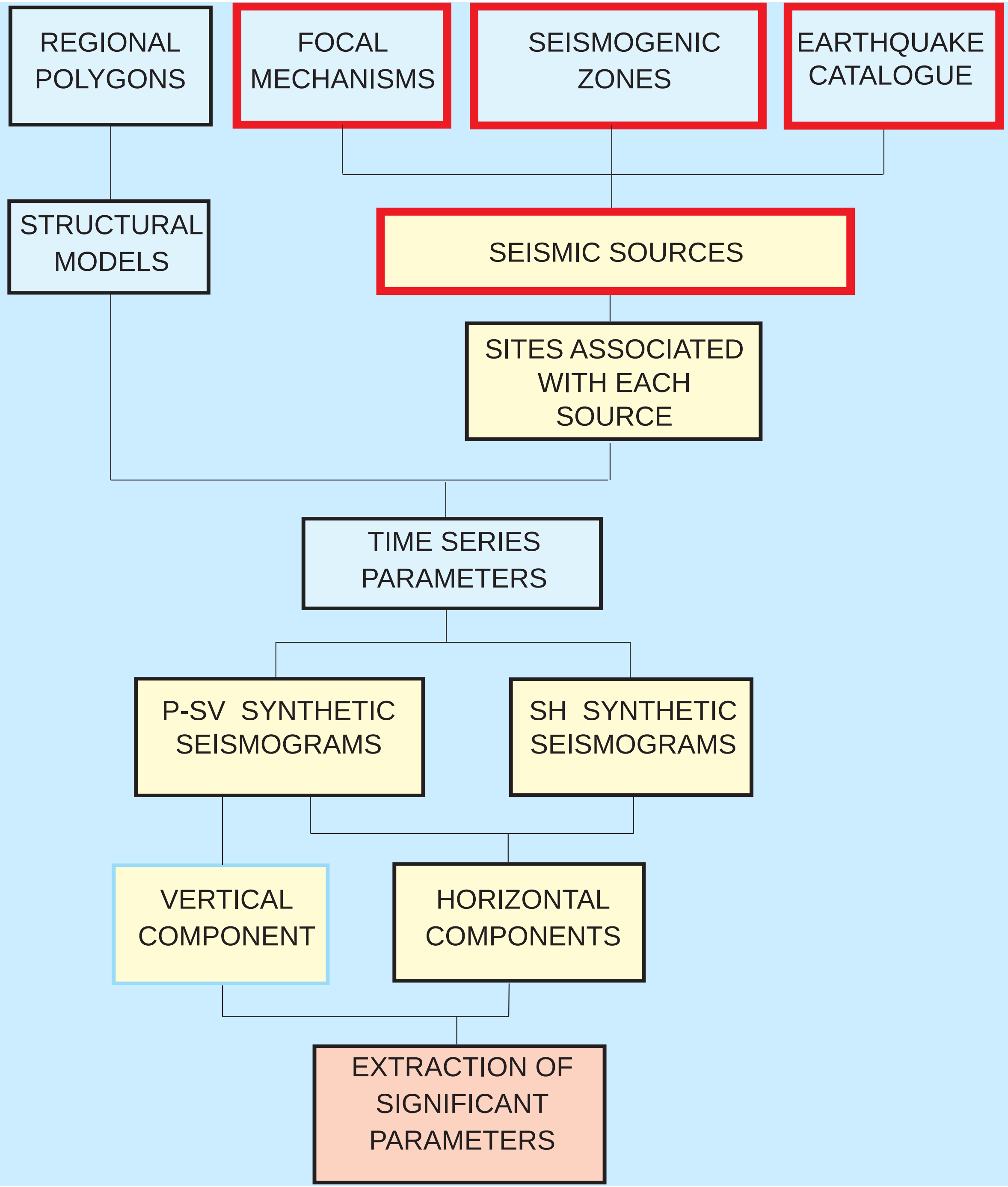

Flow-chart of the method

SMOOTHING OF SEISMICITY
for the definition of seismic sources

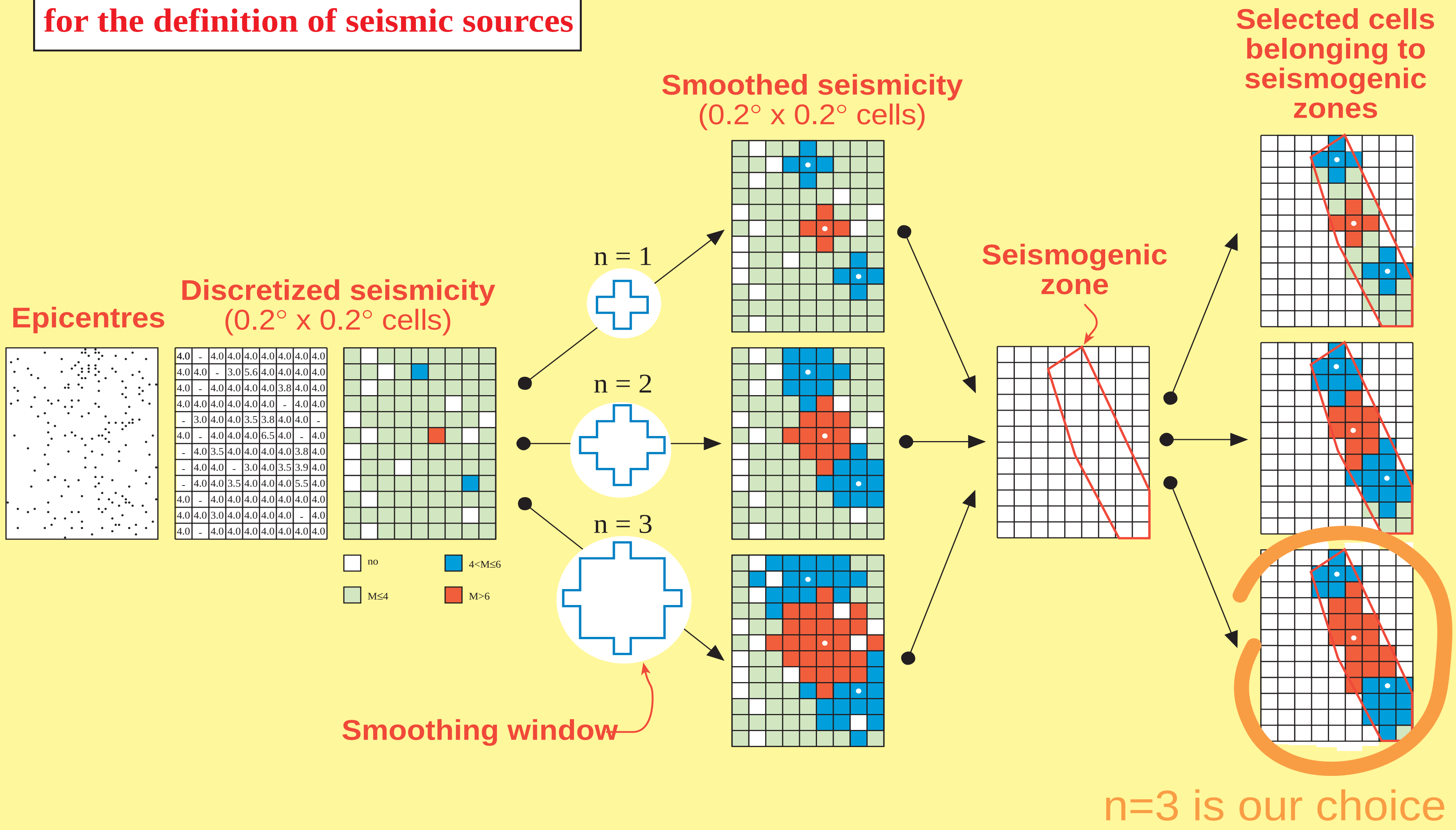

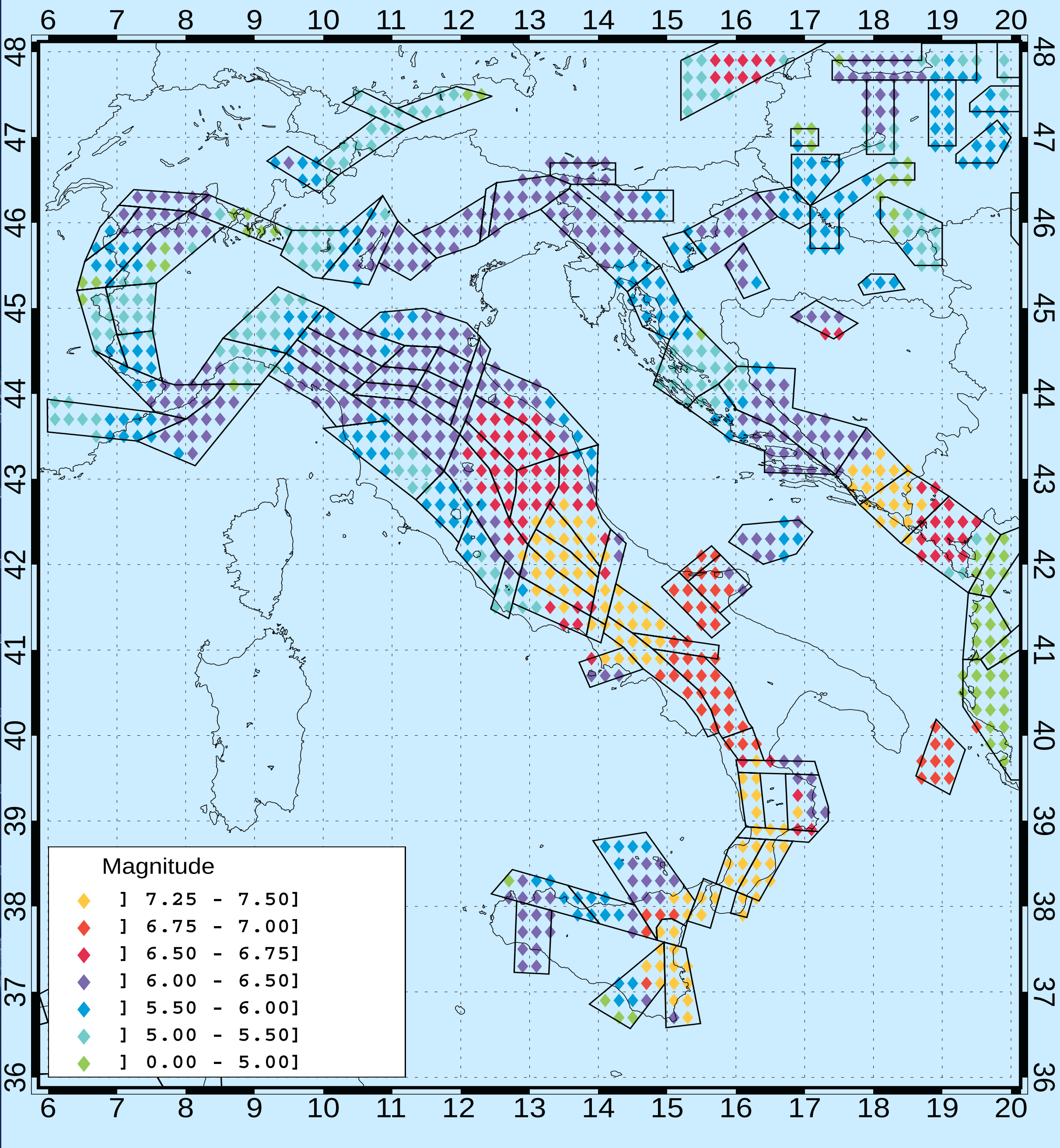

Smoothed magnitudes bounded by the seismotectonic model polygons

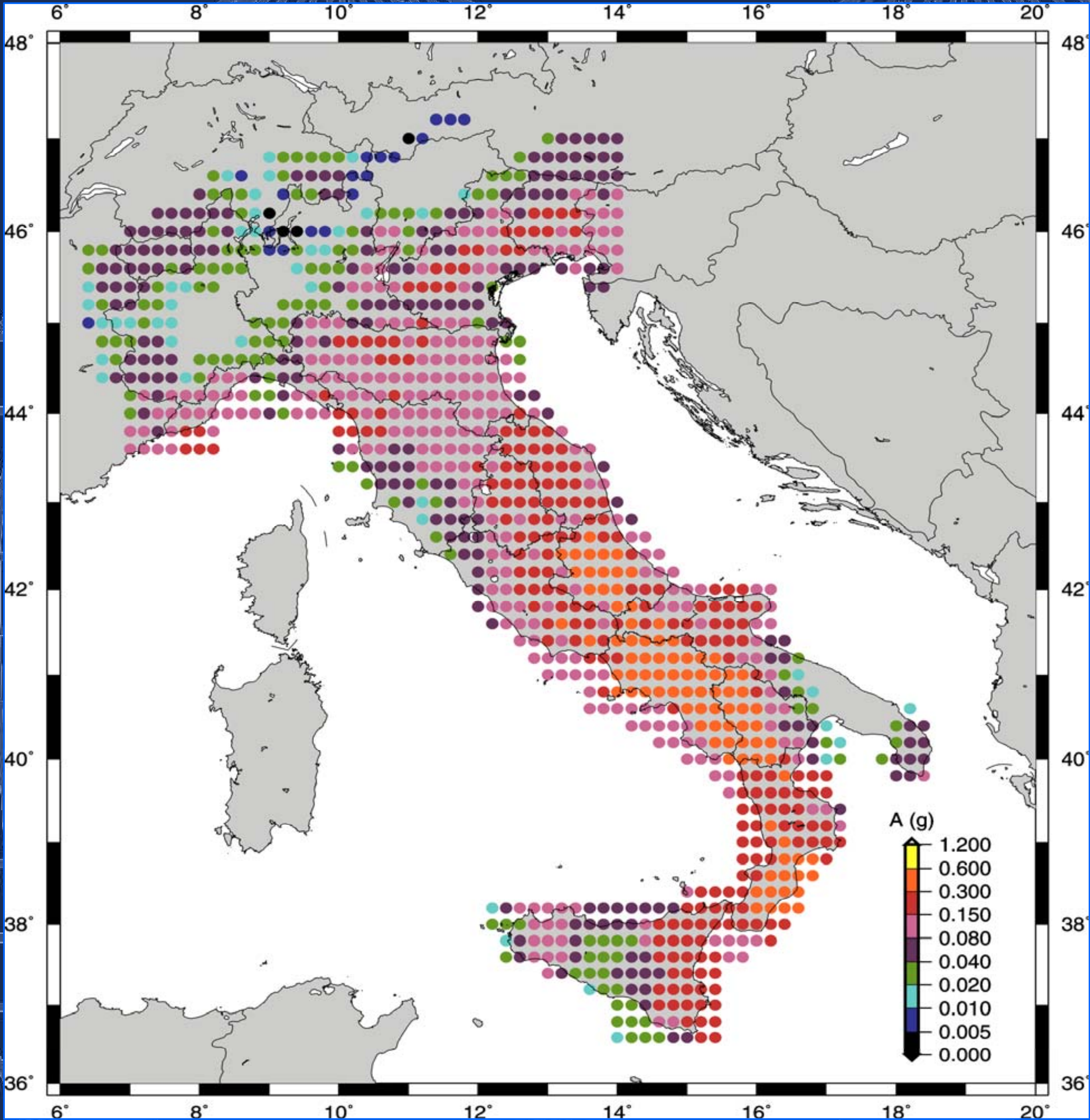

DGA

Maximum estimated Design Ground Acceleration,consistent with Eurocode 8

Deterministic Method

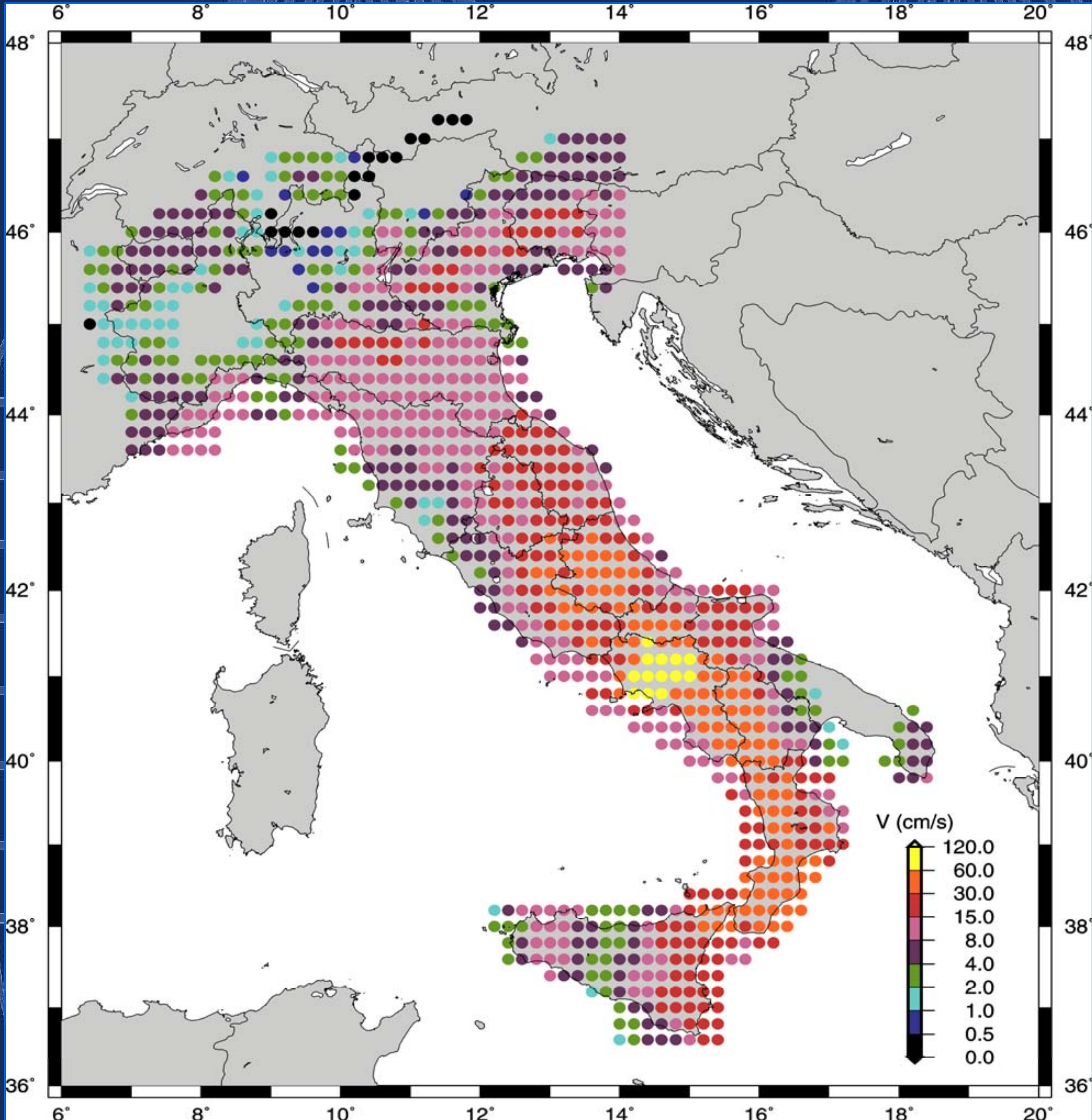

PGV

Maximum estimated velocity

Deterministic Method

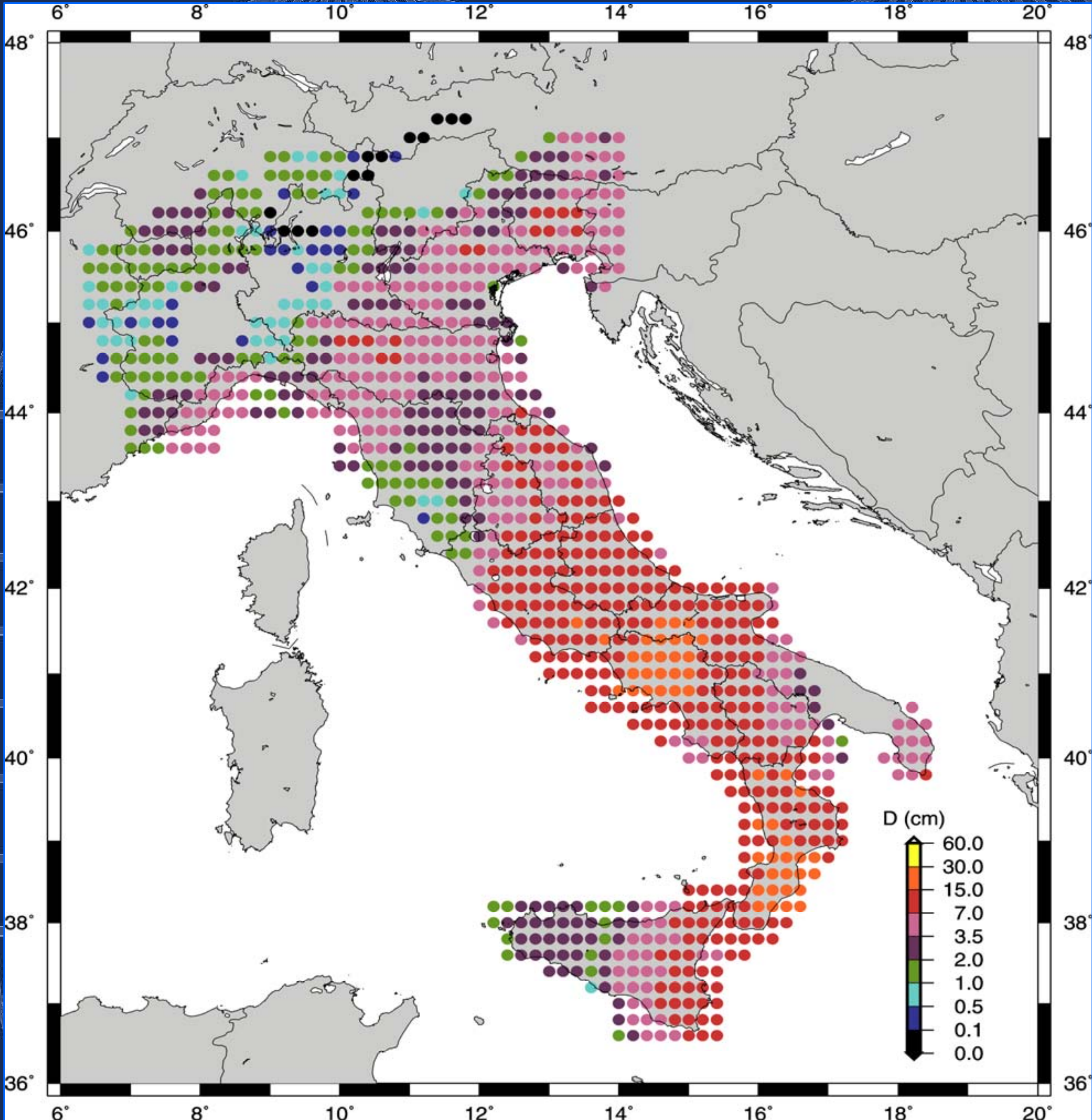

PGD

Maximum estimated displacement, particularly relevant for seismic isolation

Deterministic Method

Our modelling gives the envelope of the ground motion (like acceleration, velocity or displacement) determined considering scenario earthquakes consistent with the seismic history and the seismotectonic of the study area.

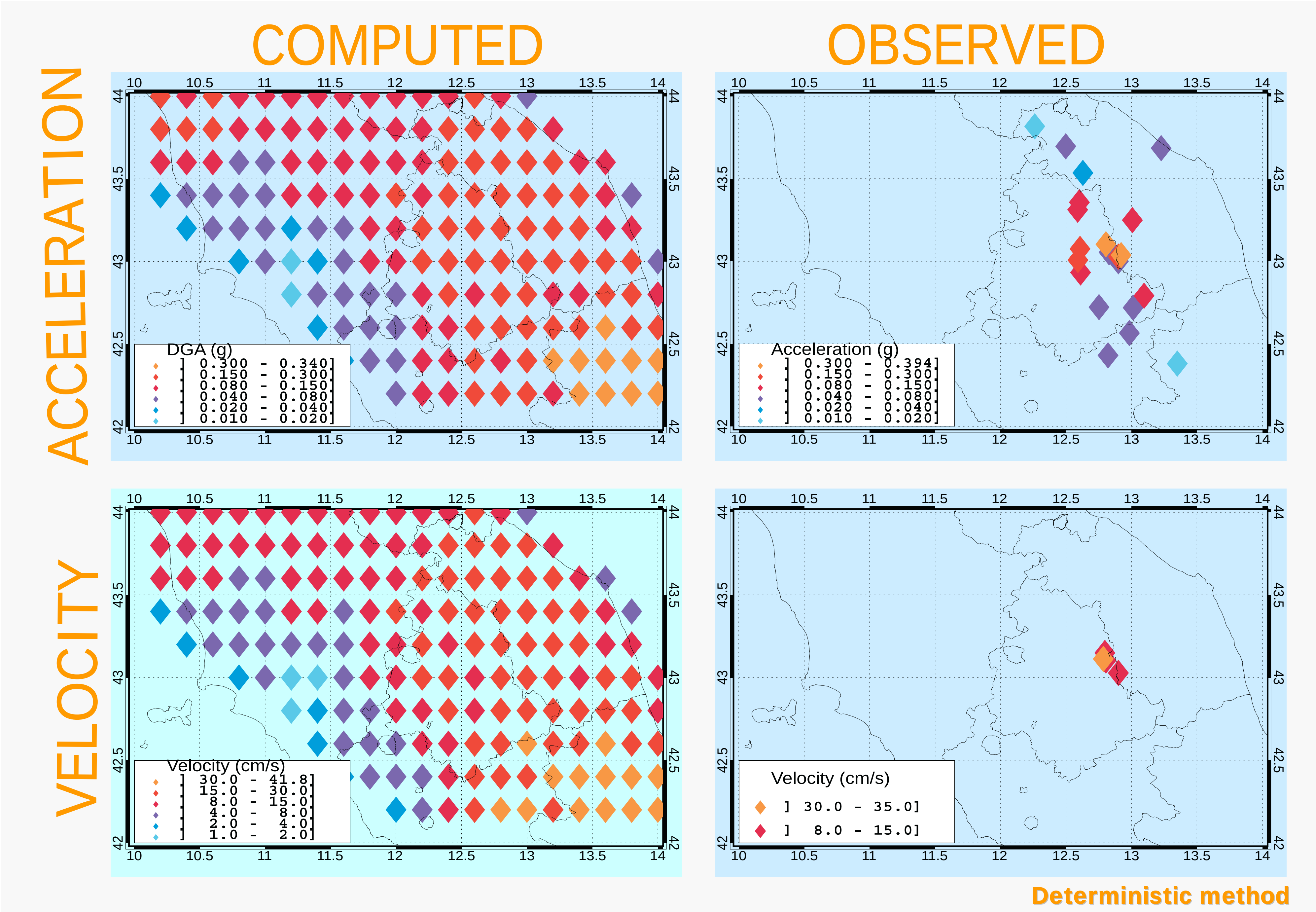
COMPUTED
OBSERVED
ACCELERATION
VELOCITY
DGA (g)
] 0.300 - 0.340]
] 0.150 - 0.300]
] 0.080 - 0.150]
] 0.040 - 0.080]
] 0.020 - 0.040]
] 0.010 - 0.020]
Acceleration (g)
] 0.300 - 0.394]
] 0.150 - 0.300]
] 0.080 - 0.150]
] 0.040 - 0.080]
] 0.020 - 0.040]
] 0.010 - 0.020]
Velocity (cm/s)
] 30.0 - 41.8]
] 15.0 - 30.0]
] 8.0 - 15.0]
] 4.0 - 8.0]
] 2.0 - 4.0]
] 1.0 - 2.0]
Velocity (cm/s)
] 30.0 - 35.0]
] 8.0 - 15.0]
10 10.5 11 11.5 12 12.5 13 13.5 14
42 42.5 43 43.5 44
Deterministic method

Conversion between Intensity (MCS) and Peak ground motion parameters in ITALY

ING Intensity data – NT4.1.1 Magnitudes

Intensity	Displacement (cm)	Velocity (cm/s)	DGA (g)
V	0.1 – 0.5	0.5 – 1.0	0.005 – 0.01
VI	0.5 – 1.0	1.0 – 2.0	0.01 – 0.02
VII	1.0 – 2.0	2.0 – 4.0	0.02 – 0.04
VIII	2.0 – 3.5.	4.0 – 8.0	0.04 – 0.08
IX	3.5 – 7.0	8.0 – 15.0	0.08 – 0.15
X	7.0 – 15.0	15.0 – 30.0	0.15 – 0.30
XI	15.0 – 30.0	30.0 – 60.0	0.30 – 0.60

Conversion between Intensity (MCS) and Peak ground motion parameters in ITALY

ISG Intensity data – NT4.1.1 Magnitudes

Intensity	**Displacement (cm)**	**Velocity (cm/s)**	**DGA (g)**
VI	1.0 – 1.5	1.0 – 2.0	0.01 – 0.025
VII	1.5 – 3.0	2.0 – 5.0	0.025 – 0.05
VIII	3.0 – 6.0	5.0 – 11.0	0.05 – 0.1
IX	6.0 – 13.0	11.0 – 25.0	0.1 – 0.2
X	13.0 – 26.0	25.0 – 56.0	0.2 – 0.4

$$DGA(I) / DGA(I-1) = 2$$

$$PGV(I) / PGV(I-1) = 2$$

$$PGD(I) / PGD(I-1) = 2$$

The slope of the regression maximum observed macroseismic intensity, I (MCS), and computed peak values of ground motion is always close to 0.3, a value common to many empirical relations (Shteinberg et al., 1993) found considering Peak Ground Accelerations. Cancani in 1904 modified the original Mercalli scale, defining the MCS scale, indeed with the declared purpose to obtain the slope 0.3.

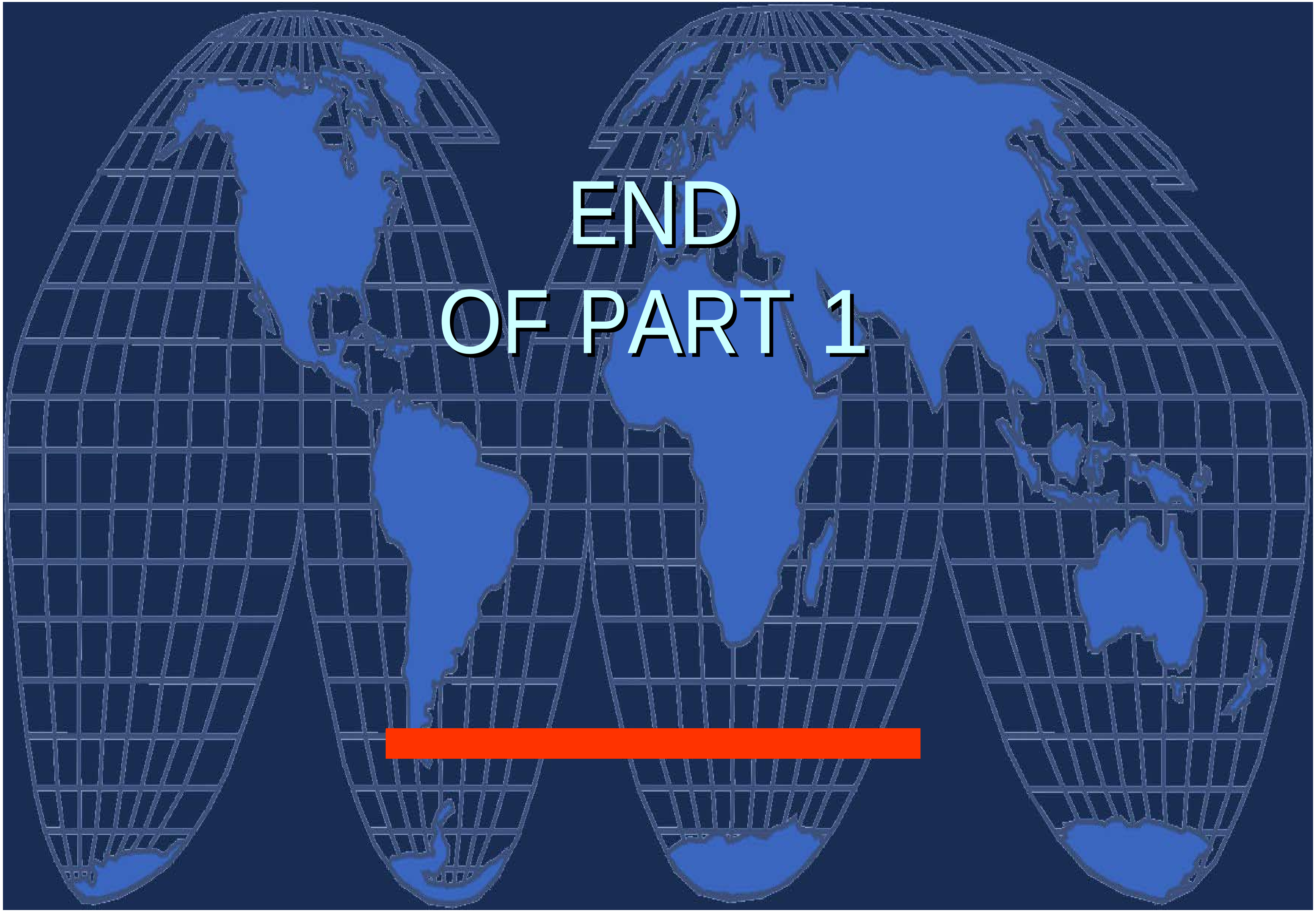
END
OF PART 1

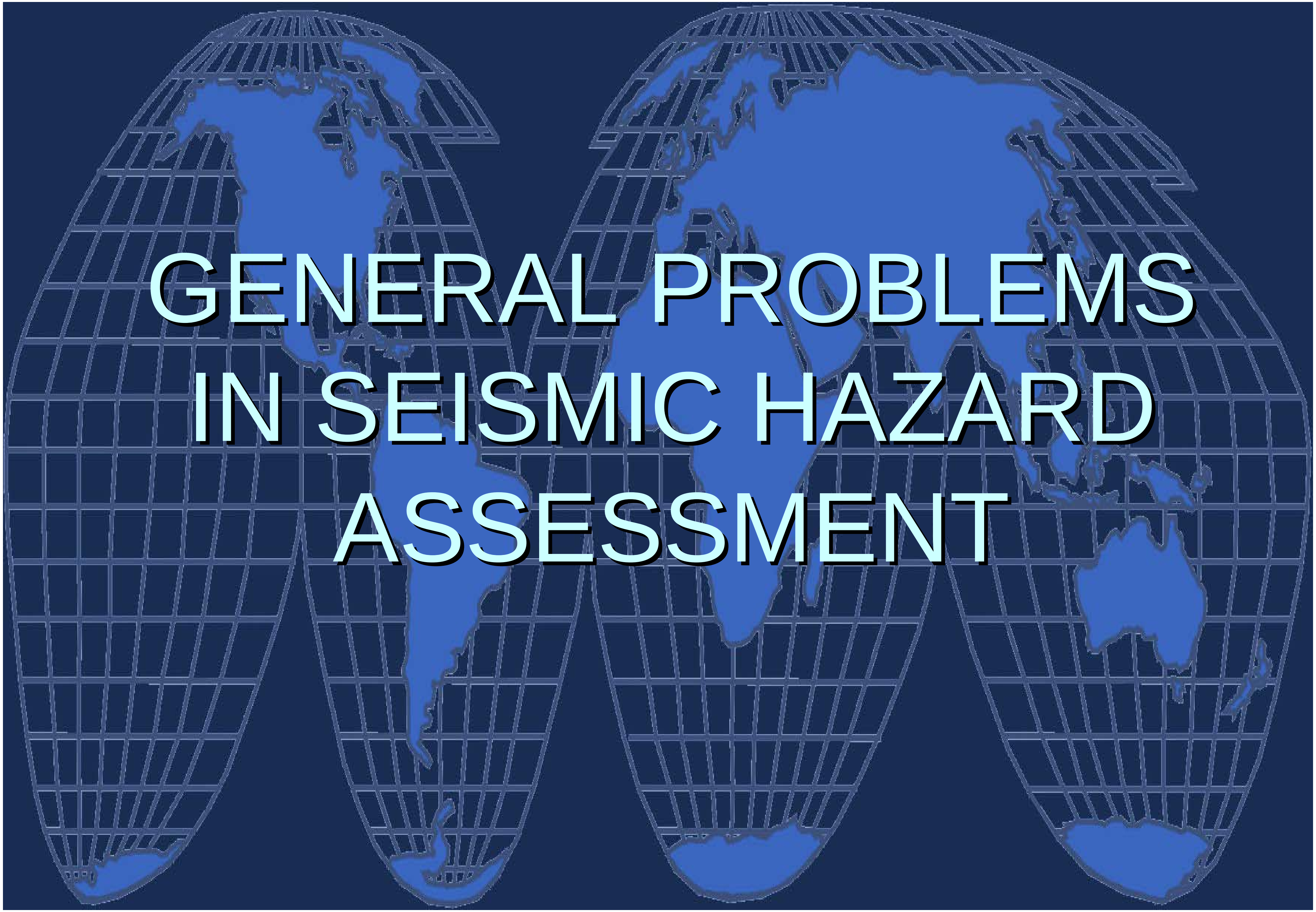

GENERAL PROBLEMS IN SEISMIC HAZARD ASSESSMENT

Case studies indicate the limits of the currently used methodologies, deeply rooted in engineering practice, based on a probabilistic approach.

The probabilistic analysis supplies indications that can be useful but are not sufficiently reliable to characterize seismic hazard. Recent examples Kobe (17.1.1995), Bhuj (26.1.2001), Boumerdes (21.5.2003) and Bam (26.12.2003) events.

? GSHAP ?

Kobe (17.1.1995), Gujarat (26.1.2001), Boumerdes (21.5.2003) and Bam (26.12.2003) earthquakes PGA(g)

	Expected with a probability of exceedence of 10% in 50 years (return period 475 years)	Observed
Kobe	0.40-0.48	0.7-0.8
Gujarat	0.16-0.24	0.5-0.6
Boumerdes	0.08-0.16	0.3-0.4*
Bam	0.16-0.24	0.7-0.8

* from I, if liquefaction is considered the value may be smaller

The mathematical modelling, based on probabilistic concepts **cannot fill in the gap due to the lack of knowledge about the physical process** behind an earthquake, at the most it can supply some guidelines.

The mathematical modelling **may loose validity** in dealing with **uncertainties** that are **so large** that may not be quantifiable in a meaningful sense (Chandler et al., 2001) as it happens in low to moderate seismicity regions, or regions lacking historical and instrumental earthquake data.

A proper definition of the seismic input at a given site can be done following **two main approaches**.

The first approach is based on the analysis of the available strong motion databases, collected by existing seismic networks, and on the grouping of those accelerograms that contain similar source, path and site effects (*e.g. Decanini and Mollaioli, 1998*).

The second approach is based on modelling techniques, developed from the knowledge of the seismic source process and of the propagation of seismic waves, that can realistically simulate the ground motion (*Panza et al., 1996; Field et al., 2000*).

The ideal procedure is to follow the two complementary ways, in order to validate the numerical modelling with the available recordings (*e.g. Decanini et al., 1999; Panza et al., 2000a,b,c*).

For example, in constructing design input motions, estimates of the peak ground motions at the site can be made in a probability hazard analysis (including interoccurrence probabilities). Then final selection of appropriate accelerograms with their associated ground velocities and displacements would follow a deterministic approach. The choices would be guided by wave propagation modelling that includes appropriate phasing and duration of the dominant waves in the time histories (Bolt, 2003).

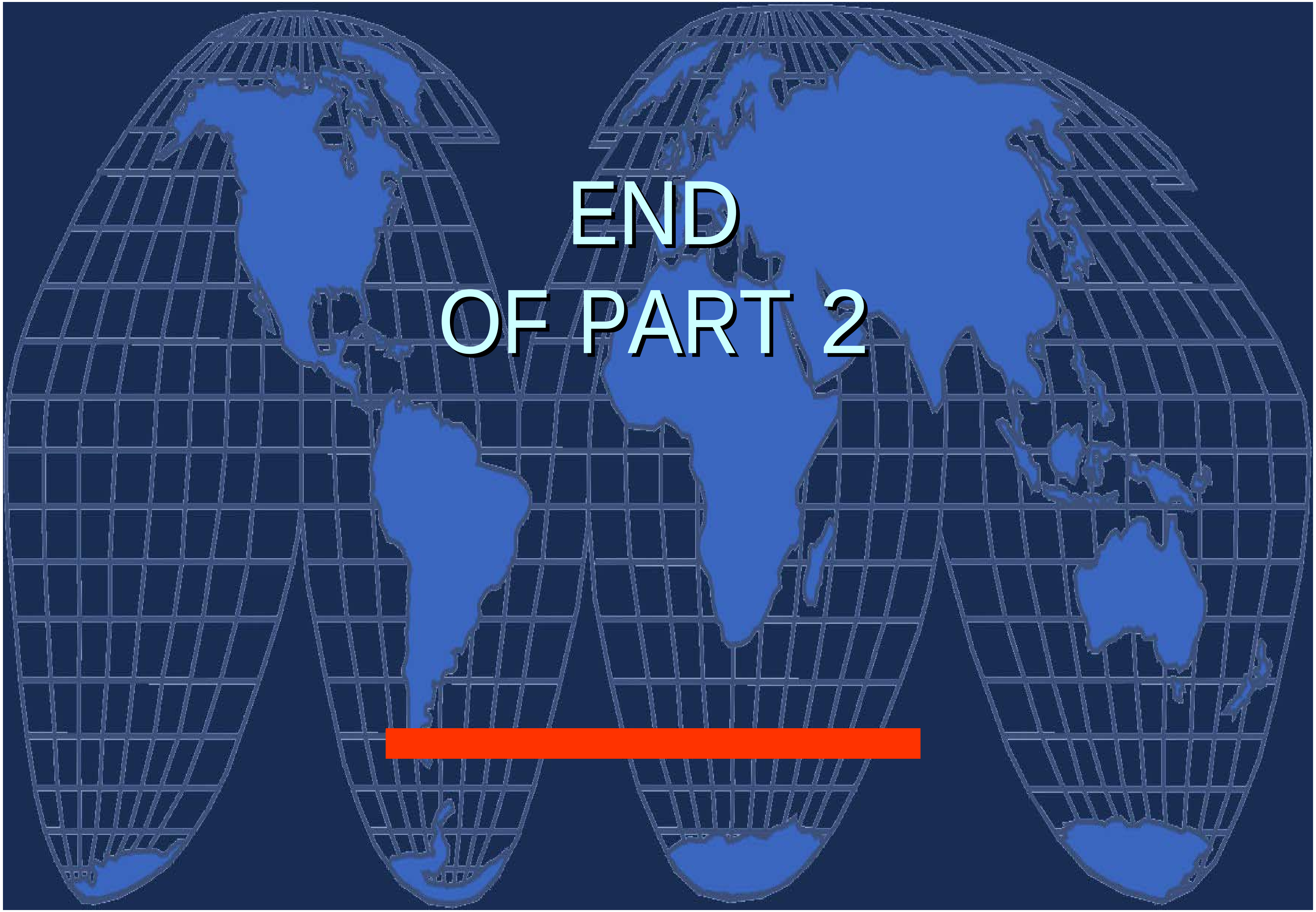
END
OF PART 2

BASE SEISMIC ISOLATION

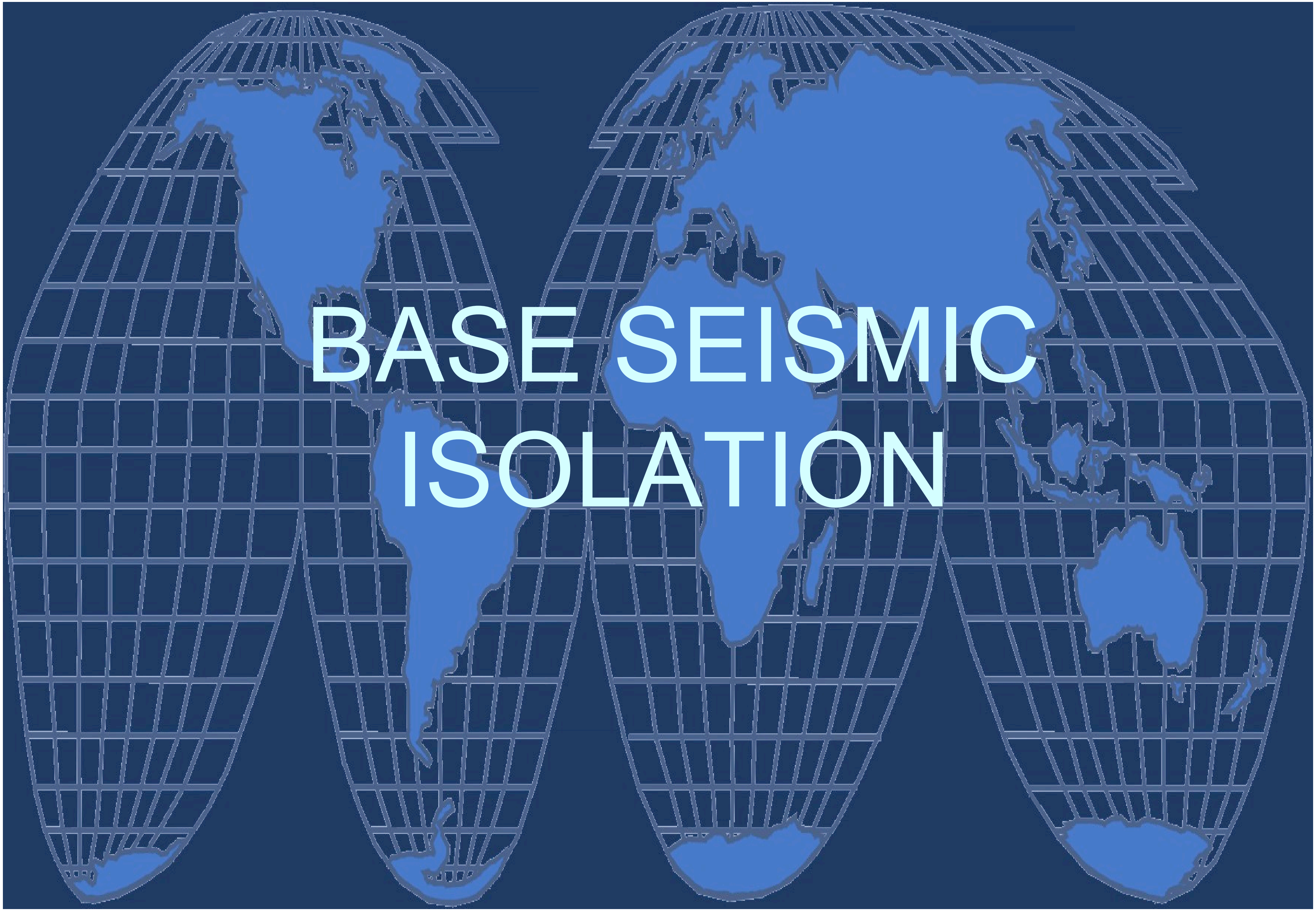

- Where the **deterministic** numerical modelling is successfully compared with records, the synthetic seismograms permit the microzoning, based upon a set of possible **scenario earthquakes**.

- Where no recordings are available the synthetic signals can be used to estimate the ground motion without having to wait for a strong earthquake to occur.

- The use of modelling is necessary because, contrary to the common practice, the so-called local site effects cannot be modelled by a convolutive method, since they can be ***strongly dependent upon the properties of the seismic source***.

- The wide use of realistic synthetic time histories, **which model the waves propagation from source to site**, allows us to easily construct scenarios based on significant ground motion parameters (velocity and displacement).

- Among the cost effective advance action aimed at creating knowledge based hazard resilient public assets a particular role is played by **seismic isolation**, an innovative technology that is getting a steadily increasing diffusion on global scale.

Base
Seismic
Isolation

Dynamic test of a base isolated building in Rapolla (*Braga and Laterza, 2000*)

Base
Seismic
Isolation

Dynamic test of a base isolated building in Rapolla (*Braga and Laterza, 2000*)

Base Seismic Isolation

Dynamic test of a base isolated building in Rapolla (*Braga and Laterza, 2000*)

- Generally, for isolated structures, the seismic isolation systems (rubber bearings, frictional type systems, etc.) need to have sufficient displacement and energy dissipation capacities.

- In order to cope with these requirements, the evaluation of the critical input for this kind of seismic protection systems should consider, beyond strength demands, the significant influence of the displacement and energy demands.

- It is then evident that the importance of the outlined aspects, and the corresponding structural design choices, depends on the **evaluation of the complete possible strong motion at the base of the isolator-building system**, from which energetic parameters can be extracted.


END
OF PART 3

MICROZONATION

Hybrid Method:
Modes Summation+Finite Differences.

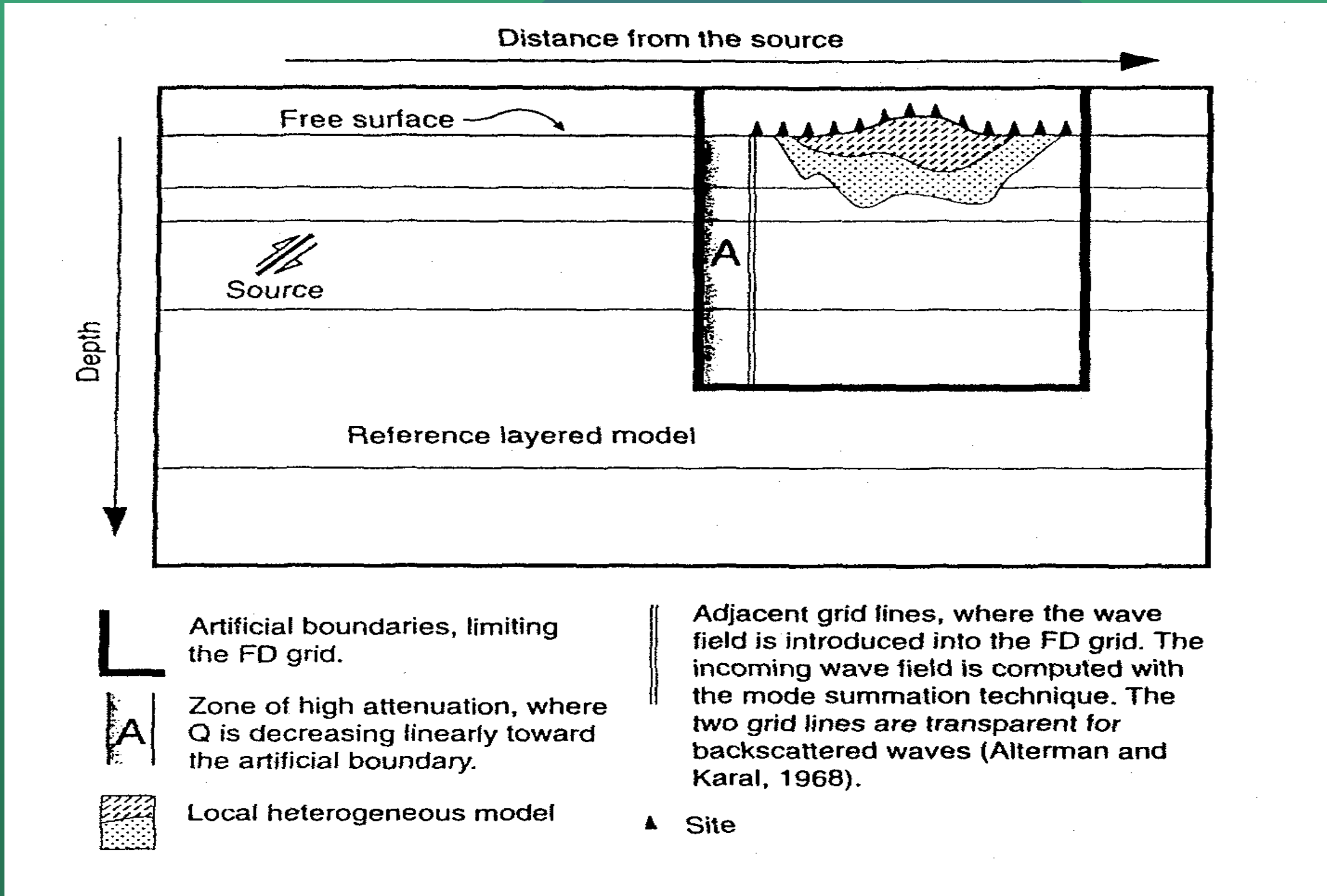

Wave propagation is treated by means of the **modal summation** technique from the source to the vicinity of the local structure (anelastic bedrock structure).

The **finite differences** technique is applied in the laterally inhomogeneous part of the model (sedimentary basin).

Synthetic seismic signal obtained consider **simultaneously** the seismic moment tensor, average mechanical characteristics of the traveled path and detailed local site conditions.

Complete synthetic seismograms in terms of displacement, velocity and acceleration are computed separately for the SH and P-SV waves in the frequency range of interest.

A comprehensive description of the theory used to compute the synthetic signals is given in **Advances in Geophysics, Vol. 43, 2001, Academic Press**.

For urban areas where the numerical modelling of ground motion has been successfully compared with strong motion records, the computations of synthetic seismograms permit a detailed microzoning based upon the set of possible scenario earthquakes.

For areas where very limited or no recordings are available the synthetic time series can be used to estimate the expected ground motion, thus leading to a **pre-disaster microzonation without having to wait for an earthquake to occur**.

In both cases the use of synthetic computations is necessary to overcome the fact that the so-called local site effects can be strongly dependent upon the properties of the seismic source generating the seismic input (Panza et al, 2000).

- **H/V** is the spectral ratio between the horizontal and vertical components of motion.

Modeling of seismic input
(azimuth effect)

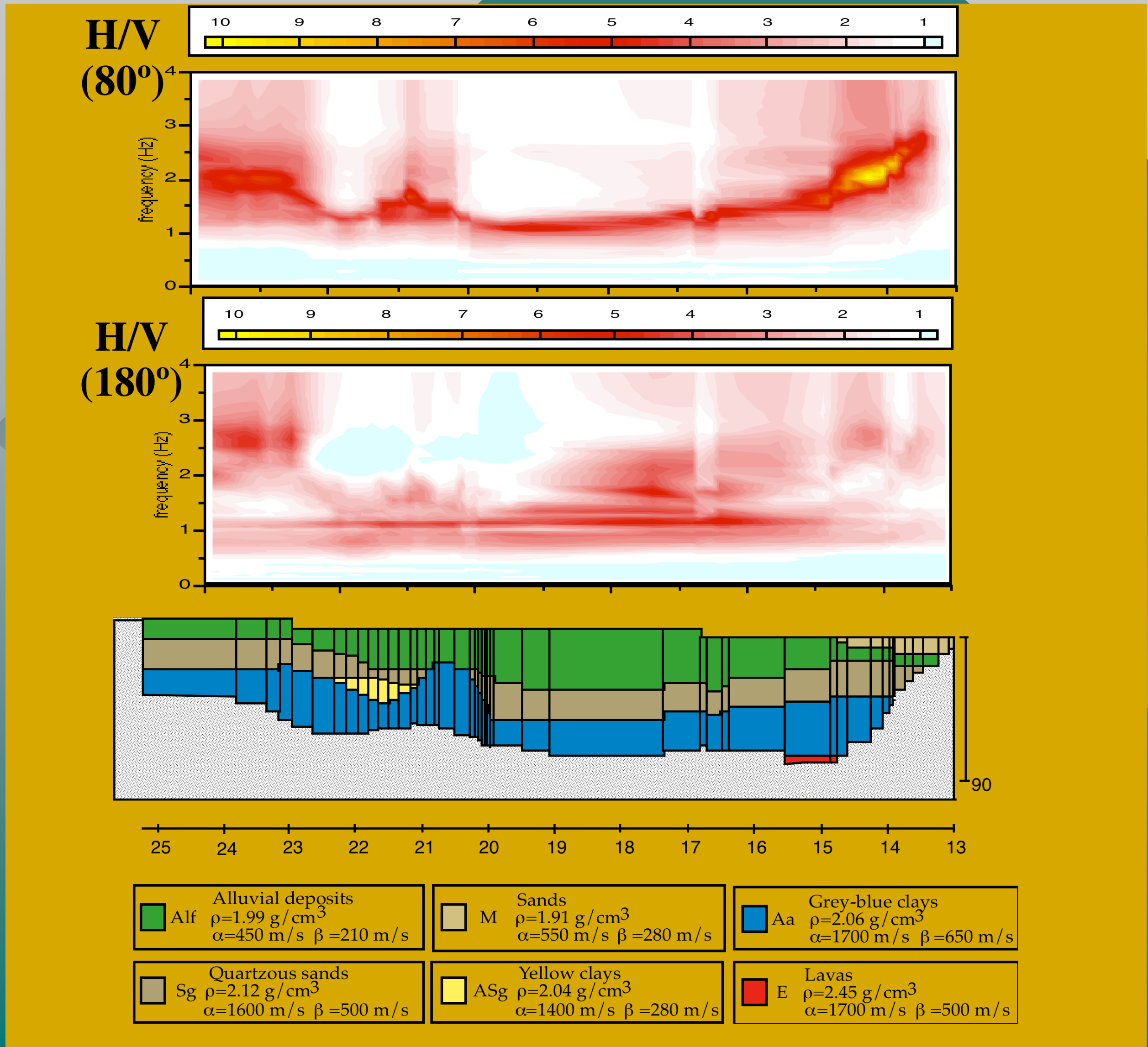

- **RSR** is the ratio between the amplitudes of the response spectra, for 5% damping, obtained considering the bedrock structure, and the corresponding values, computed taking into account the local heterogeneous medium.

Modeling of seismic input

(azimuth effect)

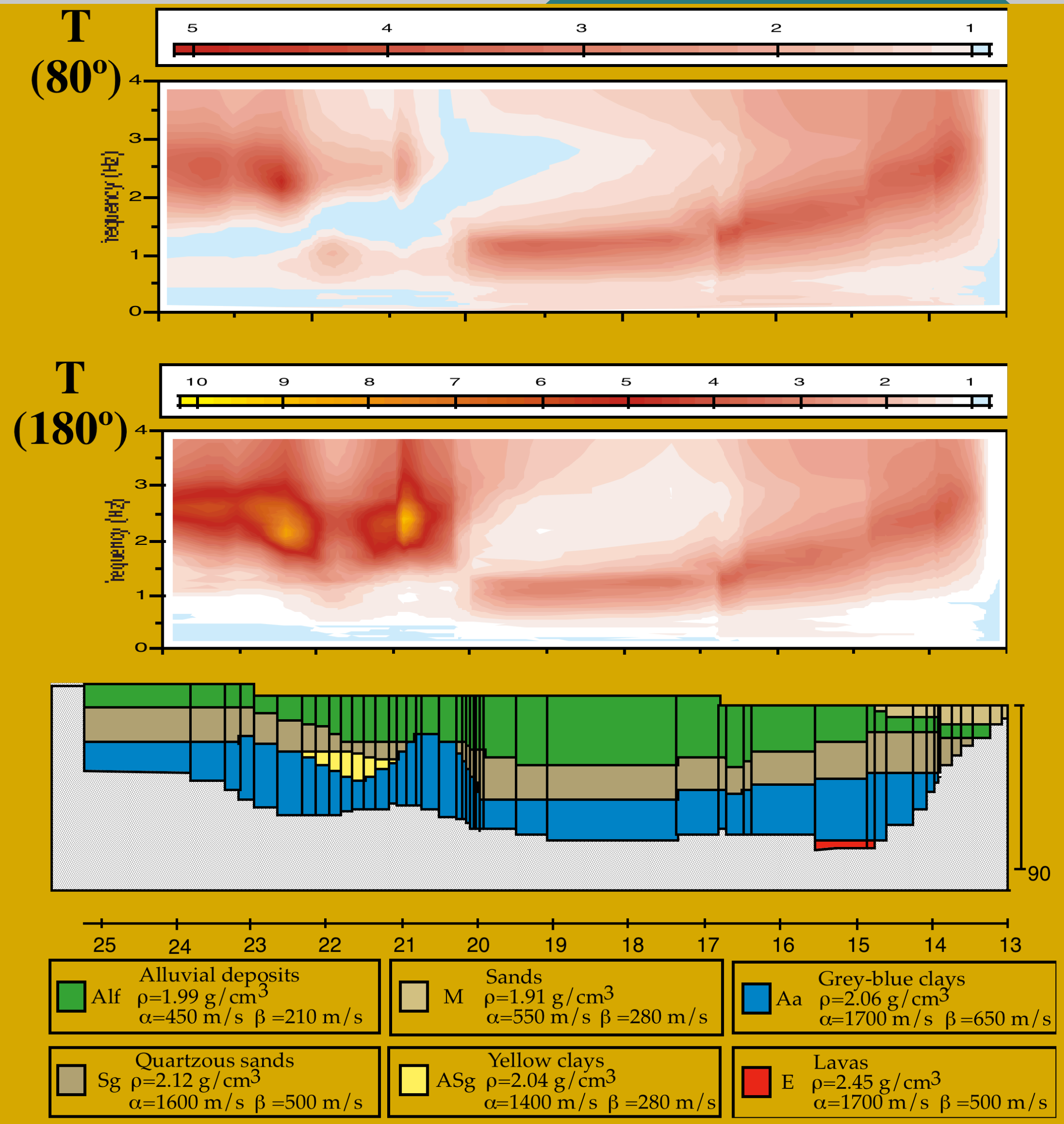

RSR for the SH component of motion

- Therefore we can conclude, in agreement with the recent paper by Field and the SCEC phase III Working Gourp (2000), that **our best hope is via waveform modeling** based on first principles of physics.

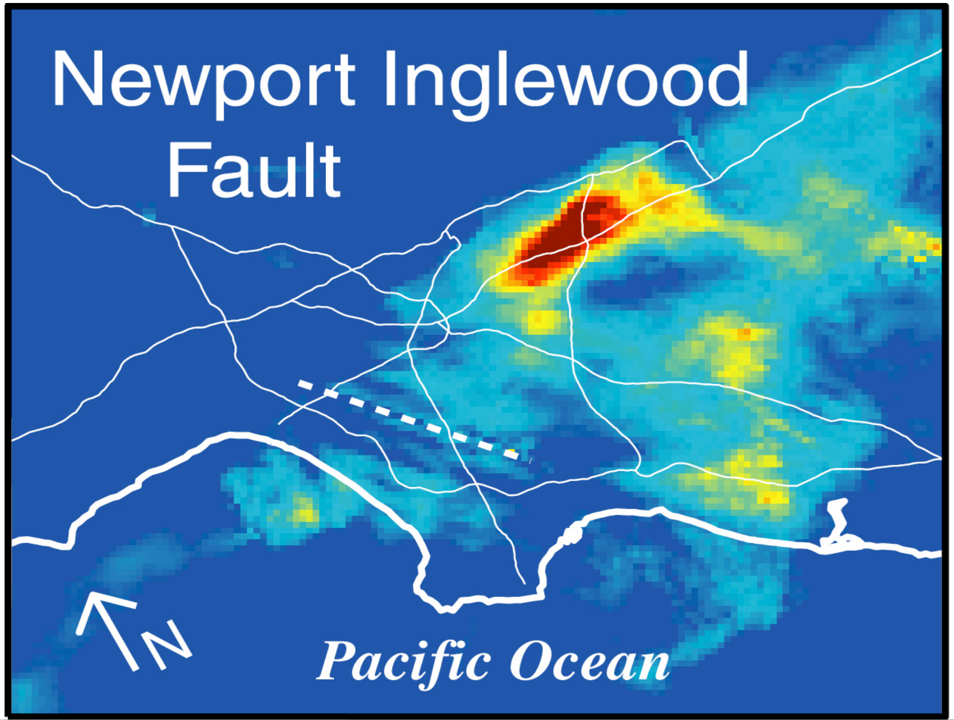

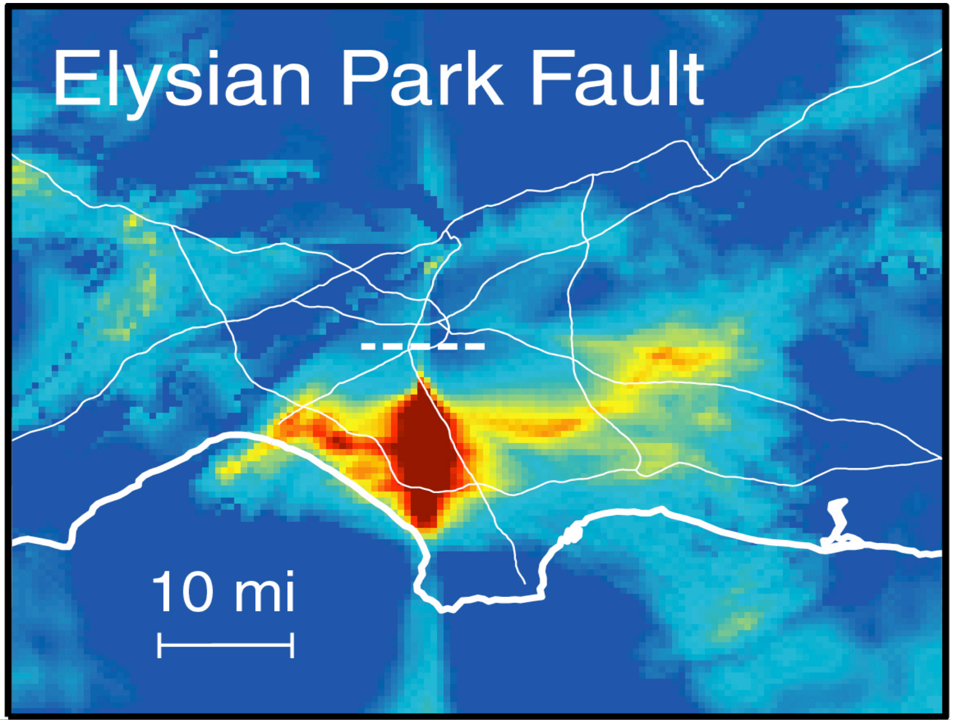

These images of the Los Angeles Basin show "hotspots" predicted from computer simulations of an earthquake on the Elysian Park Fault and an earthquake on the Newport-Inglewood Fault (represented by the white dashed lines). What is shown is **not** how much shaking was experienced at a particular site but rather how much more or less shaking (highest levels are shown in red) a site receives **relative to what is expected** from only the magnitude of the earthquake and the site's distance from the fault. These images consider only part of the total shaking (long-period motions) and were calculated by using a simplified geologic structure. (Data for images courtesy of Kim Olsen, University of California, Santa Barbara, SCEC Phase III report)

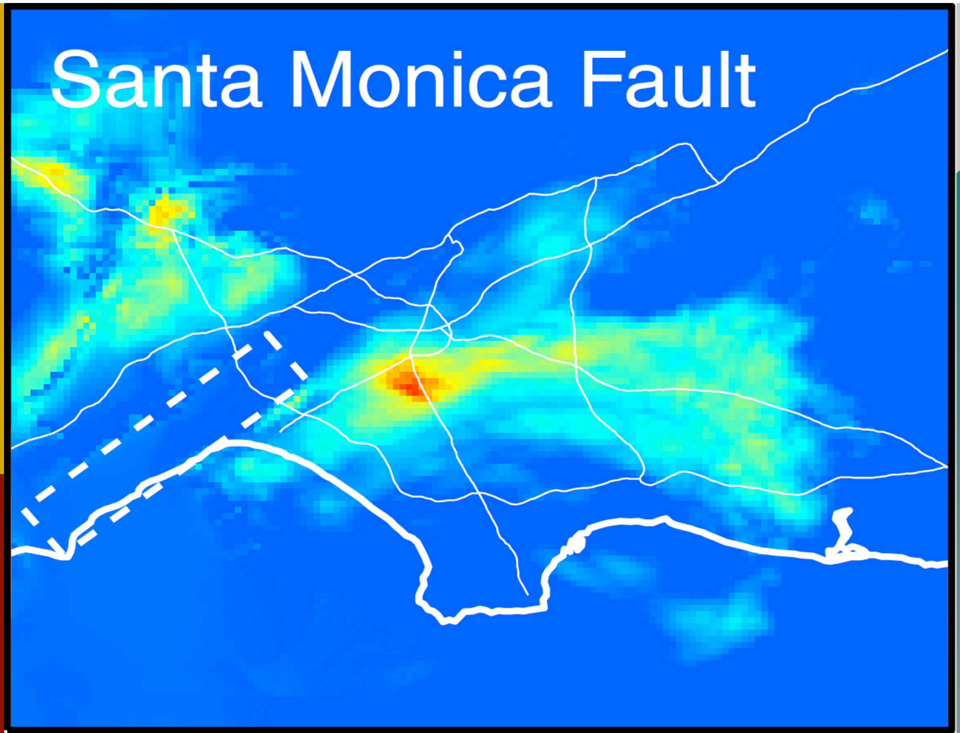

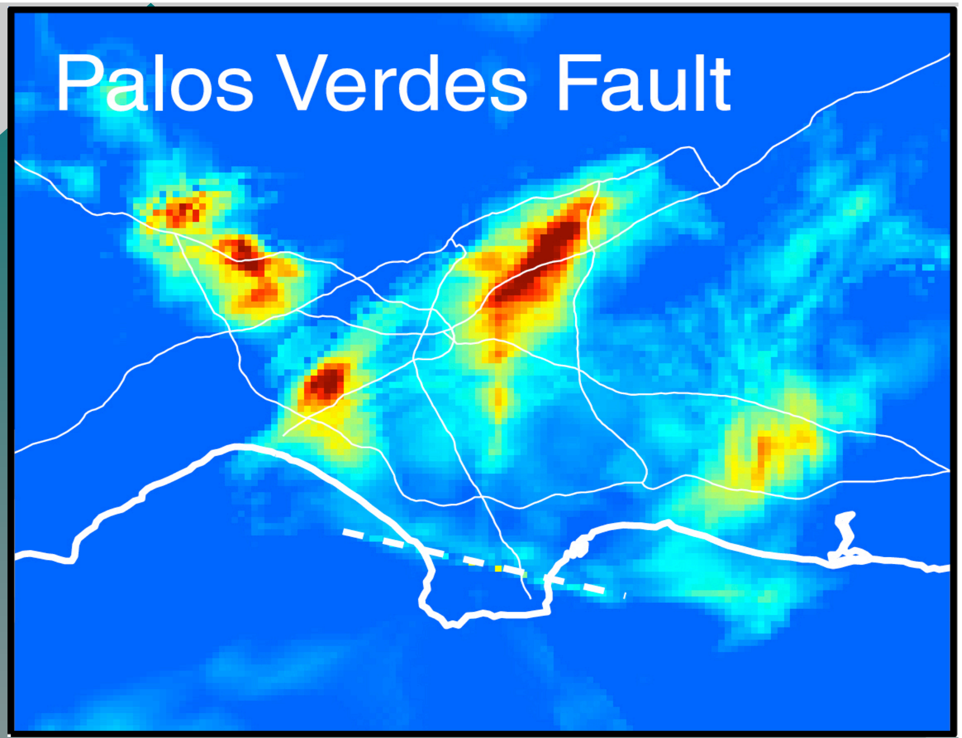

"hotspots" predicted from computer simulations of an earthquake on the Santa Monica Fault and an earthquake on the Palos Verdes Fault (represented by the white dashed lines). SCEC Phase III report, Field, 2000, BSSA, see also http://www.scec.org/phase3/

Near-Fault Ground Motions

Near-fault ground motions often contain large long-period (2-5 sec) wave pulses. There are two causes of these long-period pulses: first, constructive interference of the radiated waves due to directivity of the fault rupture; second, movement of the ground associated with the permanent geodetic offset. To keep these two effects separate, the terms “directivity pulse” and “fling-step” are used for the rupture directivity and elastic rebound effects, respectively (Bolt & Abrahamson, 2003).

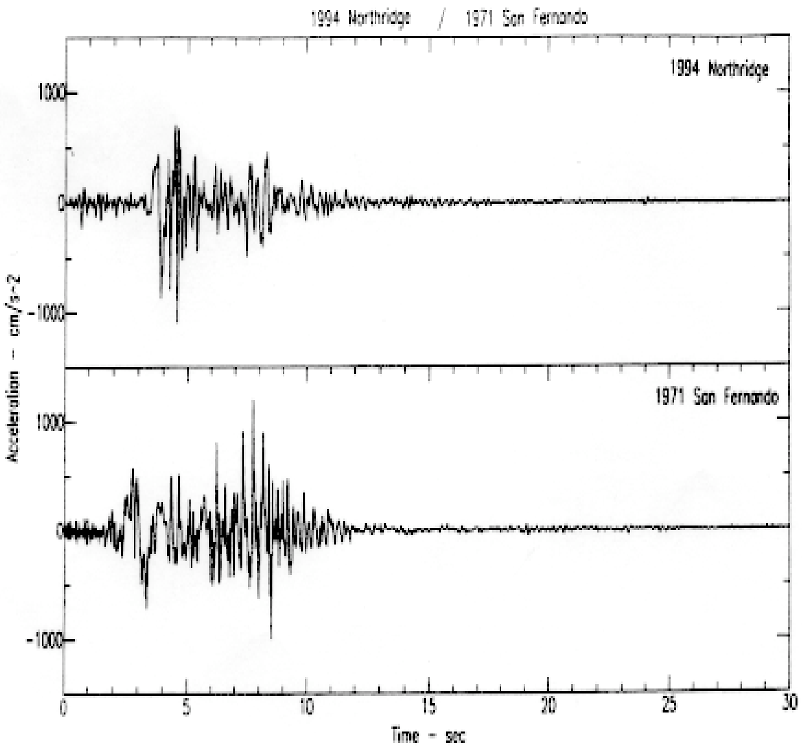

Figure 1: Strong motion recordings at the Pacoima station, California in the 1971 San Fernando (bottom) and 1994 Northridge (top) earthquakes. All are S16E horizontal components of (1a) acceleration, (1b) velocity, and (1c) displacement, respectively.

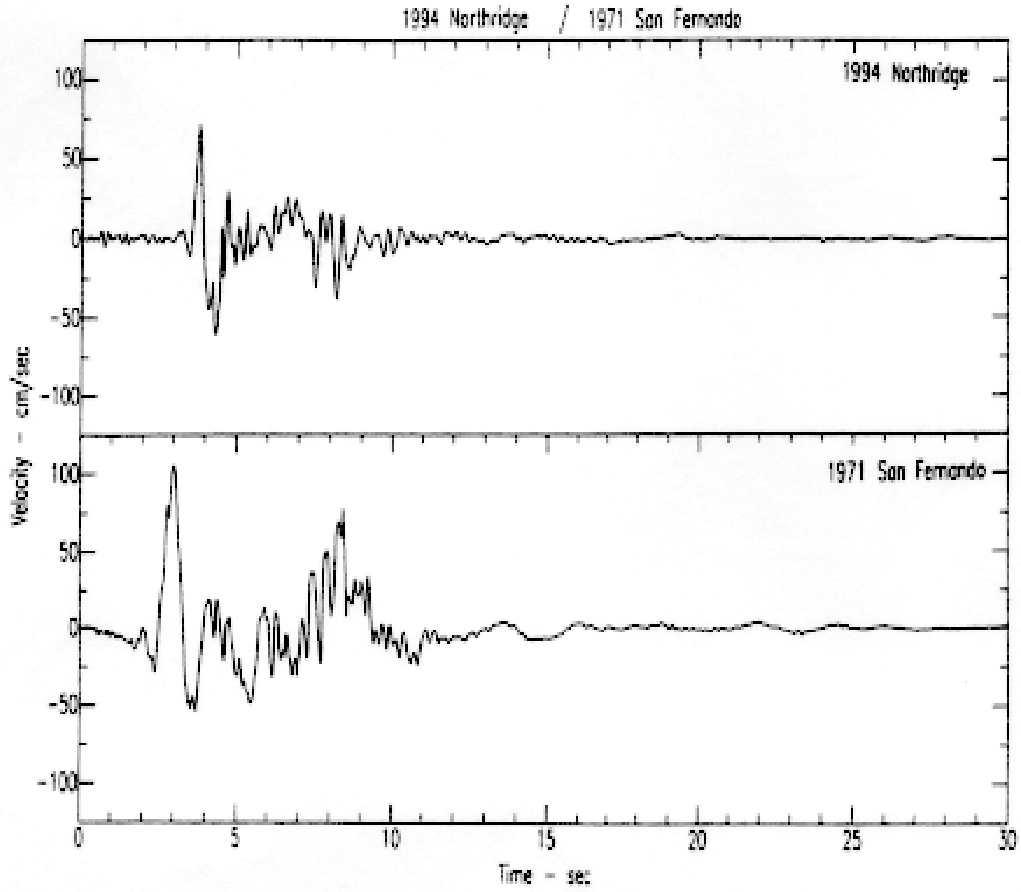

Figure 1b: Ground velocity, S16E Pacoima 1971, 1994.

Nice examples of velocity pulses

Rupture directivity effects occur when the fault ruptures toward the site and the slip direction (on the fault plane) is aligned with the rupture direction (Somerville et al., 1998). The consequent pulse is strongest on the component of motion perpendicular to the strike of the fault (fault-normal component). Fling-step ground motion occurs close to a ruptured fault with significant surface offset. It is limited to the ground displacement component parallel to the slip direction. Thus, for strike-slip earthquakes, the rupture directivity pulse and the fling-step pulse will naturally separate themselves into two horizontal components. For dip-slip earthquakes the effect is more complicated. The rupture directivity effect will be strongest on the fault normal component at a location updip from the hypocenter. The fling step will be observed on the horizontal component perpendicular to the strike of the fault. Consequently, for dip-slip faults, directivity-pulse effects and fling-step effects can be combined on the same component.

Directivity

Landers Earthquake (1992). Map showing the velocity time histories at Lucerne (forward diretivity) and Joshua Tree (backward directivity).

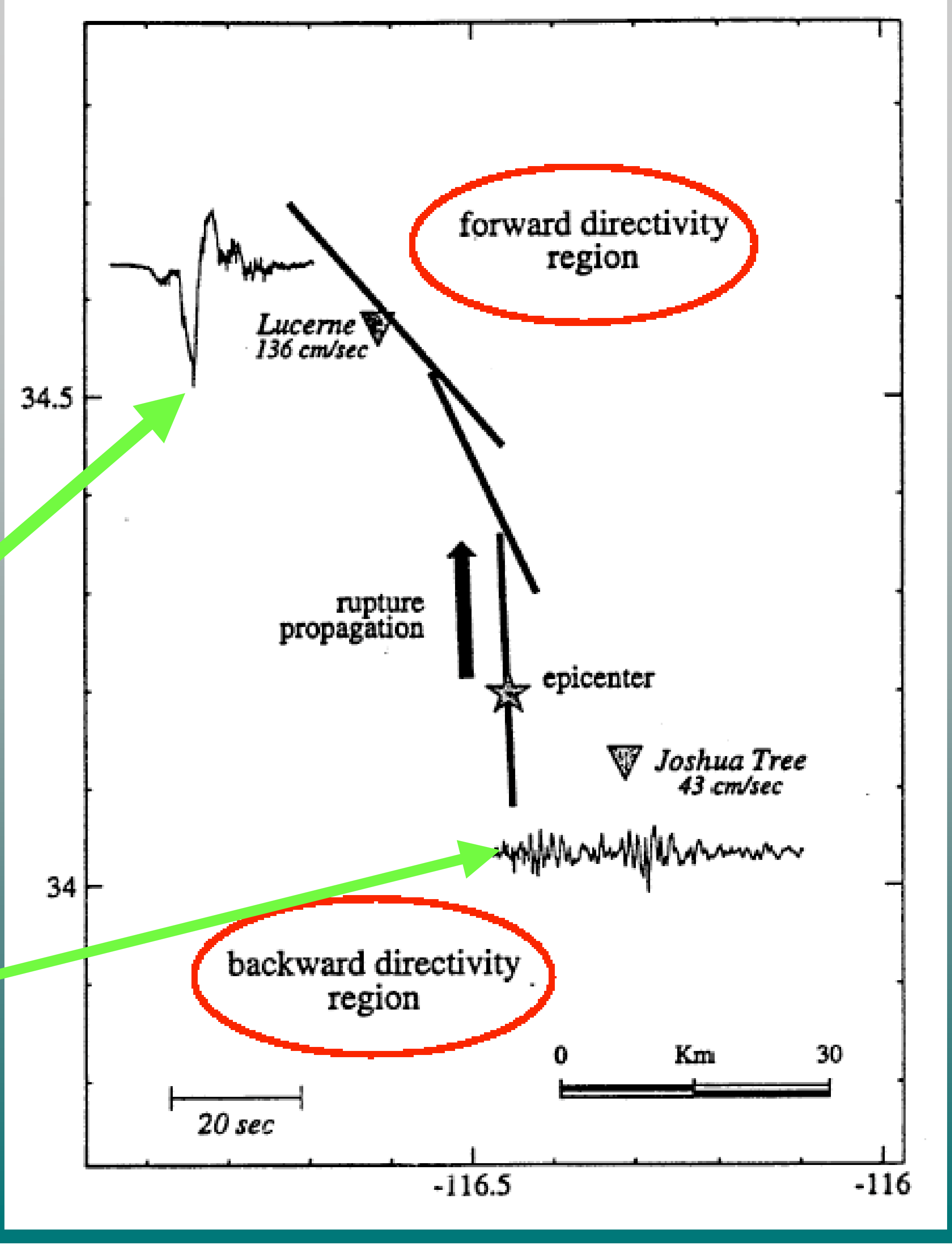

1979

Imperial Valley (Ca) quake: Velocity time histories

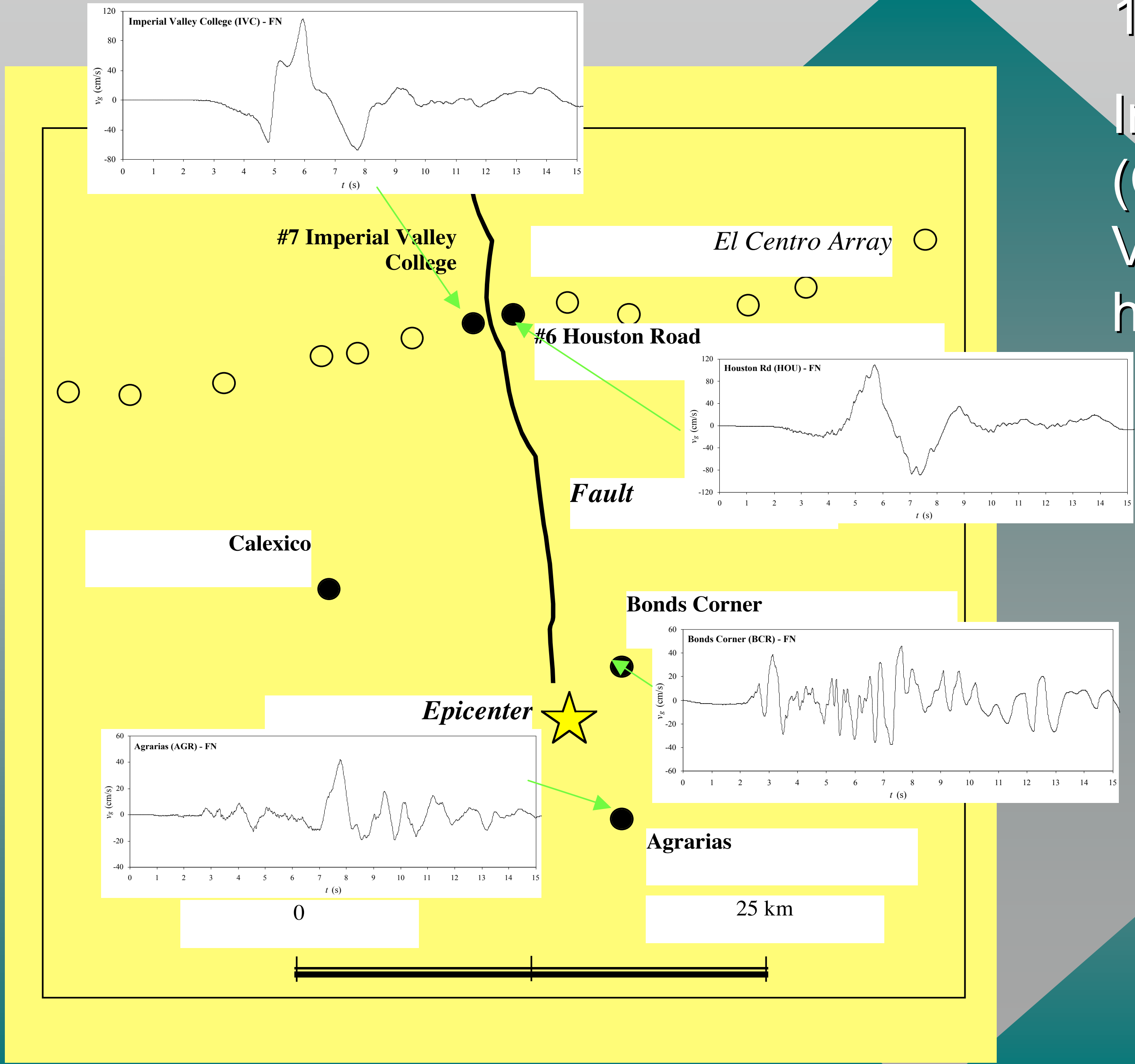

Directivity

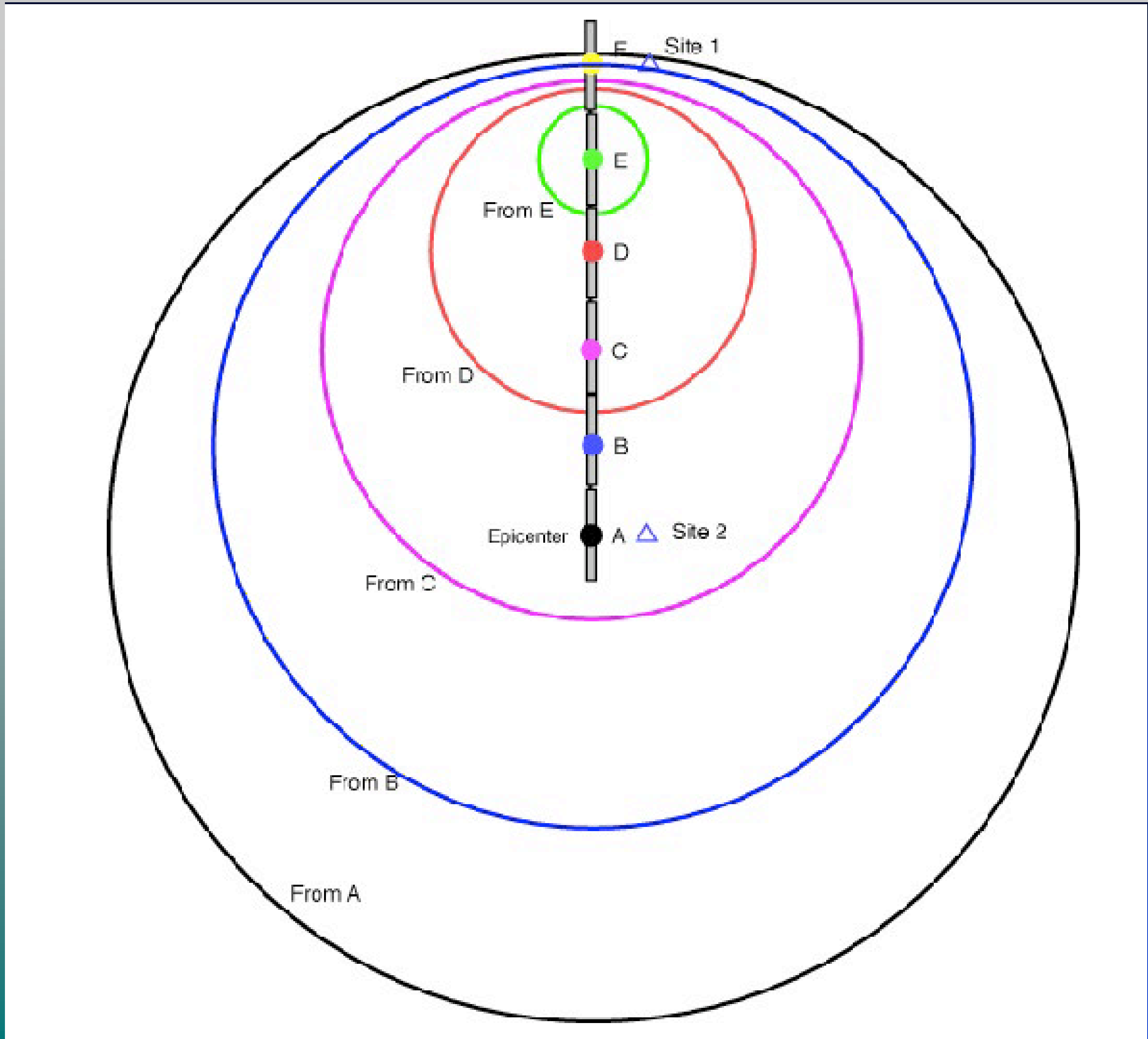

Fling

Top: schematic orientation of the rupture directivity pulse and fault displacement (fling step) for strike-slip fault (left) and dip-slip (right) faulting.

Bottom: schematic partition of the rupture directivity pulse and fault displacement between the strike normal and strike parallel components of ground displacement.

Waveforms containing static ground displacement are shown as dashed lines; versions of these waveforms with the static displacement removed are shown as dotted lines (Sommerville, 2002).

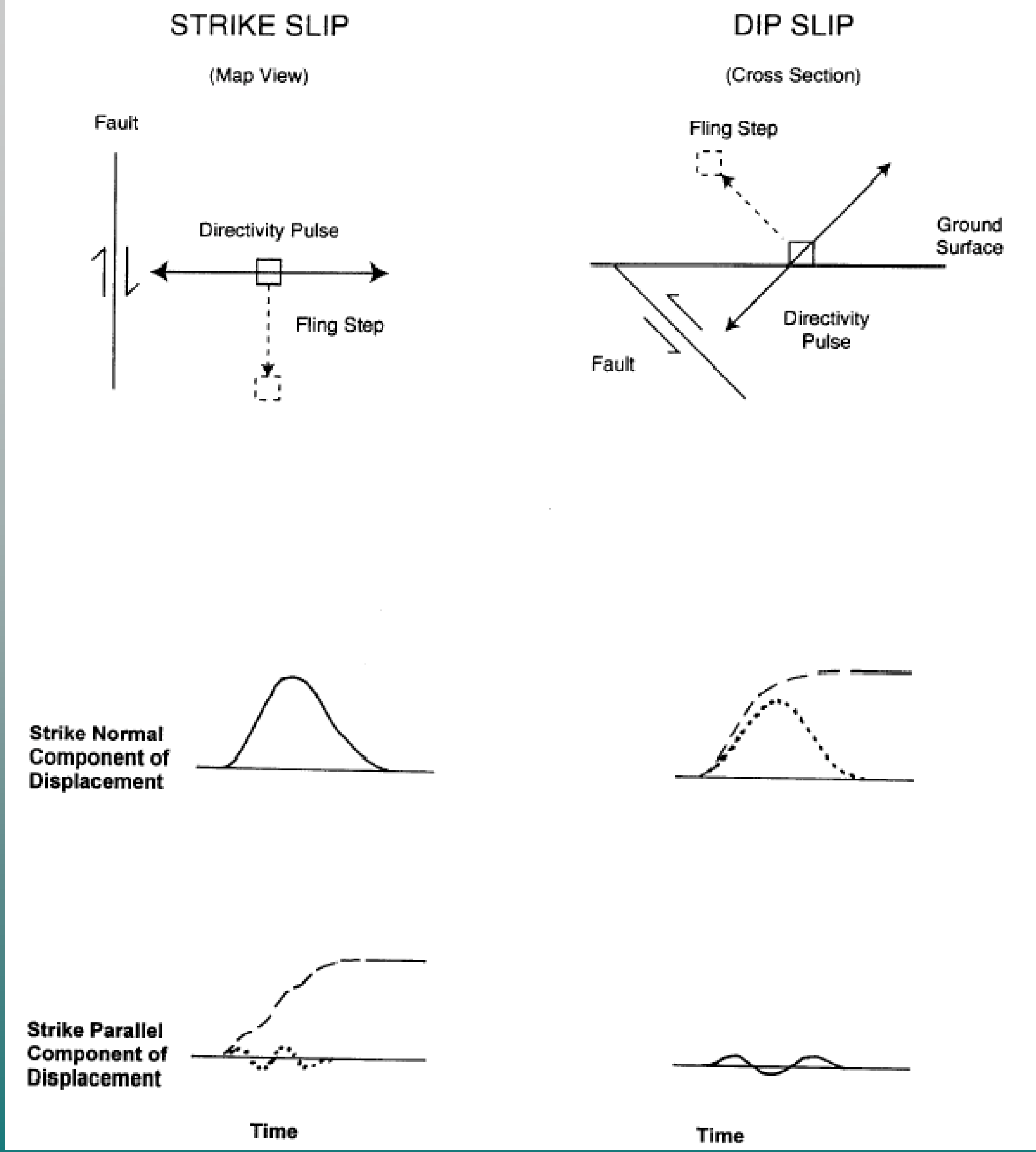

Fault normal velocity pulses recorded near 3 moderate magnitude earthquakes (left column) and 3 large magnitude earthquakes (right column), shown on the same scale (Sommerville, 2002).

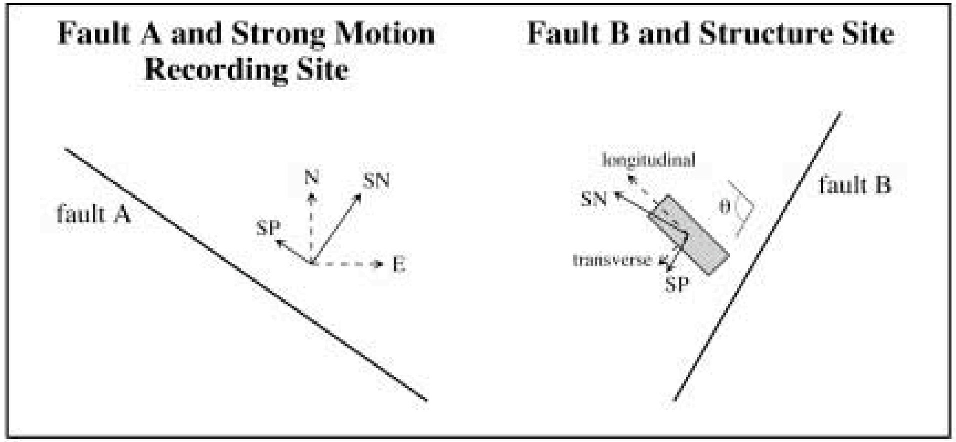

Figure 3. Archiving (left) and application (right) of strike-normal and strike-parallel components of ground motion.

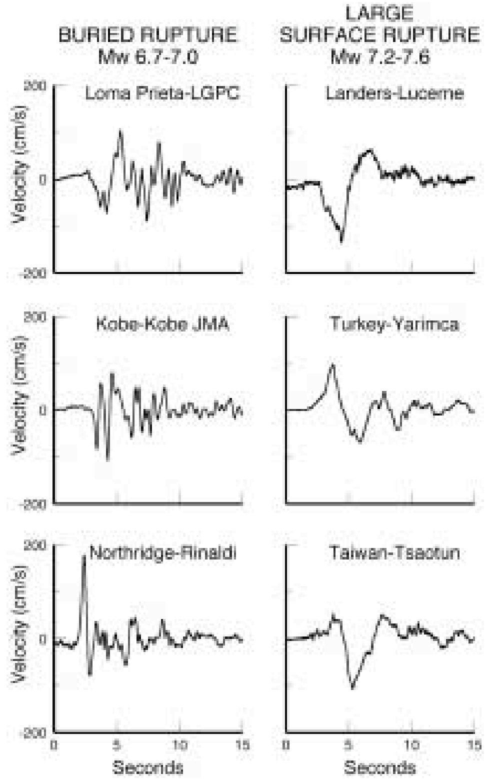

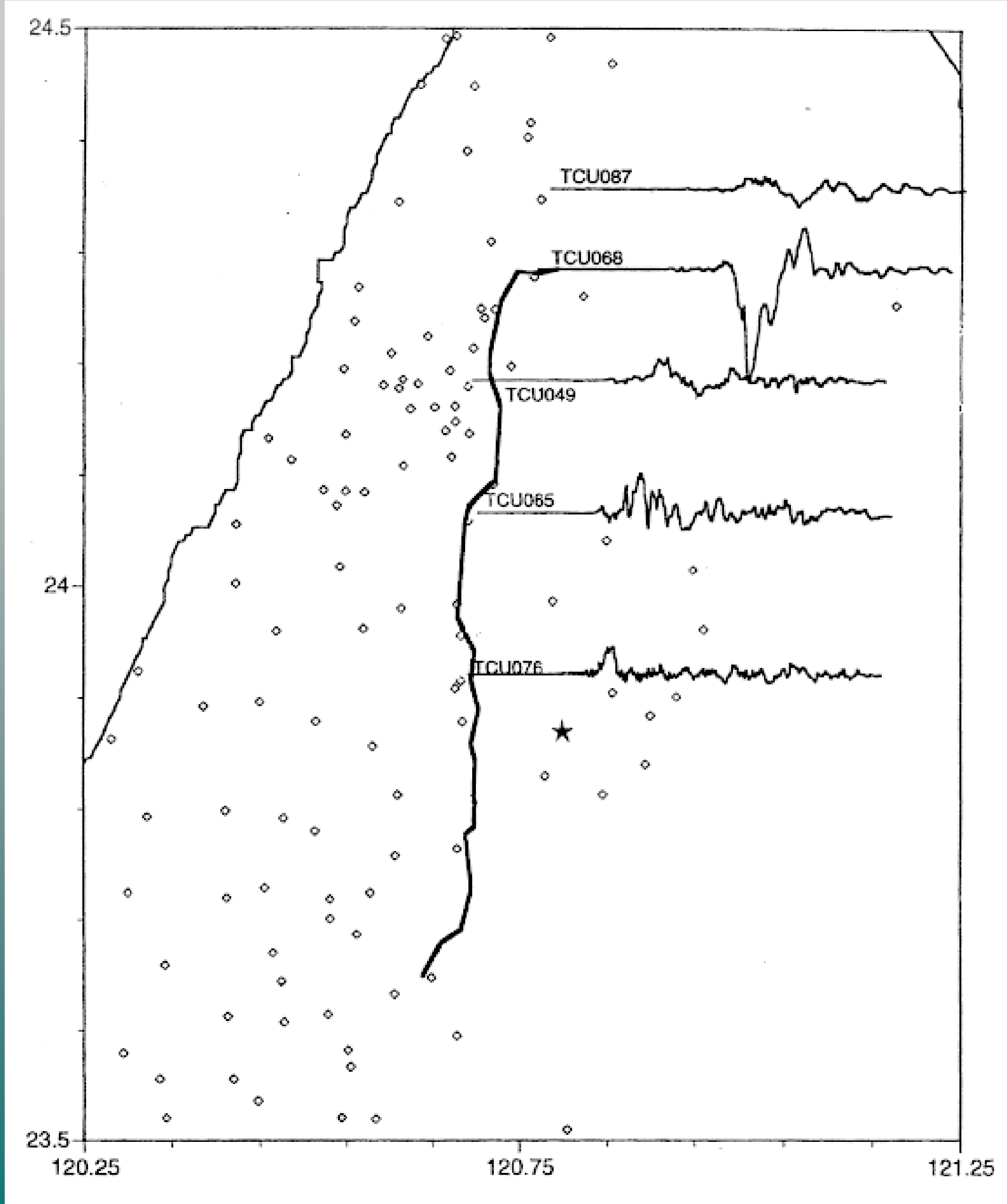

Chi Chi 1999 event (thrust fault)

Accelerations at different sites showing fling effect

3 epicenter

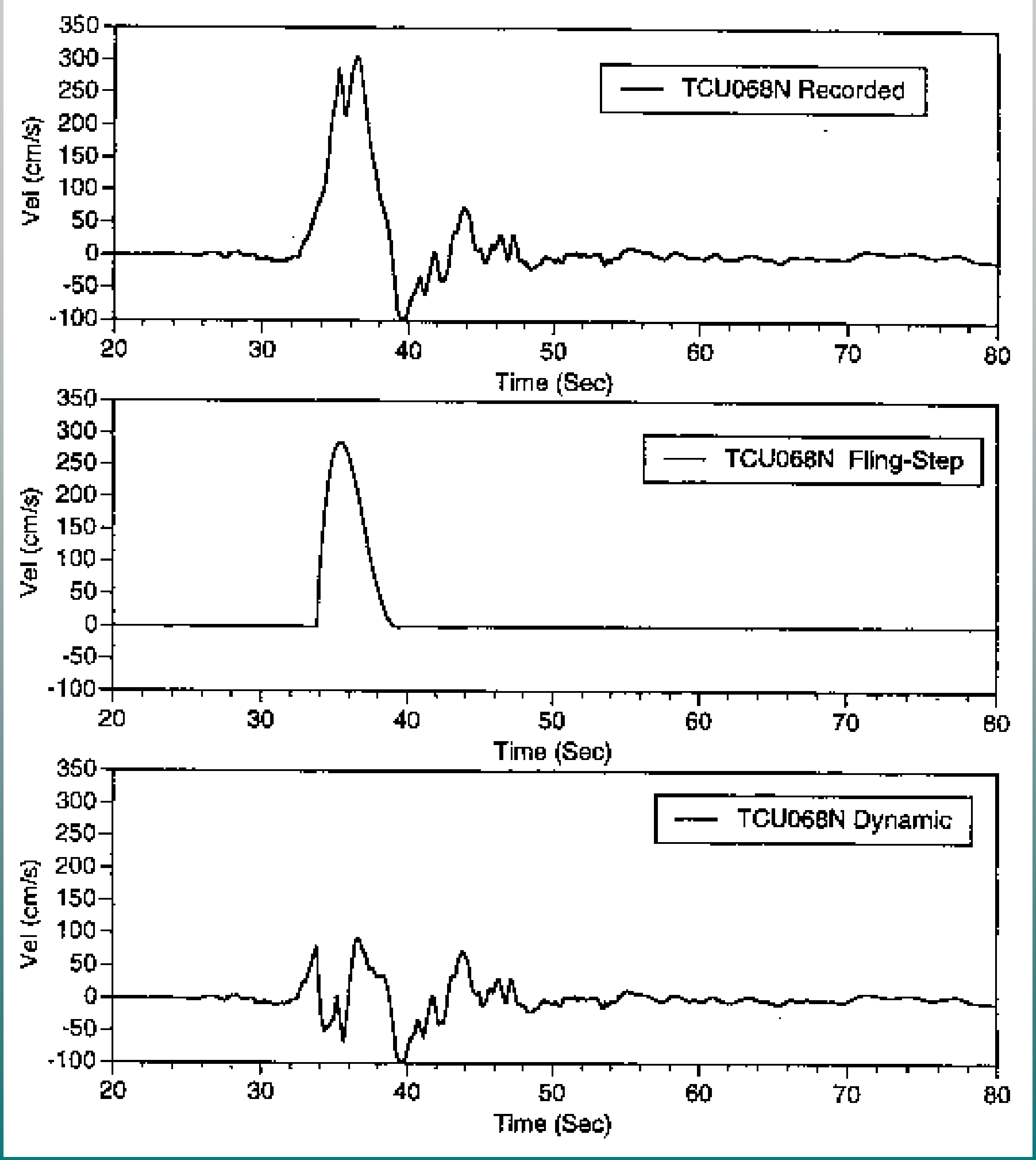
TCU068N Recorded
Vel (cm/s)
Time (Sec)
TCU068N Fling-Step
Vel (cm/s)
Time (Sec)
TCU068N Dynamic
Vel (cm/s)
Time (Sec)

UNESCO-IUGS-IGCP

Project

- In the framework of the UNESCO-IUGS-IGCP project “Realistic Modelling of Seismic Input for Megacities and Large Urban Areas” , centred at the **Abdus Salam International Center for Theoretical Physics**, a deterministic approach has been developed and applied to several urban areas for the purpose of seismic microzoning.

The full text of the summary of the main results obtained can be downloaded at:

- http://www.ictp.trieste.it/

www_users/sand/unesco-414.html

- Pilot studies show that, distances from the causative fault being equal, for events with magnitude in the range 6.5-7.1 and epicentral distances in the range 10-30 km, **the elastic spectra computed from synthetic signals are comparable with those computed from real records**.

Elastic E_I (cm^2/s^2) spectra. Comparison between Augusta synthetic signals and strong motion records of Irpinia 1980 (Calitri station) and Loma Prieta 1989 (Gav. Tower, Ucsc and Ysidro stations) earthquakes.

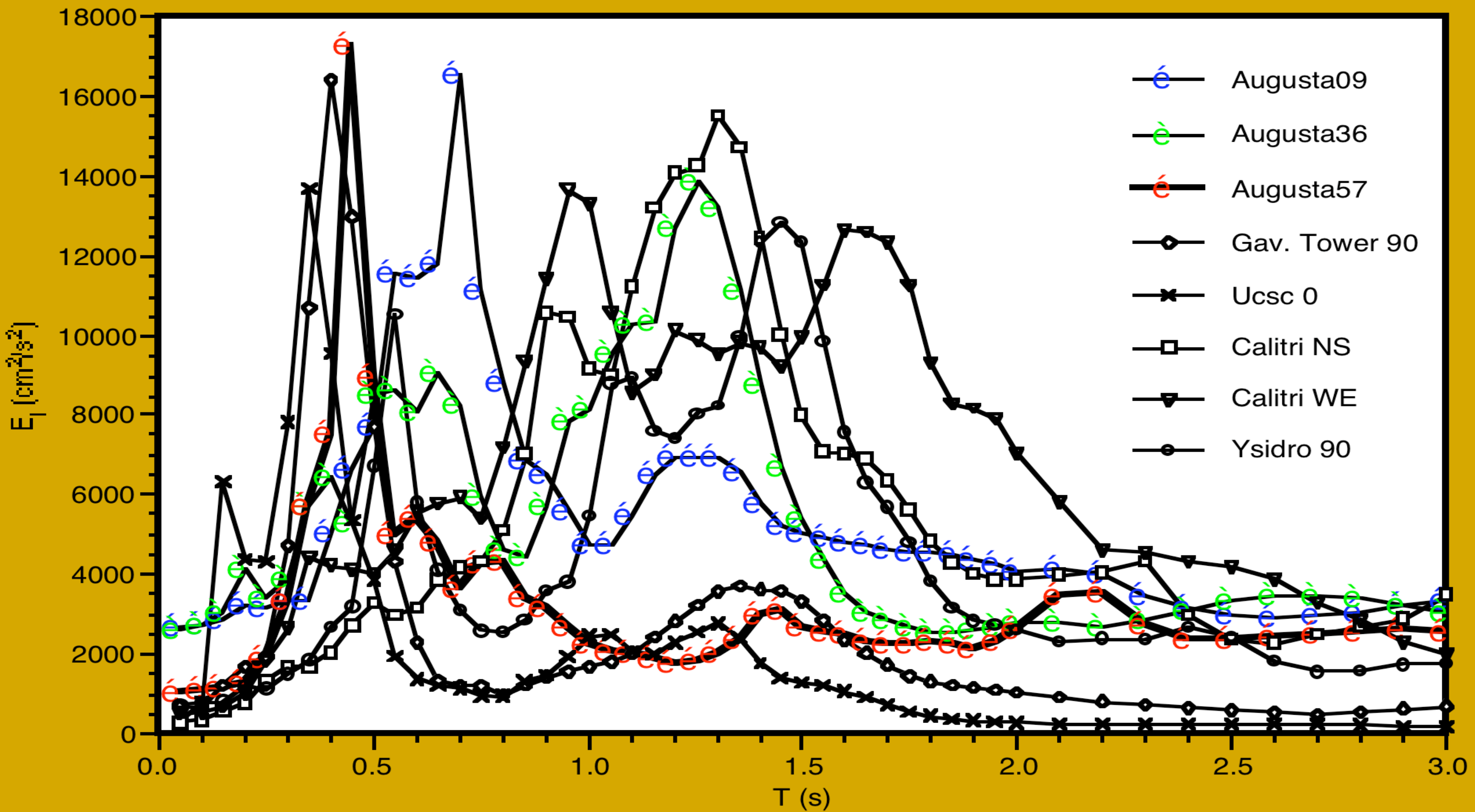

- The envelope of the synthetic elastic energy spectra can reproduce a wide distribution of energy in the most relevant frequency range from the engineering point of view.

- The data set of synthetic seismograms can be fruitfully used and analysed by civil engineers for design and reinforcement actions.

- The data set of synthetic seismograms supply a particularly powerful and economical tool for the prevention and preparedness aspects of Civil Defence.

UNESCO-IUGS-IGCP Project

Seismic microzoning of **Beijing**

The Profiles for Tangshan Earthquake

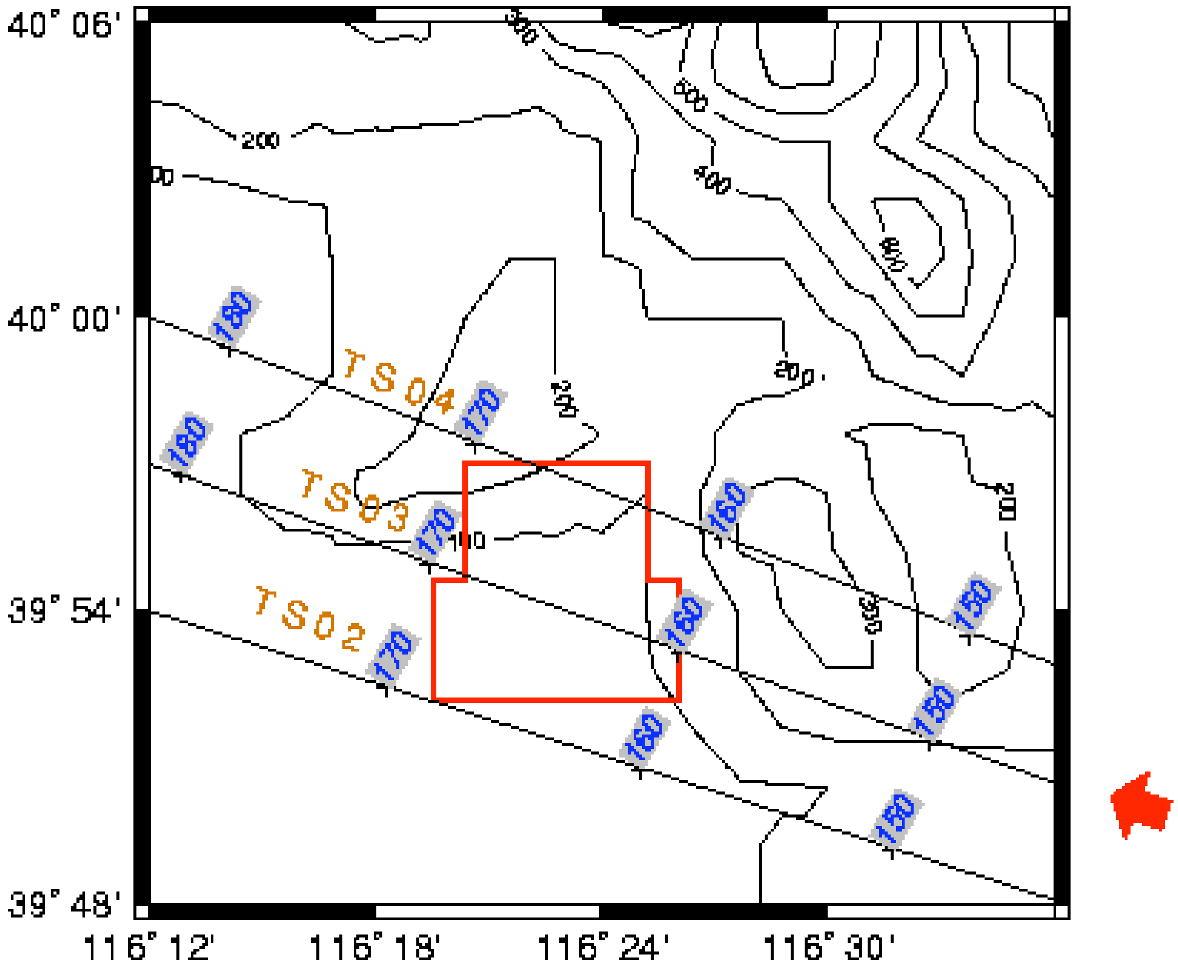

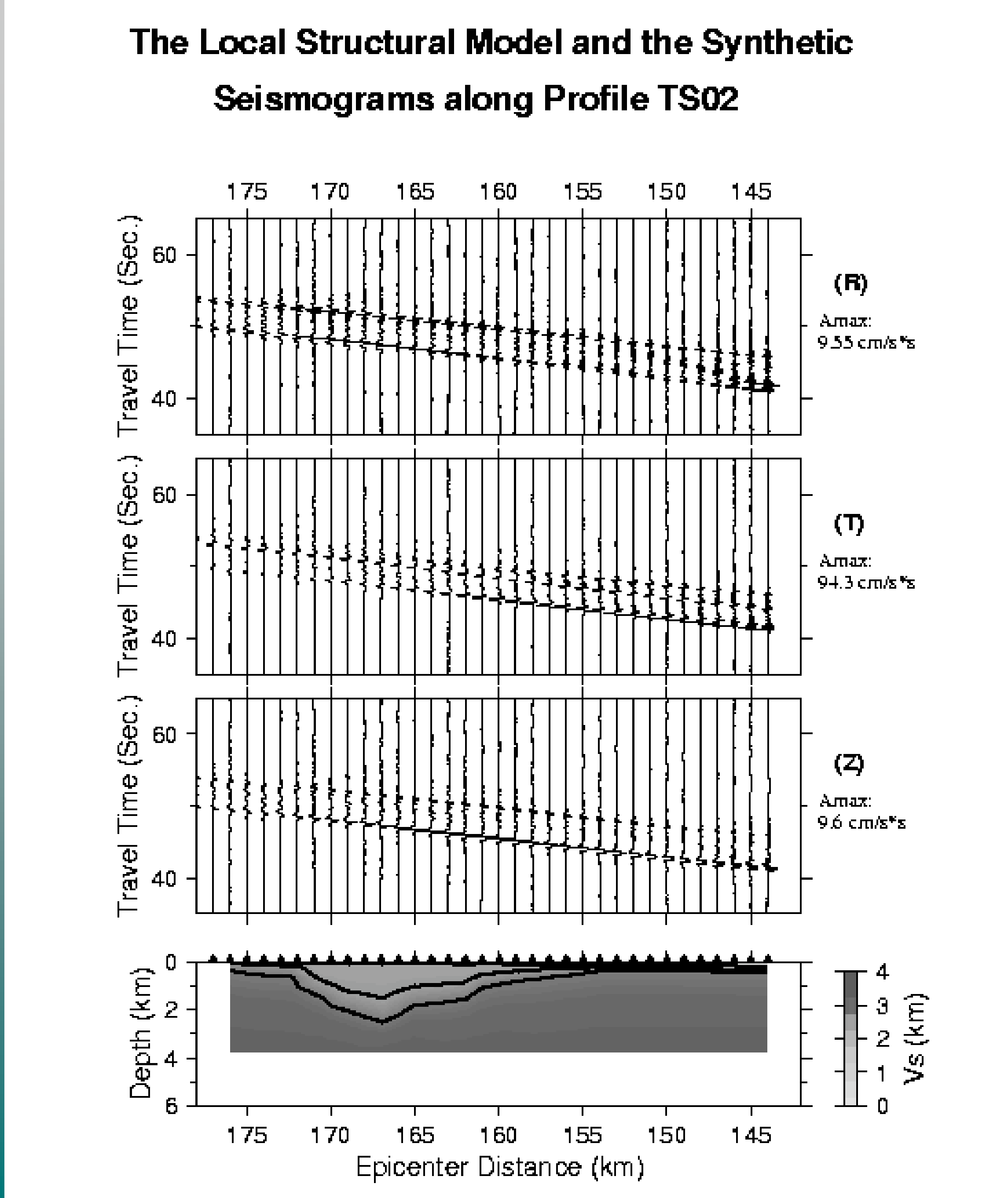

The local structural model and the synthetic seismograms along the profile TS02.

The lines in the bottom figure outline the three sediment layers.

Radial, transverse and vertical components of the synthetic ground acceleration

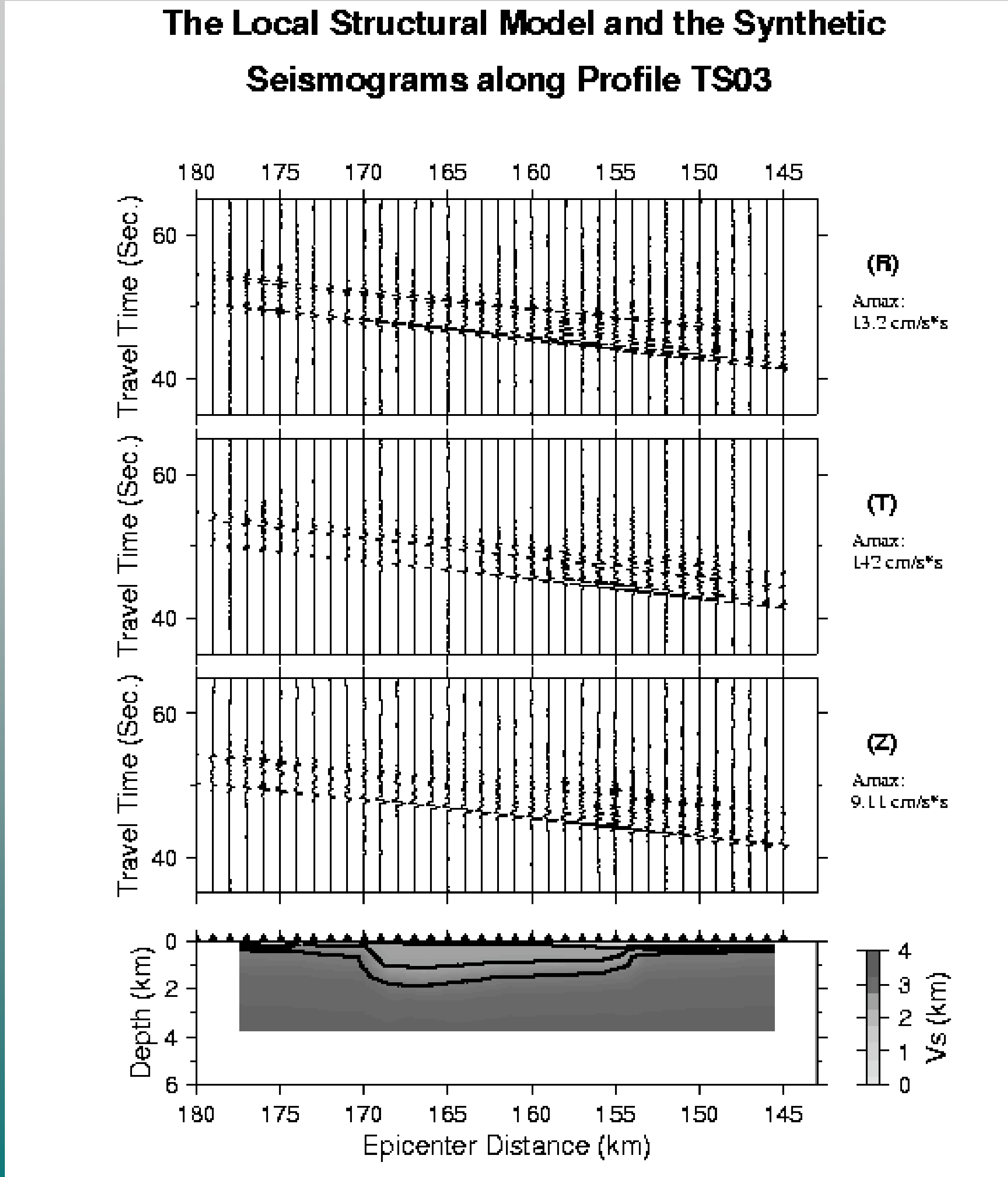

The local structural model and the synthetic seismograms along the profile TS03.

The lines in the bottom figure outline the three sediment layers.

Radial, transverse and vertical components of the synthetic ground acceleration.

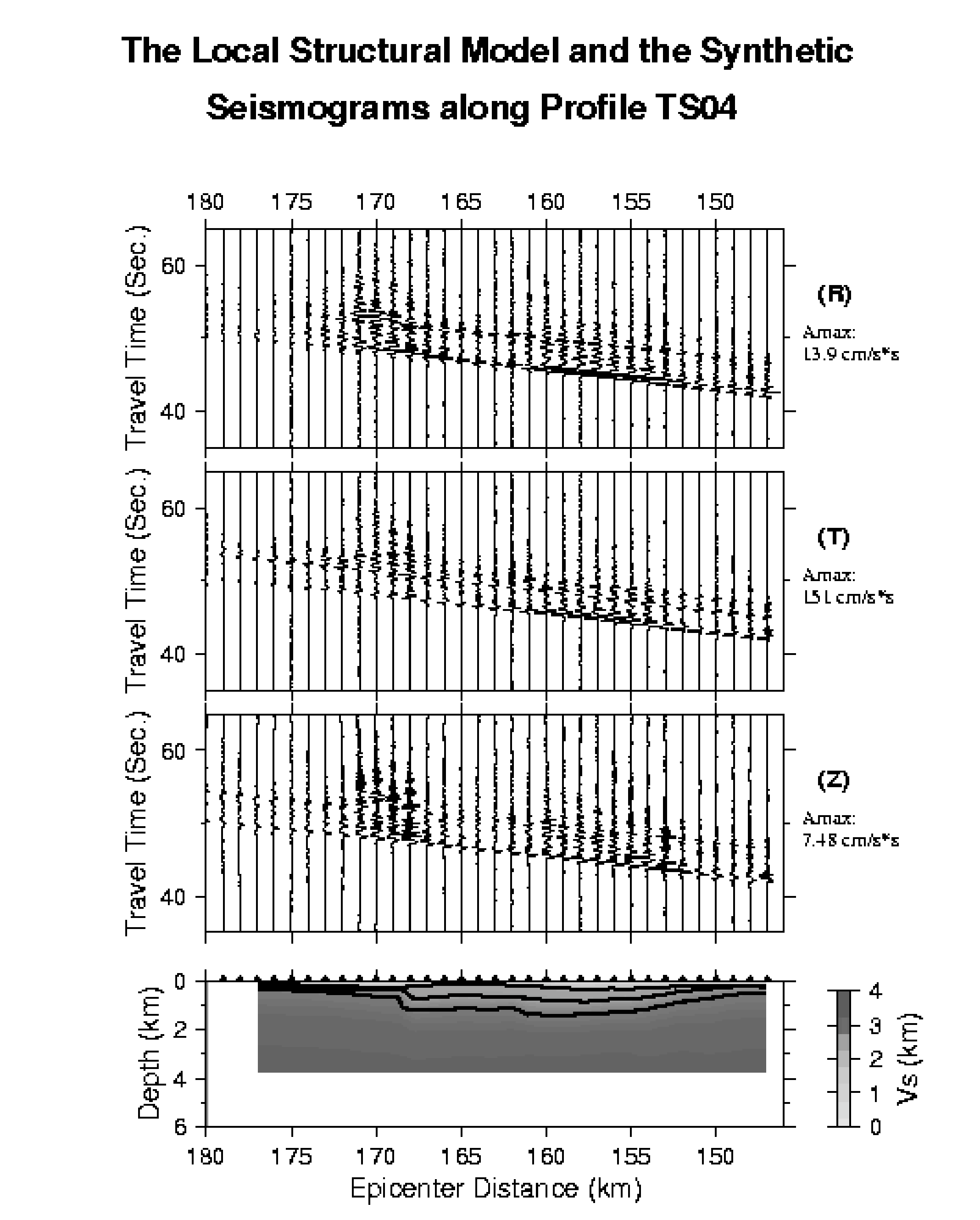

The local structural model and the synthetic seismograms along the profile TS04.

The lines in the bottom figure outline the three sediment layers. Radial, transverse and vertical components of the synthetic ground acceleration.

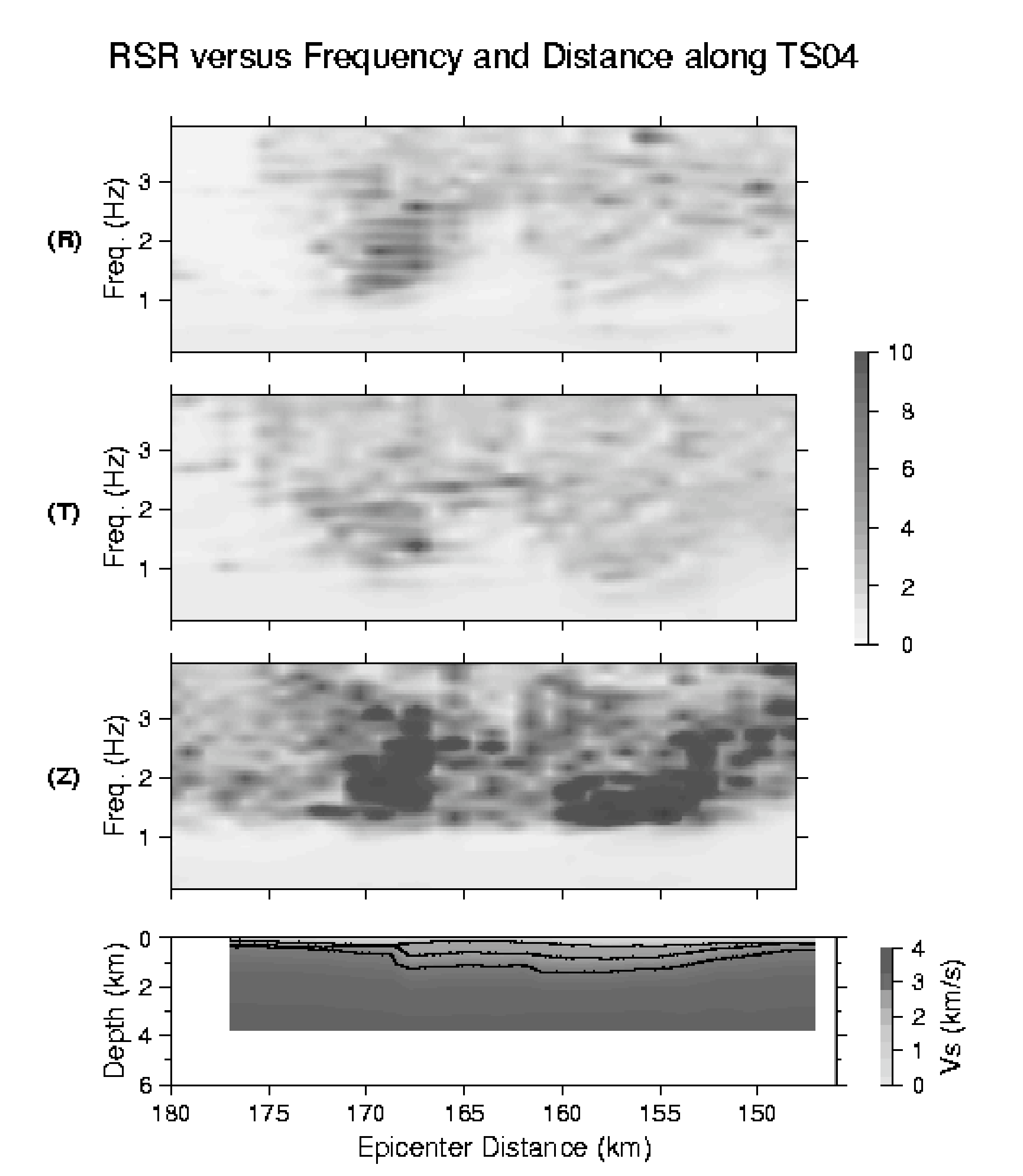

RSR versus frequency and distance along Profile TS04

RSR of SH-waves at Selected Sites along Profile TS04

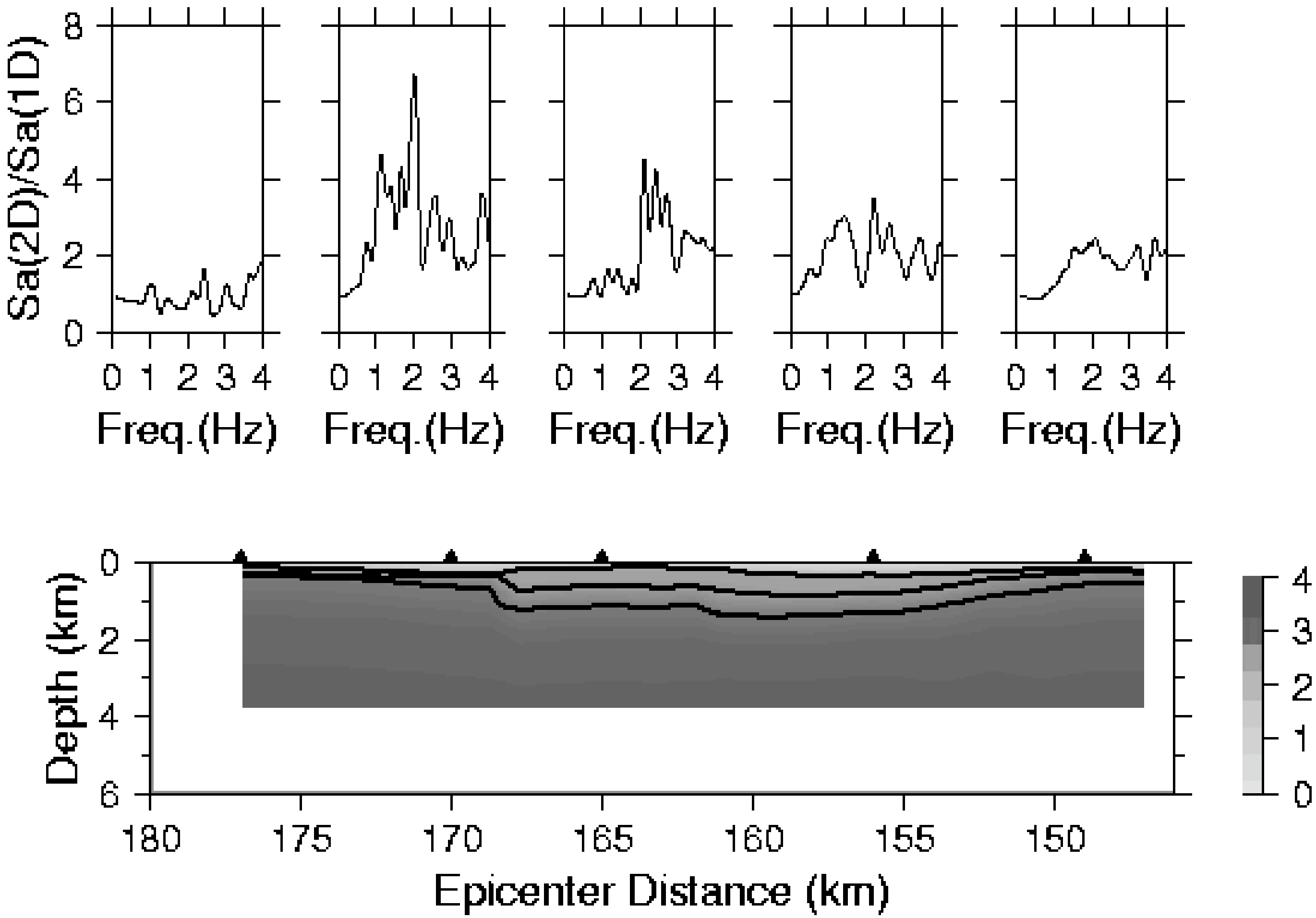

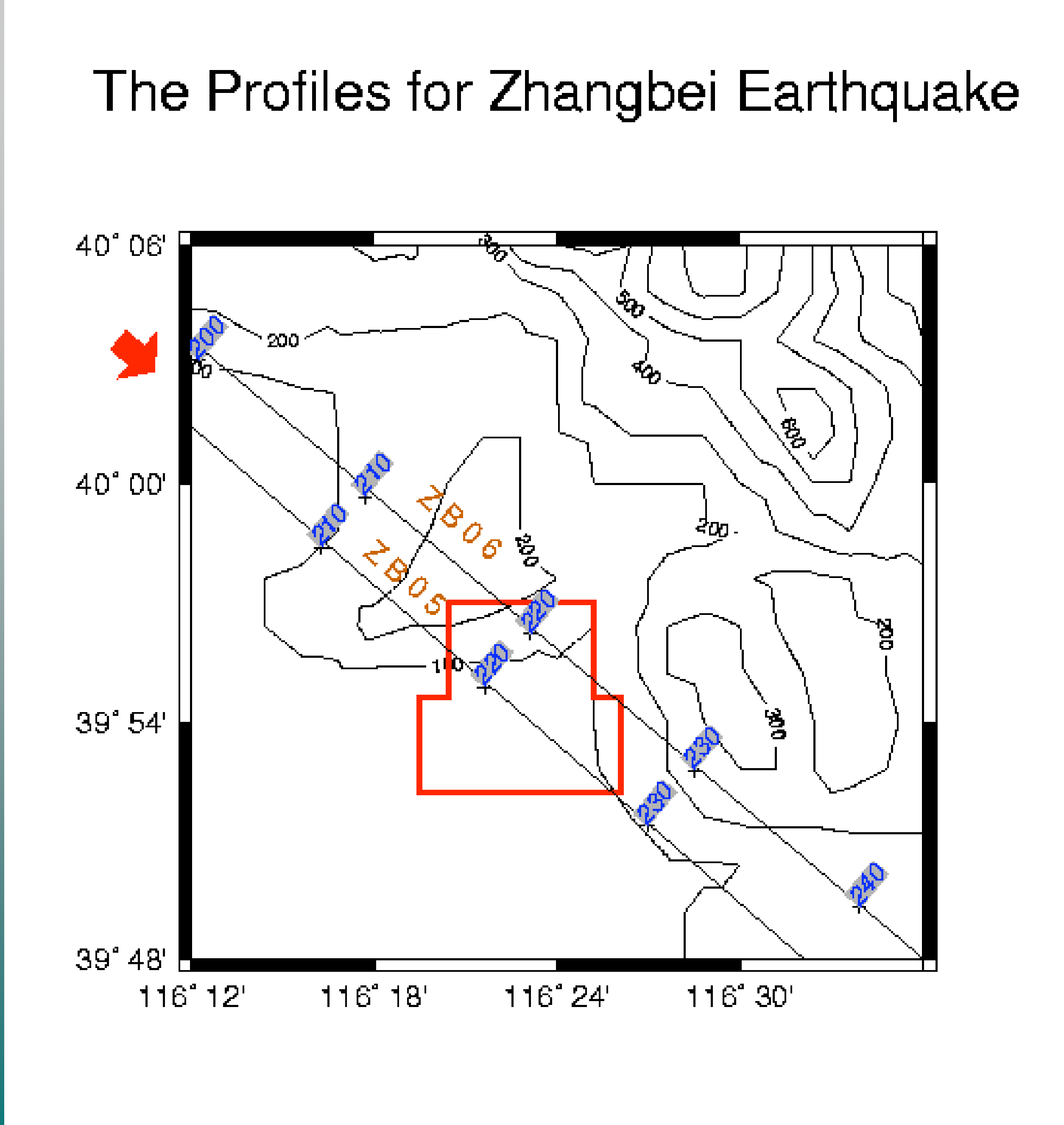

Profiles for Zhangbei Earthquake.
The background contours represent the Quaternary sediment depth in meters.
The polygon represents the town of Beijing.
Two profiles, ZB05 and ZB06 are shown in the figure.
The profiles point towards to the epicenter of the 1998 Zhangbei earthquake, which is located in the northwest.
The numbers along the profiles are the distances from the epicenter, in km.

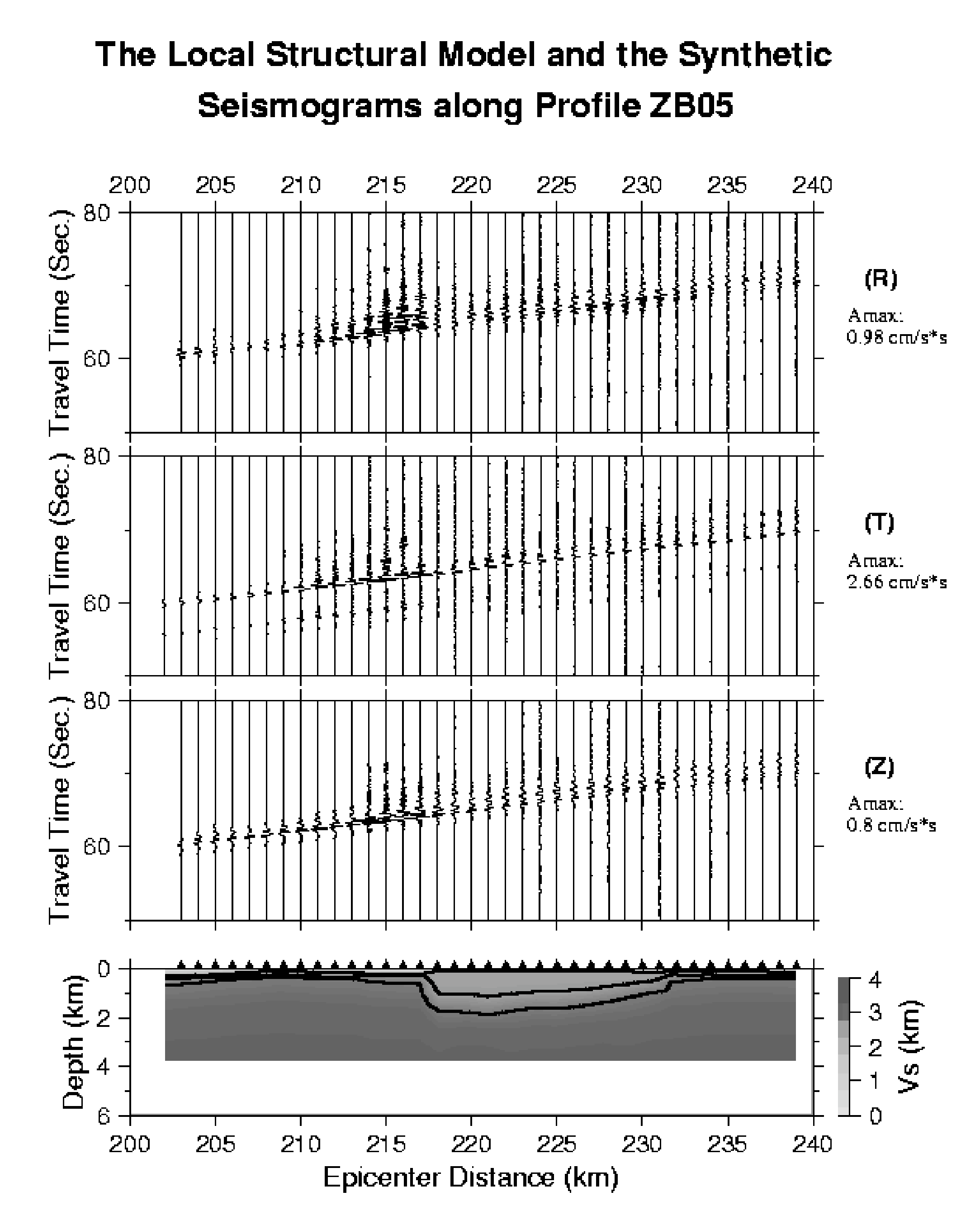

The local structural model and the synthetic seismograms along the profile ZB05.

The lines in the bottom figure outline the three sediment layers.

Radial, transverse and vertical components of the synthetic ground acceleration.

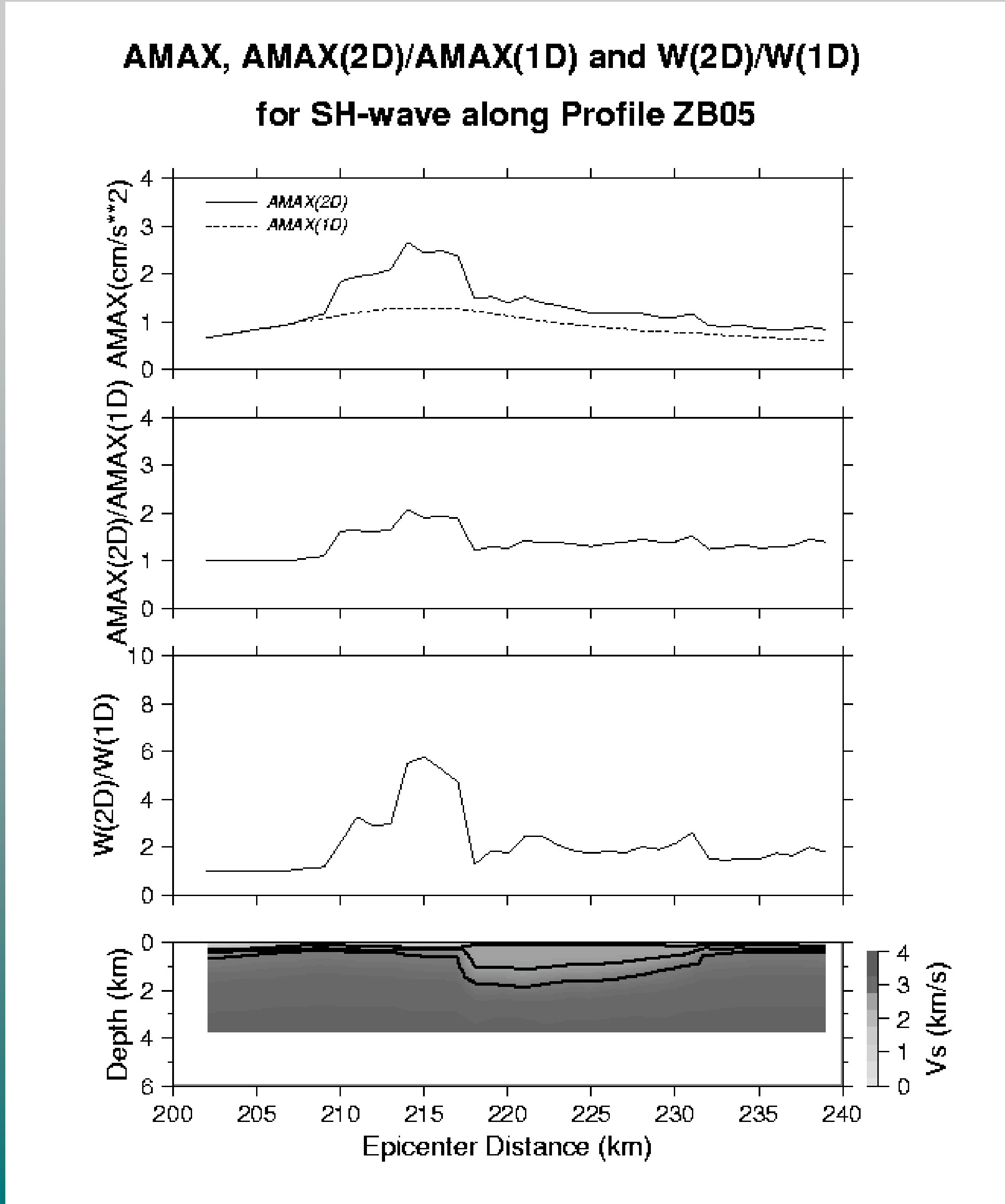
AMAX, AMAX(2D)/AMAX(1D) and W(2D)/W(1D)
for SH-wave along Profile ZB05
AMAX(2D)
AMAX(1D)
AMAX(cm/s**2)
AMAX(2D)/AMAX(1D)
W(2D)/W(1D)
Depth (km)
Vs (km/s)
Epicenter Distance (km)
200
205
210
215
220
225
230
235
240

RSR of SH-waves at Selected Sites along Profile ZB05

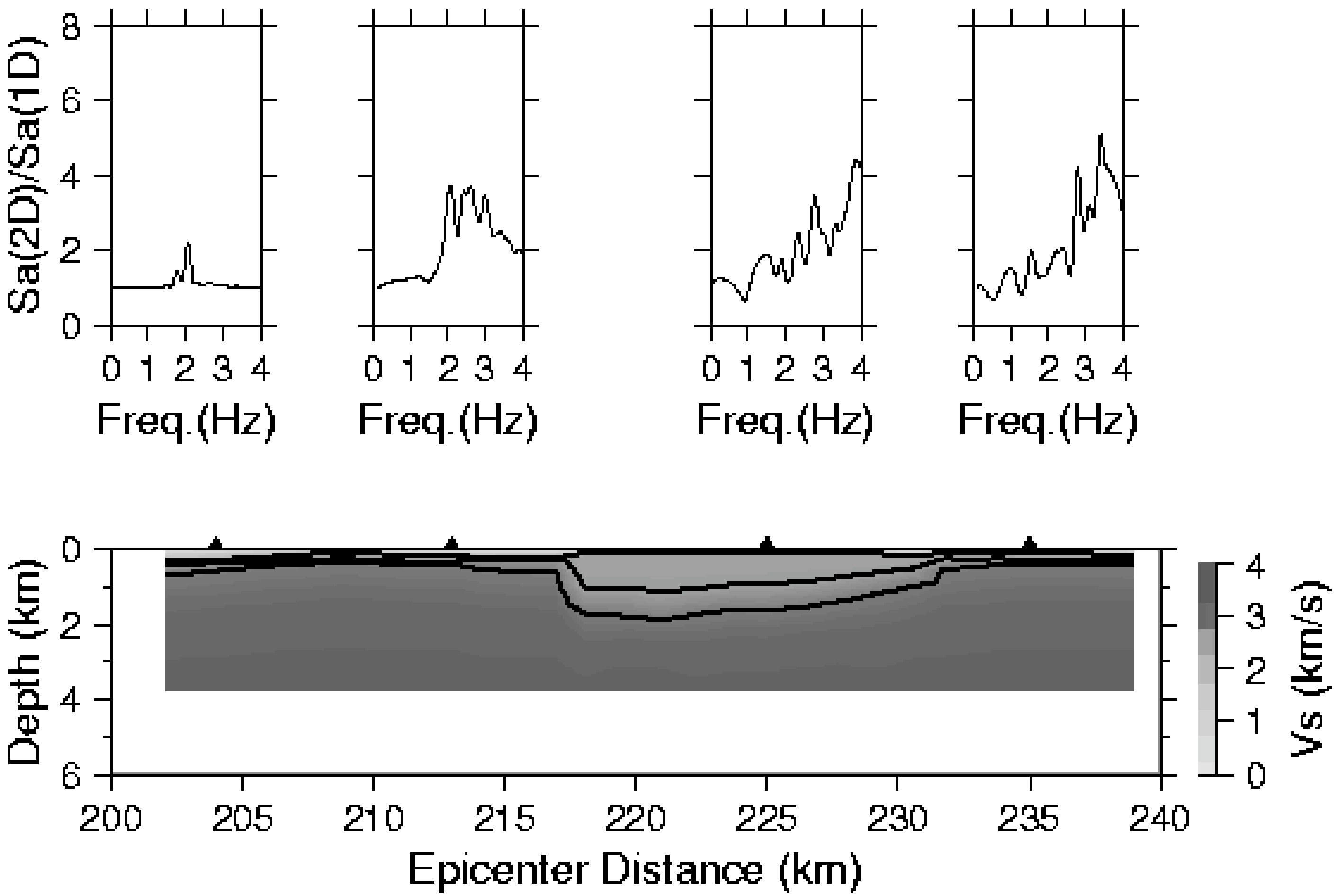

The Local Structural Model and the Synthetic Seismograms along Profile ZB06

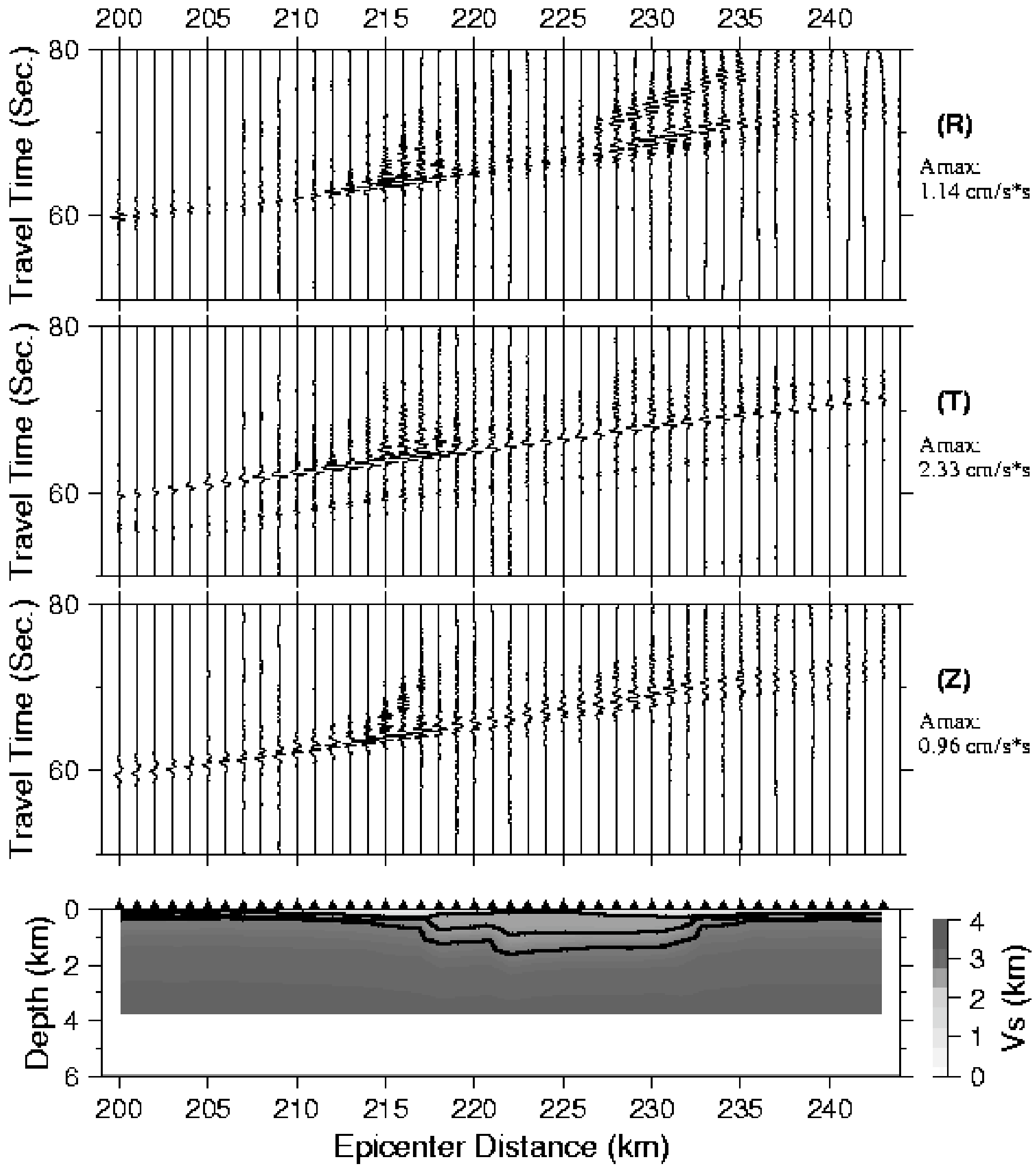

Different Site Effect Zones in Beijing City

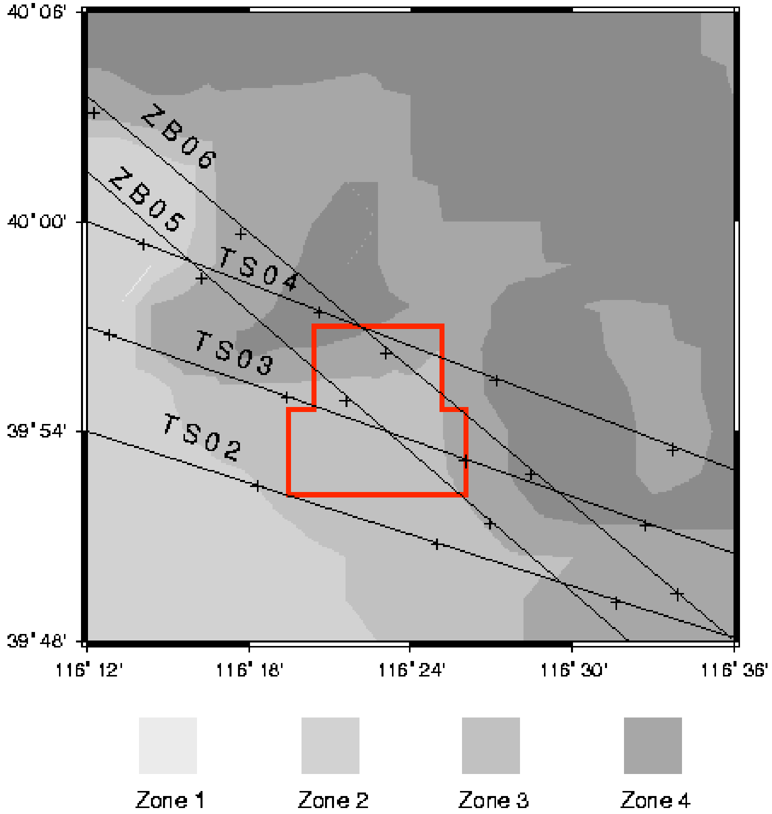

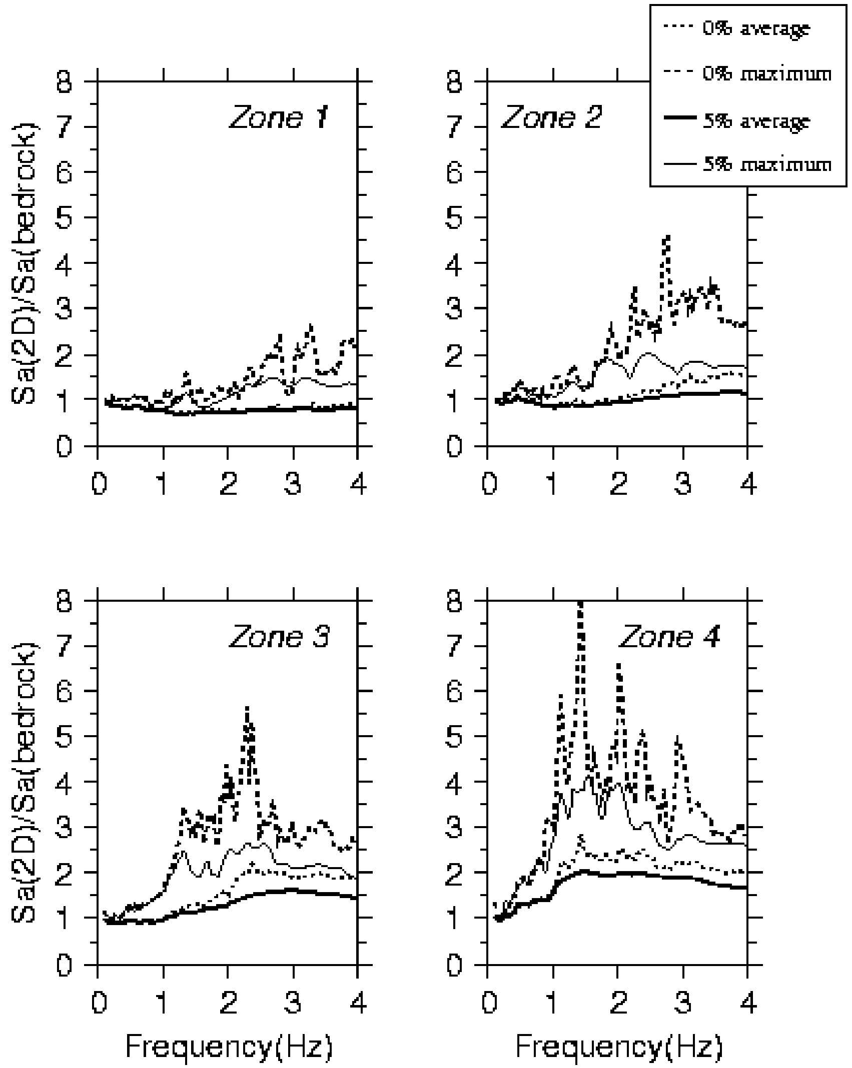

Maxmum and average RSR for 4 zones for zero damping and 5% damping.

Absolute spectral accelerations consistent with 1976 Tangshan earthquake

Different Site Effect Zones in Beijing City

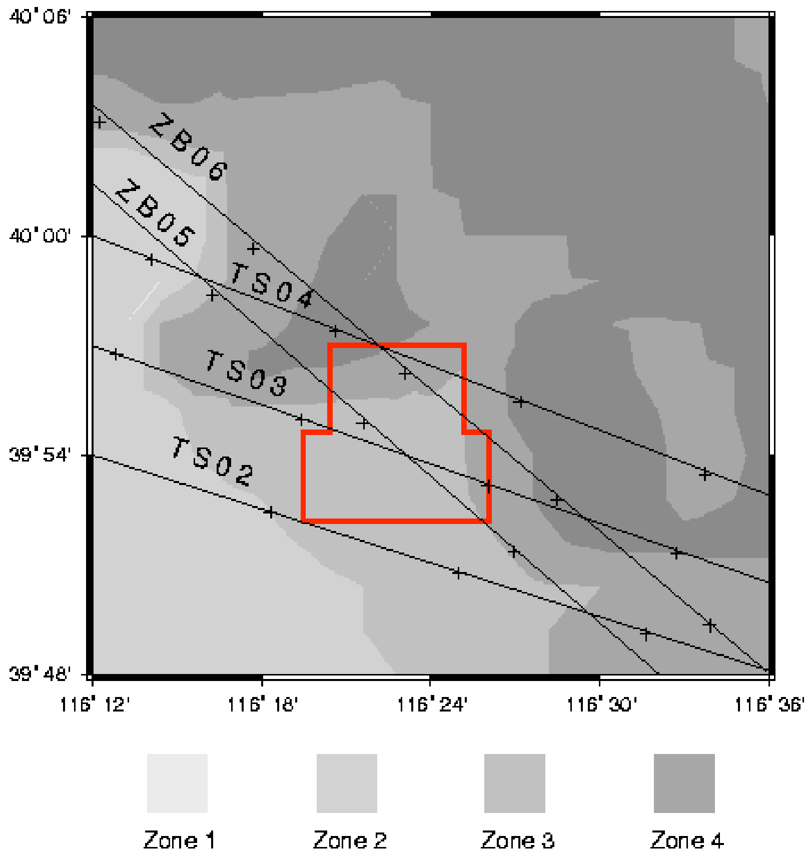

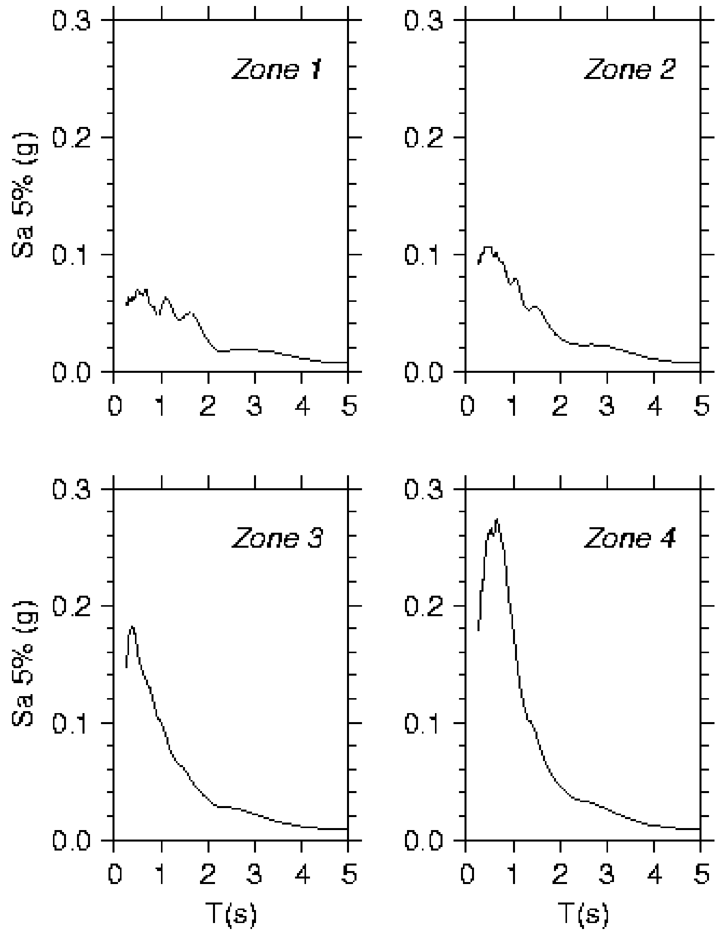

Spectral acceleration (5% damping) for the 4 zones

UNESCO-IUGS-IGCP Project

Seismic microzoning of **Rome**

Traianus (98-117) wars to conquer Dacia (101-106) are celebrated by the *Colonna Traiana*, about 30 m (excluding basement) toll, in Roma. The column is made of 17 juxtaposed blocks called *rocchi*.

Essentially equal funeral monument (*Colonna di Marco Aurelio*) was built to celebrate Marcus Aurelius (161-180) wars against Marcomanni.

Colonna Traiana sits on solid soil and is well preserved, while *Colonna di Marco Aurelio* sits on Tiber sediments and shows a dislocation of about 8 cm between two central *rocchi*.

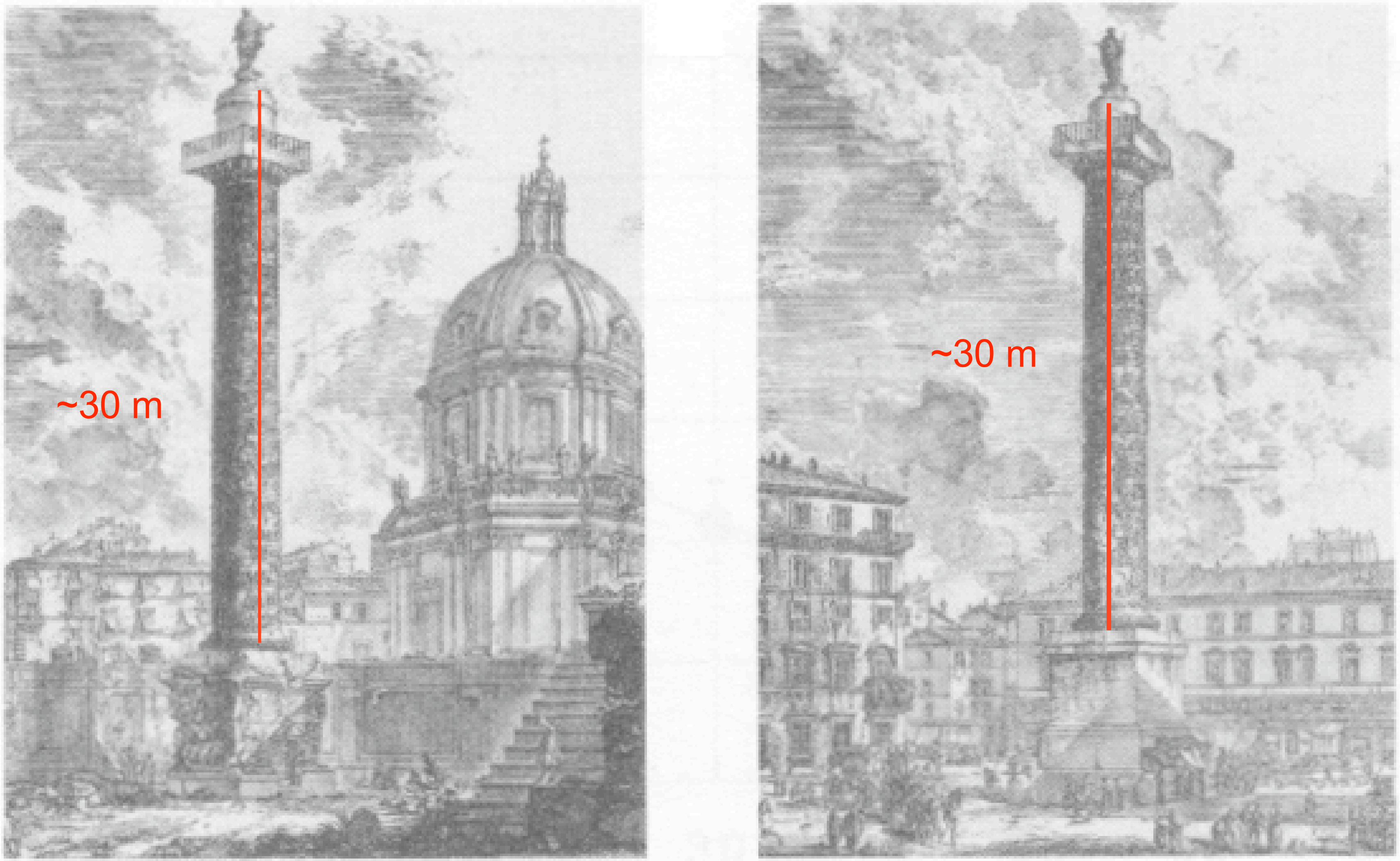

Colonna Traiana (sinistra) e *Colonna di Marco Aurelio* (destra)

30 m

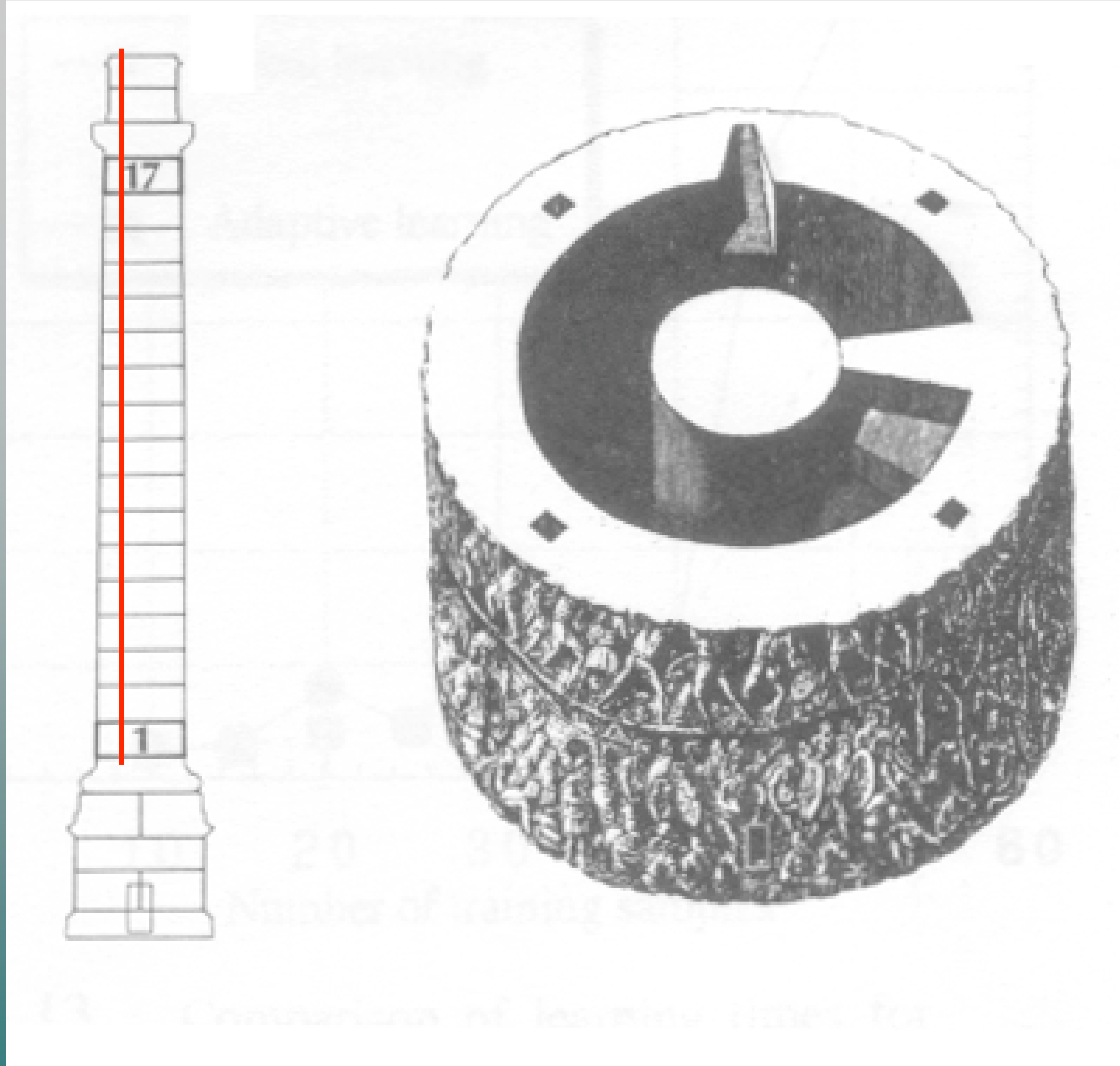

Rocco basic element of the two columns

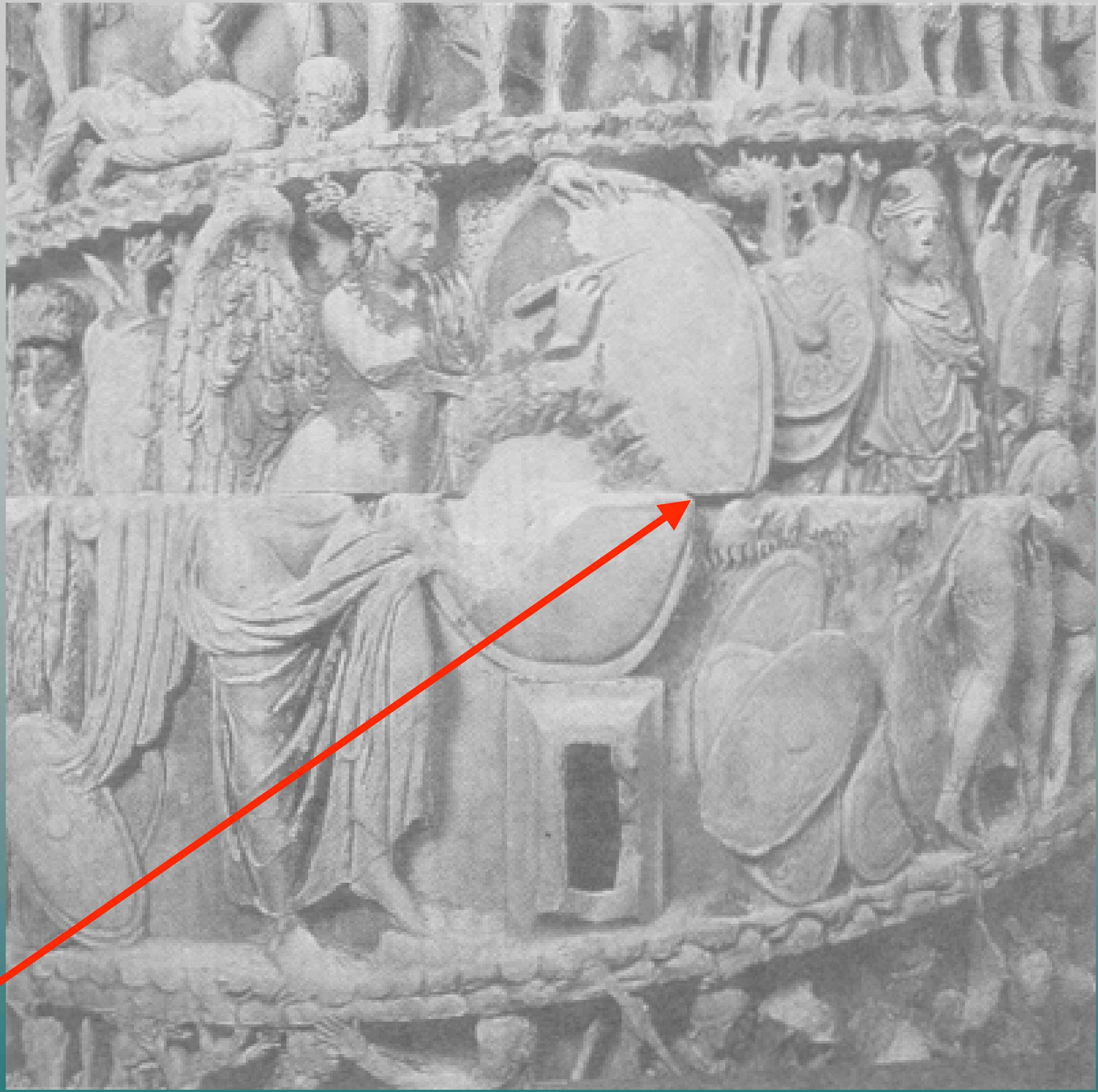

Dislocation of about 8 cm between two *rocchi* of *Colonna di Marco Aurelio*

Dislocation of about 8 cm between rocchi IX and X of *Colonna di Marco Aurelio*
(from ITALIA 2004, 32nd International Geological Congress; 1st Circular)

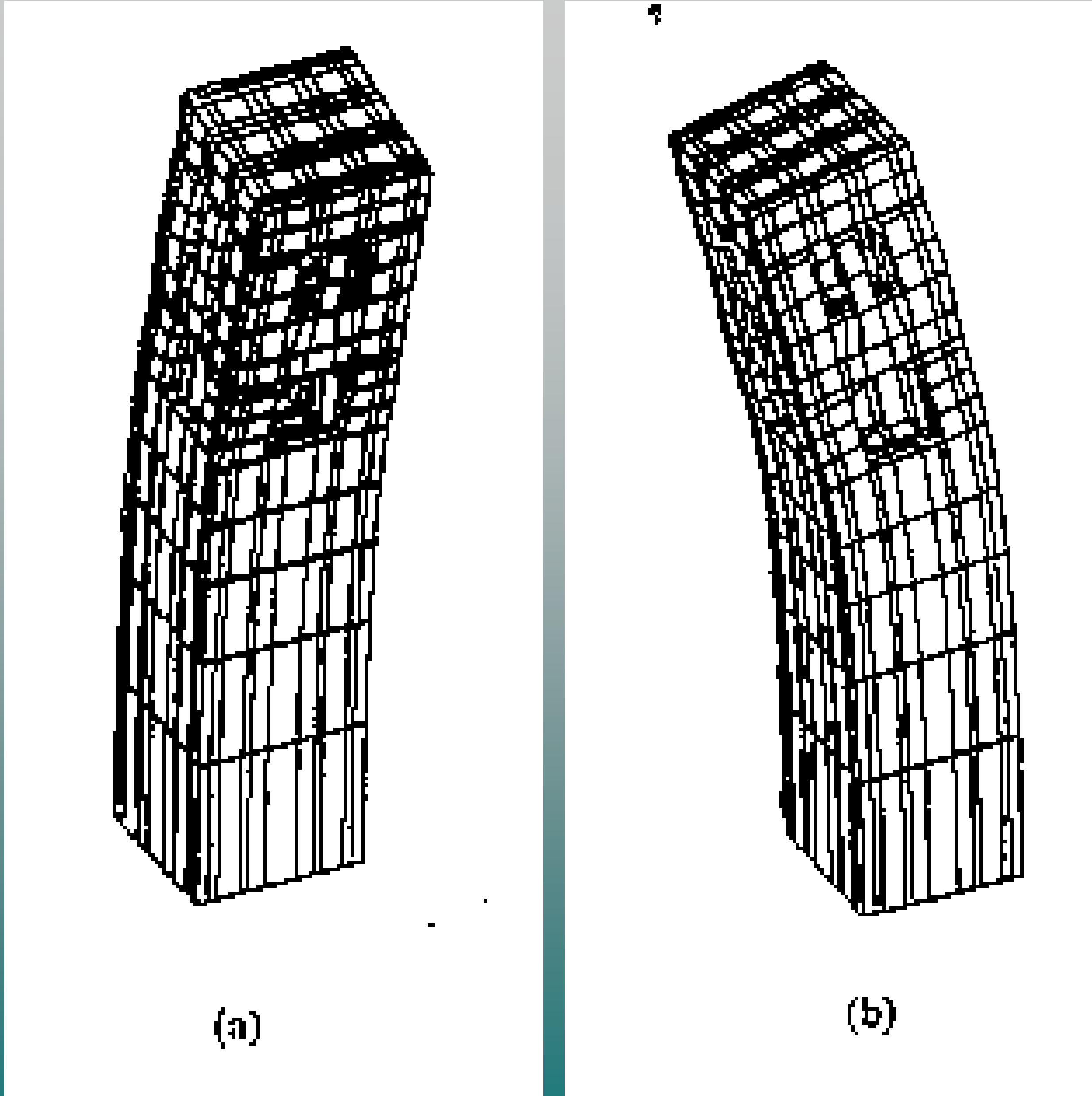

First two free modes of S. Giorgio church in Trignano

(a) 2.57Hz,
(b) 2.72 Hz

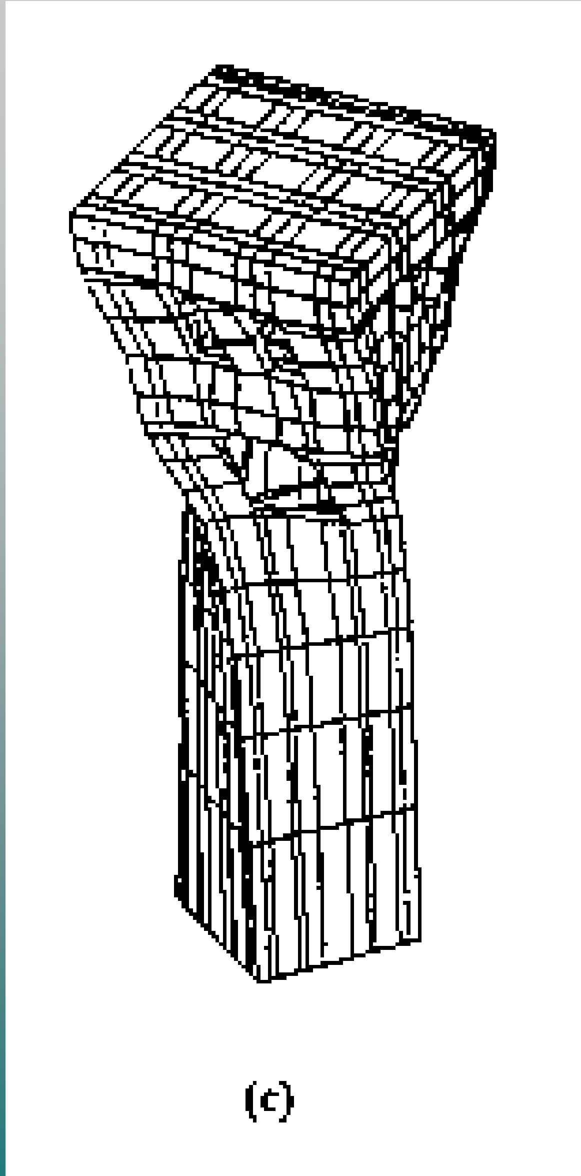

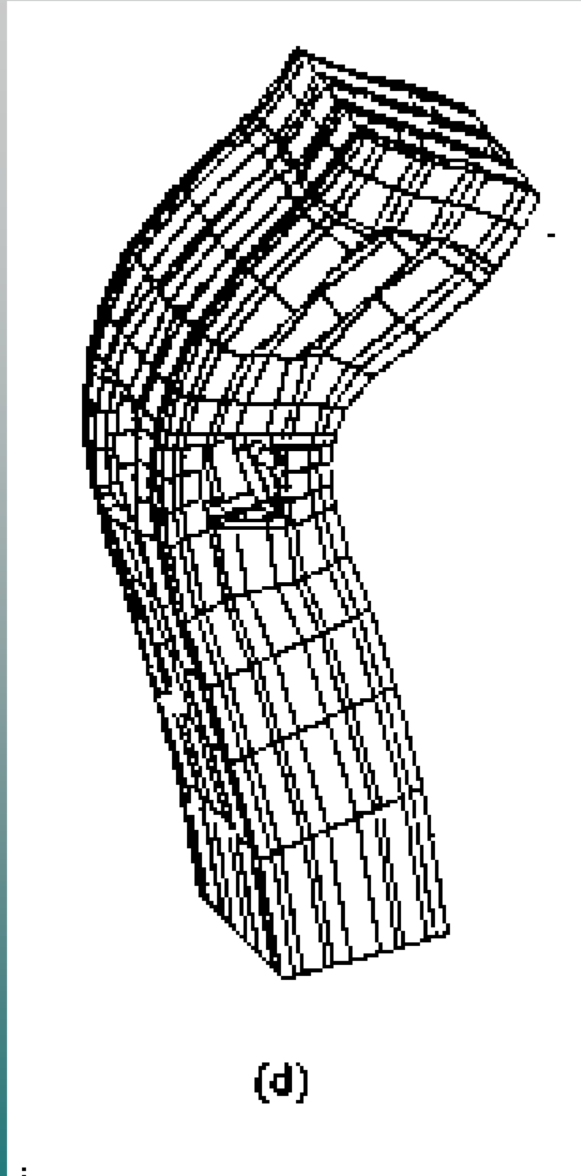

Third and fourth free modes of

S. Giorgio church in Trignano

(c) 6.26Hz,

(d) 9.22 Hz

Microzonazione della citta’ di Roma consistente con la storia sismica e la sismotettonica della regione

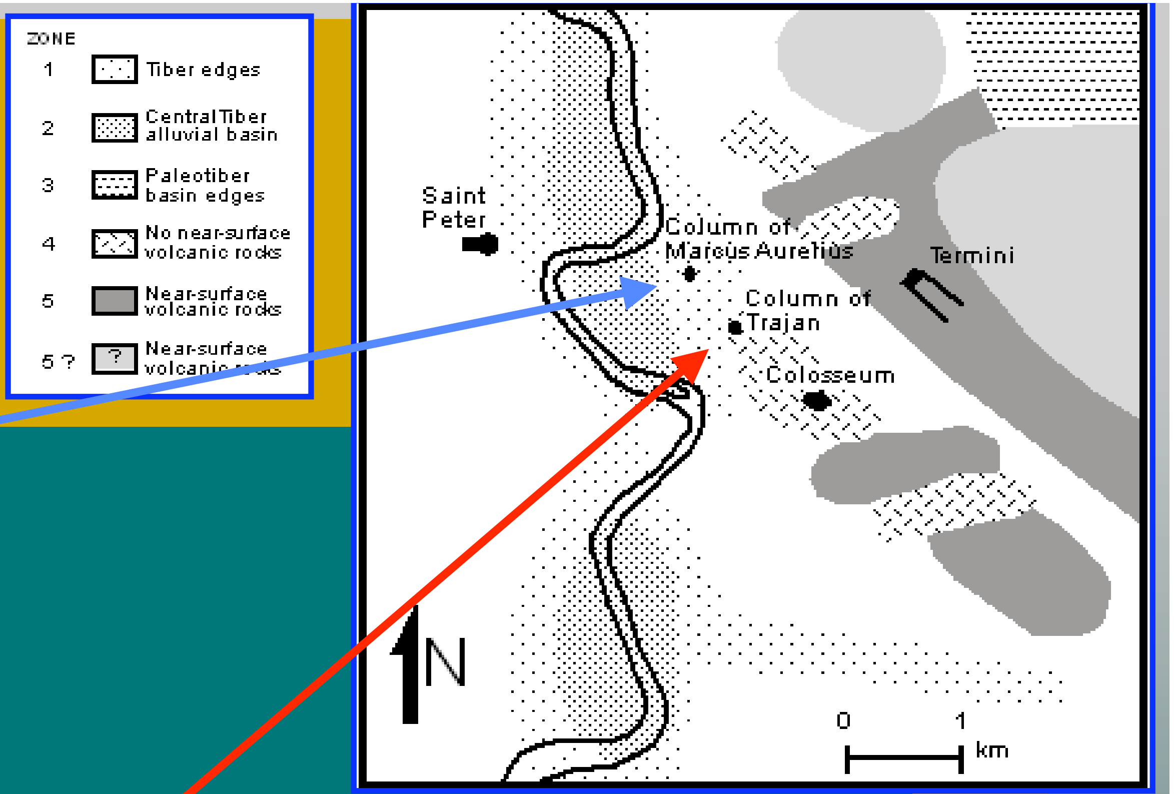

Accelerazioni spettrali attese (n=3)

La normativa sismica per la citta' di Roma

Roma: 3ª categoria

Accelerazione orizzontale di ancoraggio dello spettro di risposta elastico:

0.15 [a_g/g] ~ I=IX

Stima che considera storia sismica e sismotettonica:

max med med+σ

Zona 1: 0.24 - 0.15 - 0.30 [a_g/g] ~ I=X

Zona 4: 0.16 - 0.13 - 0.26 [a_g/g] ~ I=X

Stima che considera solo la storia sismica:

max med med+σ

Zona 1: 0.14 - 0.08 - 0.16 [a_g/g] ~ I=IX

Zona 4: 0.08 - 0.07 - 0.14 [a_g/g] ~ I=VIII

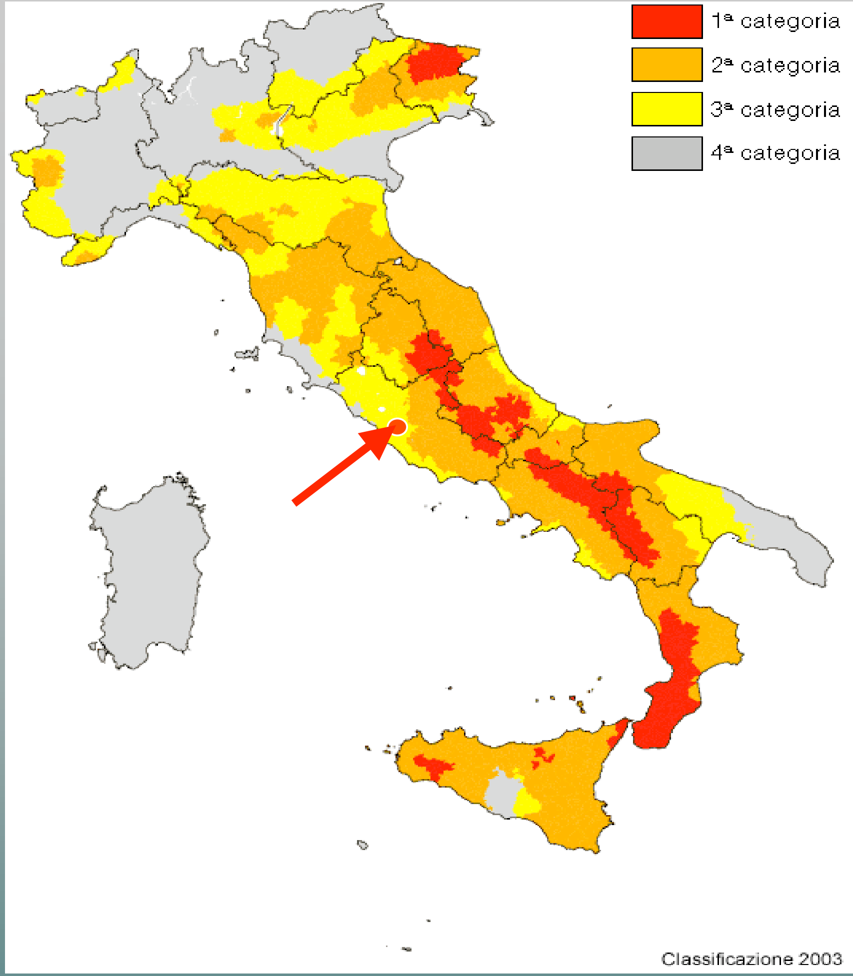

Zone sismiche del territorio italiano (2003)

zona	accelerazione orizzontale con probabilità di superamento pari al 10 % in 50 anni [a_g/g]	accelerazione orizzontale di ancoraggio dello spettro di risposta elastico (Norme Tecniche) [a_g/g]
1	> 0,25	0,35
2	0,15-0,25	0,25
3	0,05-015	0,15
4	<0,05	0,05

Microzonazione della citta’ di Roma, scalata al terremoto del Fucino del 1915 (I_{obs} a Roma=VIII).

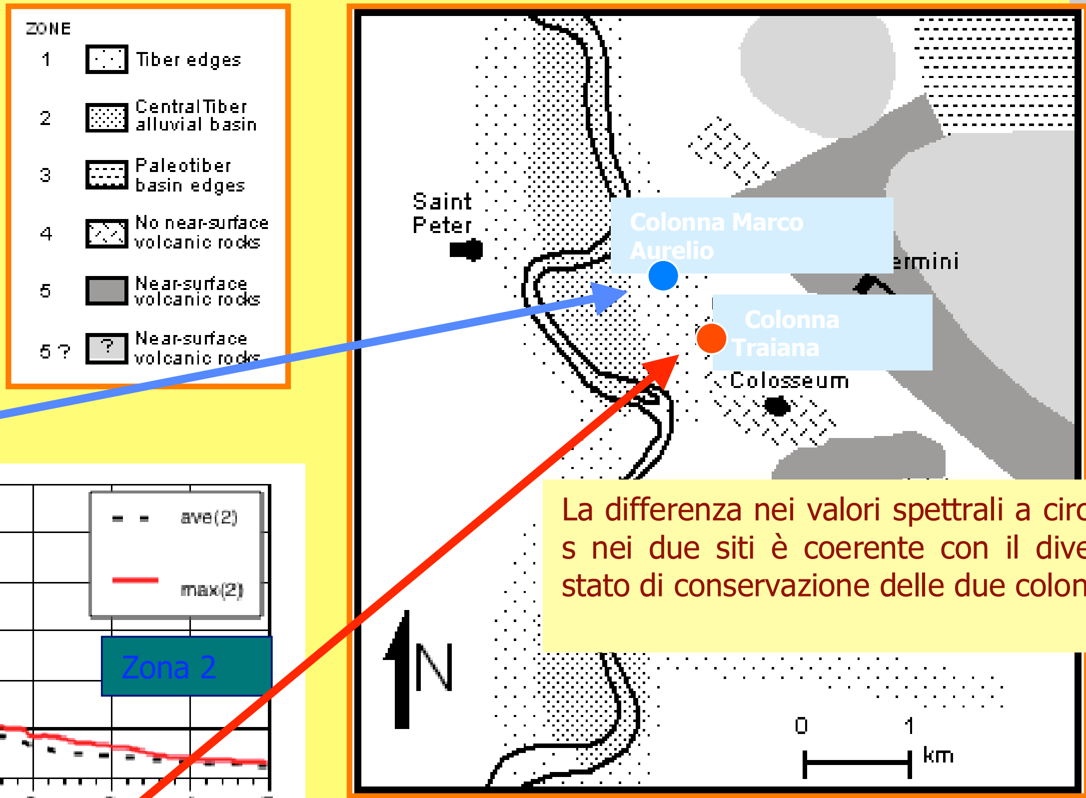

La differenza nei valori spettrali a circa 1 s nei due siti è coerente con il diverso stato di conservazione delle due colonne.

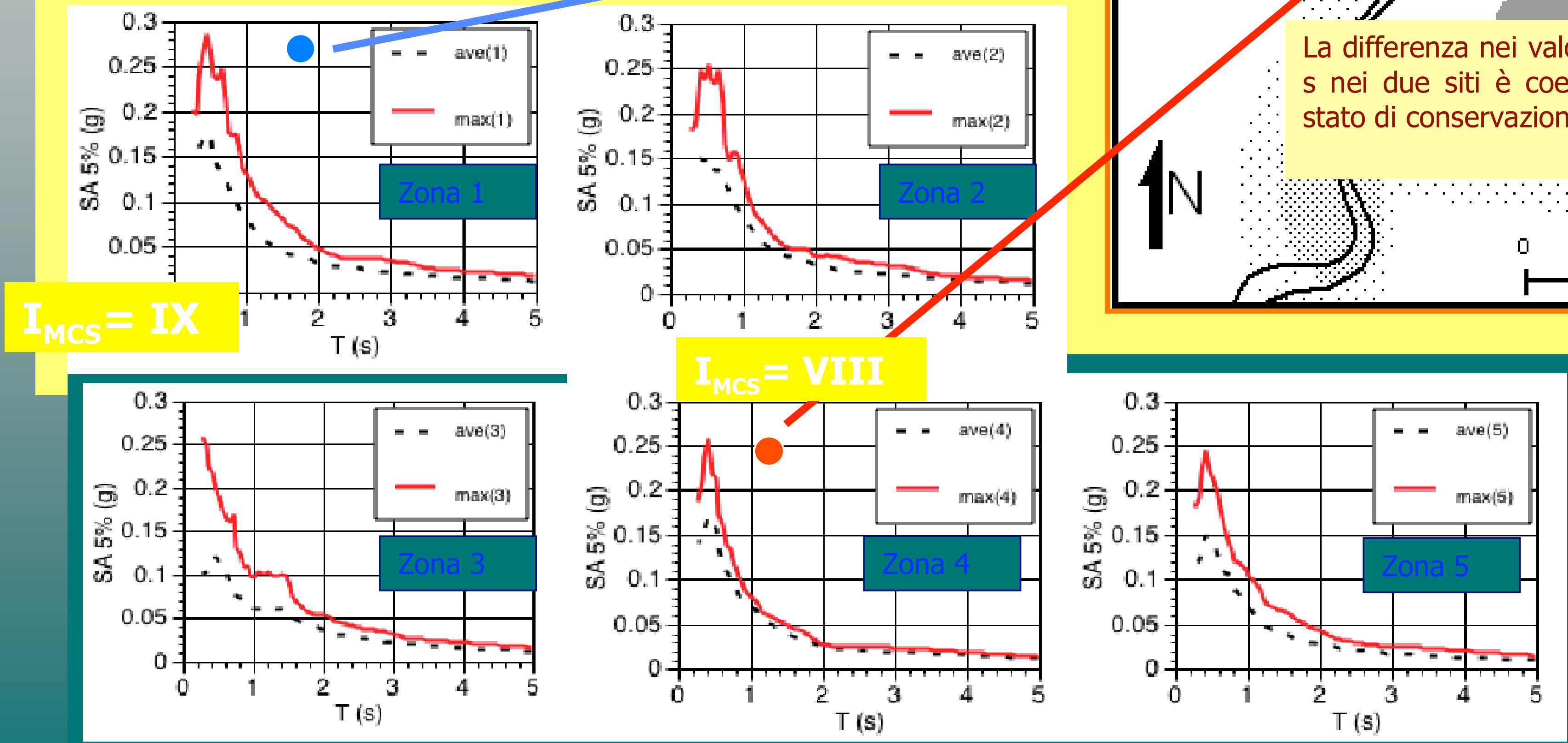

Modellazione delle Intensita’ osservate dedotte dalle accelerazioni spettrali teoriche (n=1)

From historical monuments, we can infer that strong lateral (within < 1km) variations in seismic ground motion can occur in Rome, as confirmed by realistic modeling of seismic ground motion.

Il periodo di circa 1 s in corrispondenza del quale ci sono raddoppi delle coordinate spettrali sono particolarmente rilevanti per edifici in cemento armato (CA) di alcuni piani. Un esperimento effettuato a JRC-Ispra ha mostrato che un edificio tipo in CA, di circa 10mx10mx10m (tre piani), ha un periodo proprio di 1.3 s e non 0.3 s, come comunemente stimato in base a relazioni empiriche (Fardis, comm. Pers., 2004).

CONCLUSIONI

La normativa rispecchia la sollecitazione sismica media della citta', ma non e' in grado di coprire ne' la sollecitazione derivante dal potenziale sismogenetico incombente (storia sismica e sismotettonica), ne' gli effetti locali che risultano alquanto rilevanti (almeno un grado I_{MCS} in piu') e riguardano zone abbastanza ampie (e.g. valli alluvionali).

In considerazione del deterioramento delle proprieta' meccaniche del sottosuolo (e.g. effetto acque sotterranee), negli ultimi cento anni, un terremoto simile a quello del Fucino puo' indurre in citta' valori di intensita' superiori a quelli osservati nel 1915.

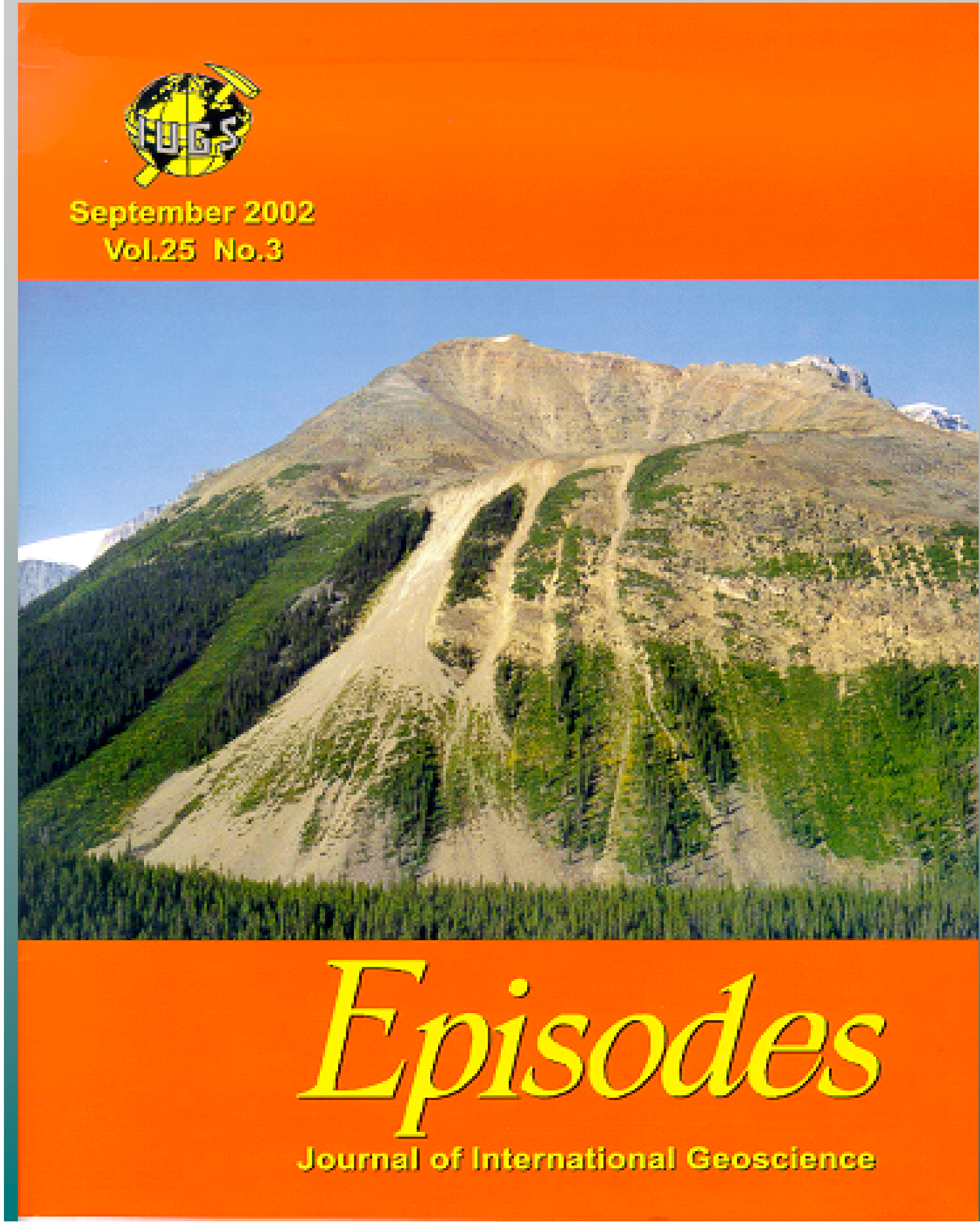

Studied Cities:

Algier
Bucharest
Cairo
Debrecen
Delhi
Naples
Bejing
Rome
Russe
Santiago de Cuba
Thessaloniki
Sofia
Zagreb

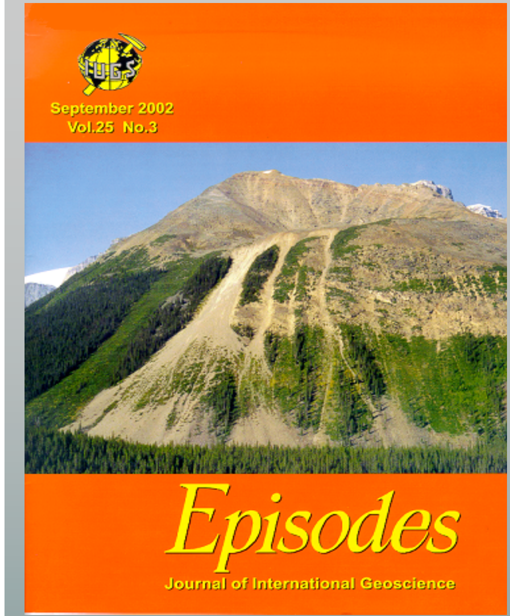

International Working Group composed by about forty scientists:

Giuliano F. Panza (Chairman), Leonardo Alvarez, Abdelkrim Aoudia, Abdelhakim Ayadi, Hadj Benhallou, Djillali Benouar, Zoltan Bus, Yun-Tai Chen, Carmen Cioflan, Zhifeng Ding, Attia El-Sayed, Julio Garcia, Bartolomeo Garofalo, Alexander Gorshkov, Katalin Gribovszki, Assia Harbi, Panagiotis Hatzidimitriou, Marijan Herak, Mihaela Kouteva, Igor Kuznetzov, Ivan Lokmer, Said Maouche, Gheorghe Marmureanu, Margarita Matova, Maddalena Natale, Concettina Nunziata, Imtyaz Parvez, Ivanka Paskaleva, Ramon Pico, Mircea Radulian, Fabio Romanelli, Alexander Soloviev, Peter Suhadolc, Gyõzõ Szeidovitz, Petros Triantafyllidis, Franco Vaccari.

UNESCO-IUGS-IGCP Project

Seismic microzoning of **Naples**

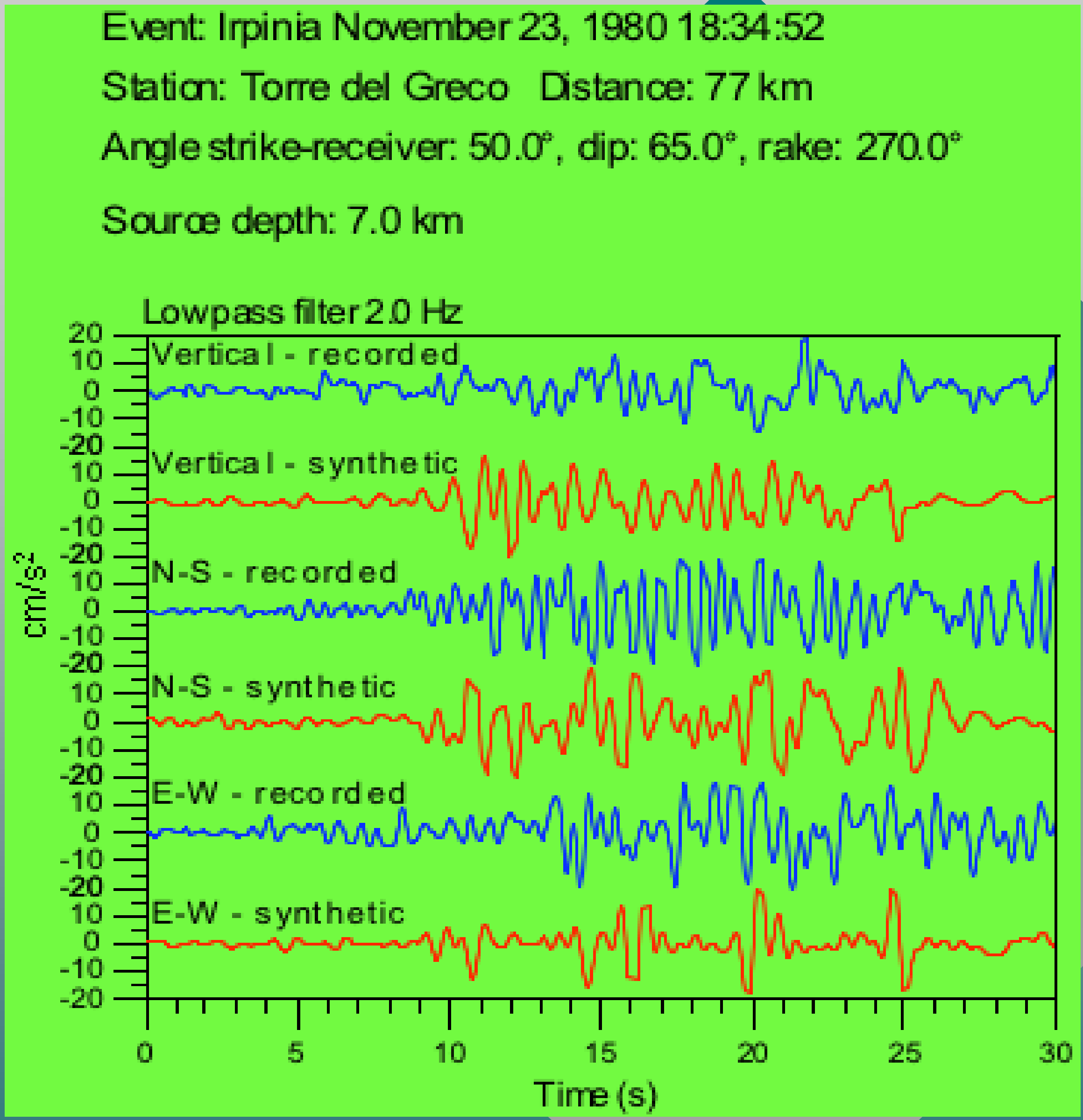

Modelling of seismic input (Torre del Greco)

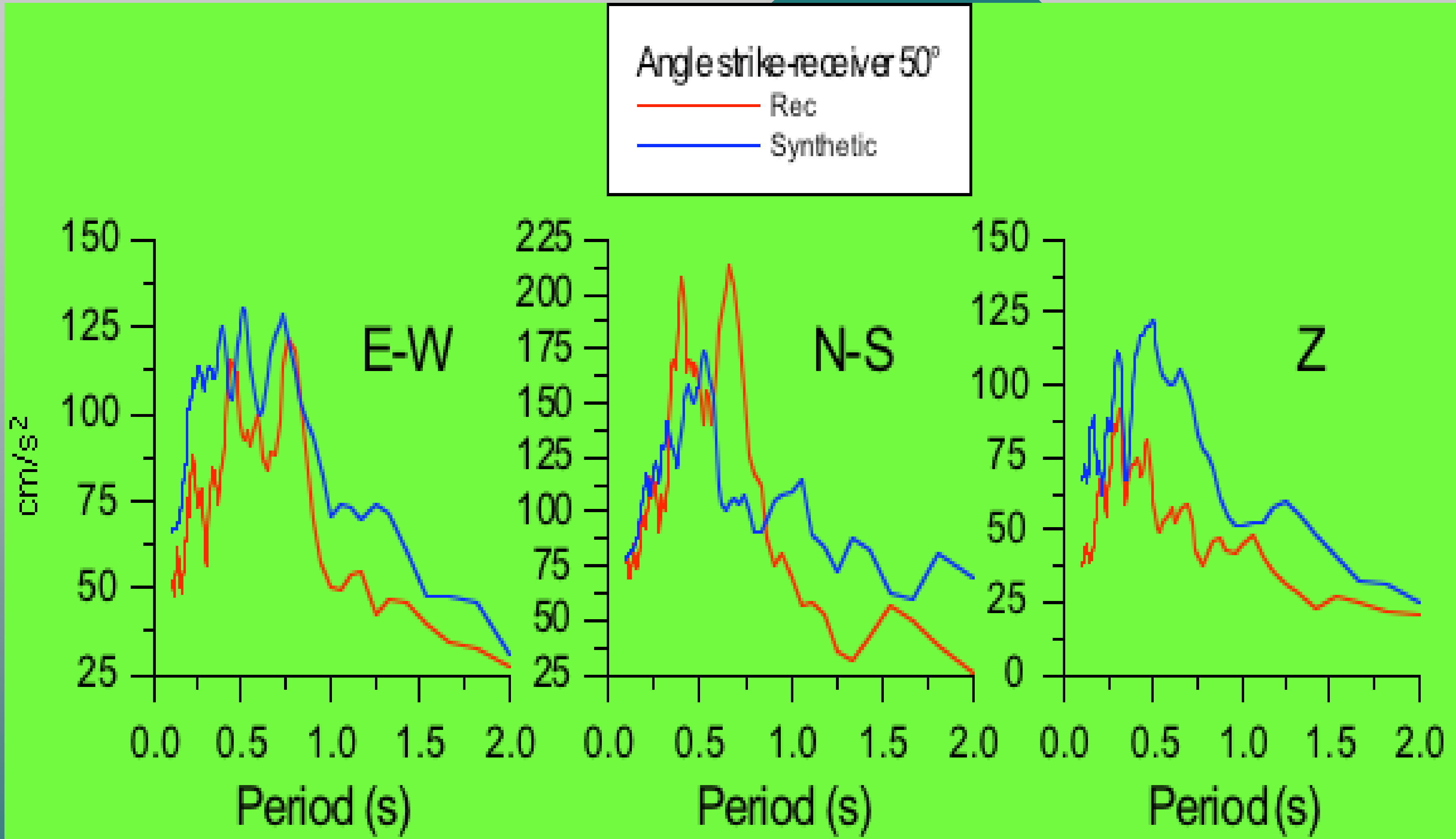

Modelling of seismic input (Torre del Greco)

Seismic Zonation

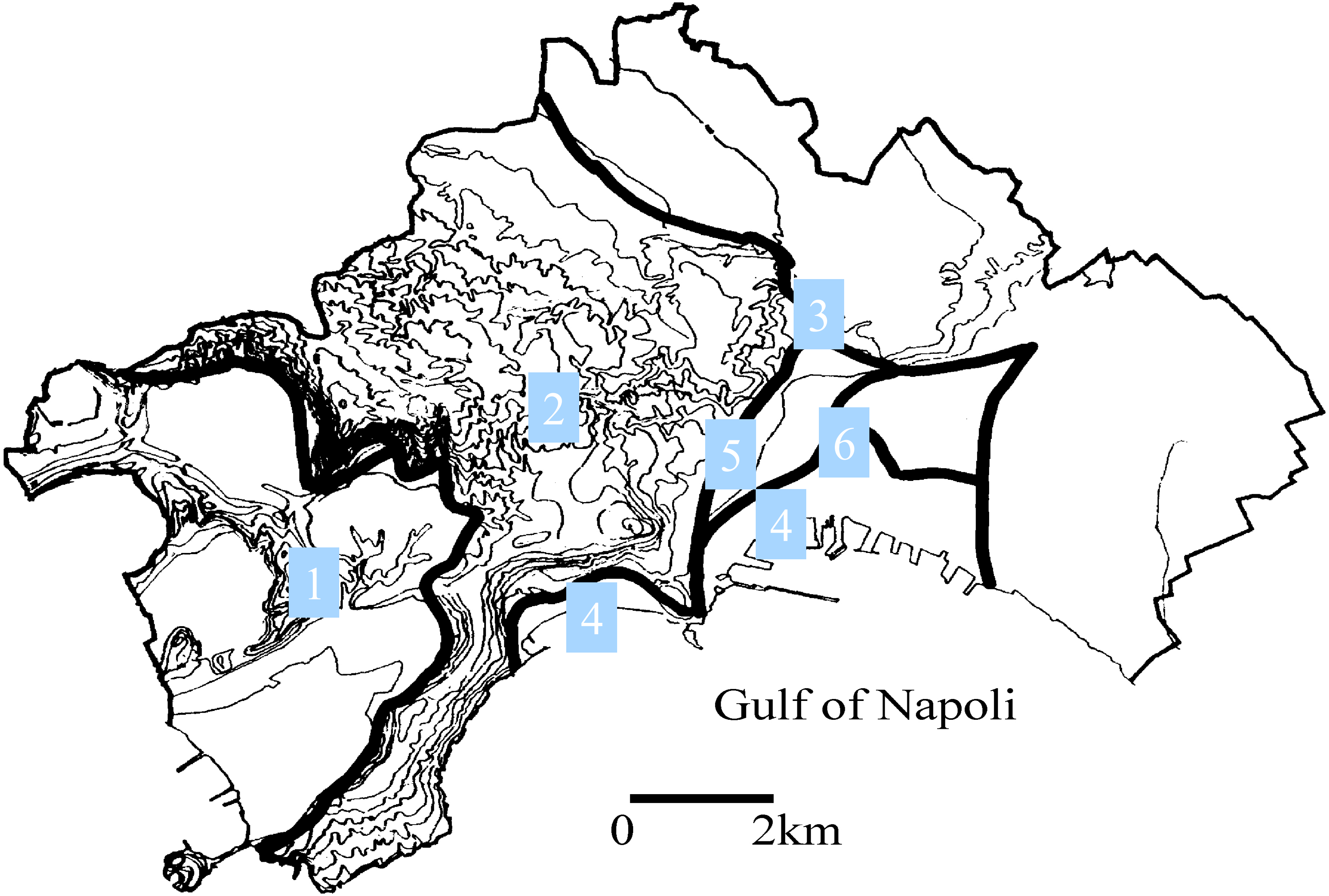

Zone 1

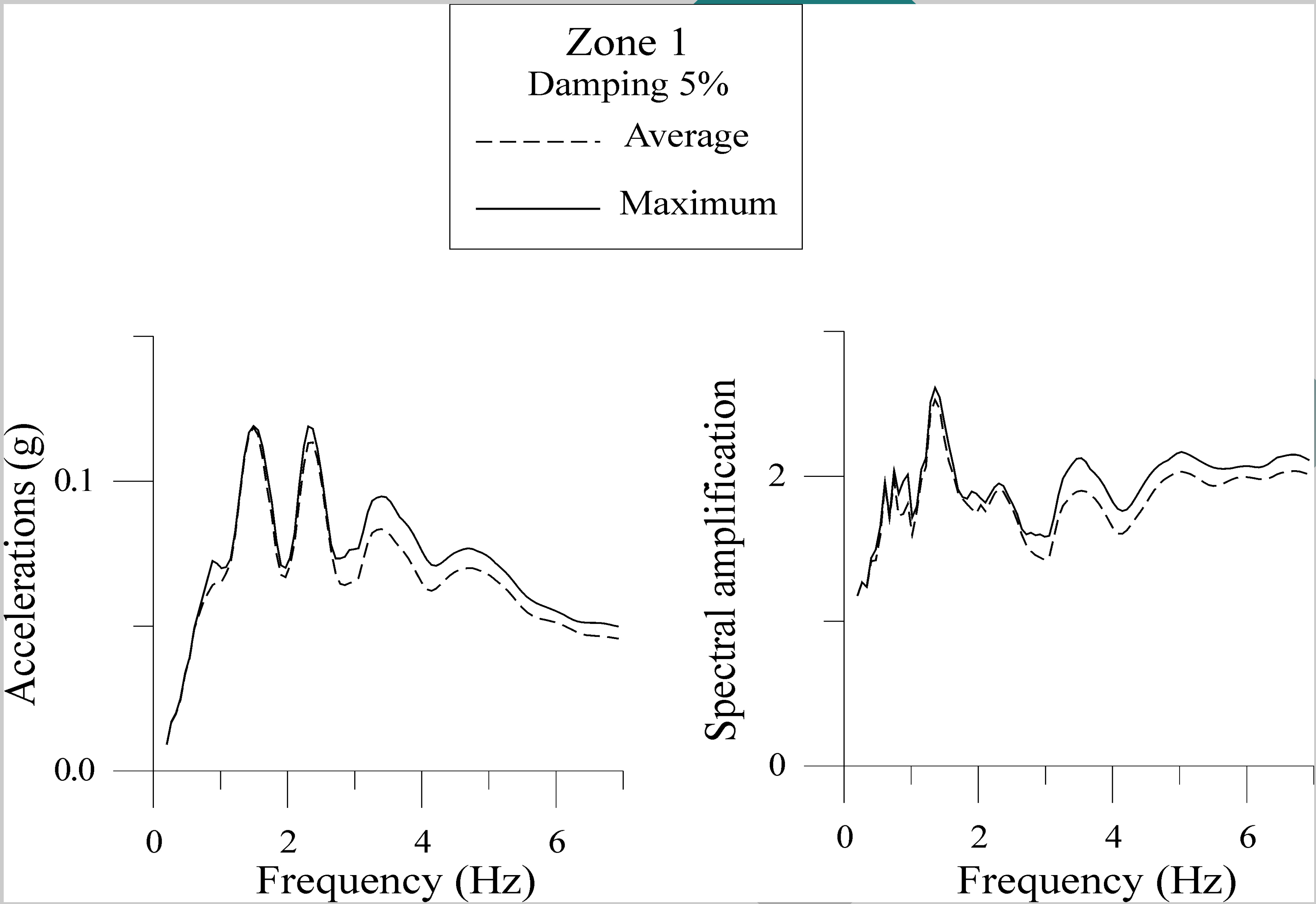

Zone 1
Damping 5%
Average
Maximum
Accelerations (g)
0.1
0.0
0
2
4
6
Frequency (Hz)
Spectral amplification
2
0
0
2
4
6
Frequency (Hz)

Zone 2

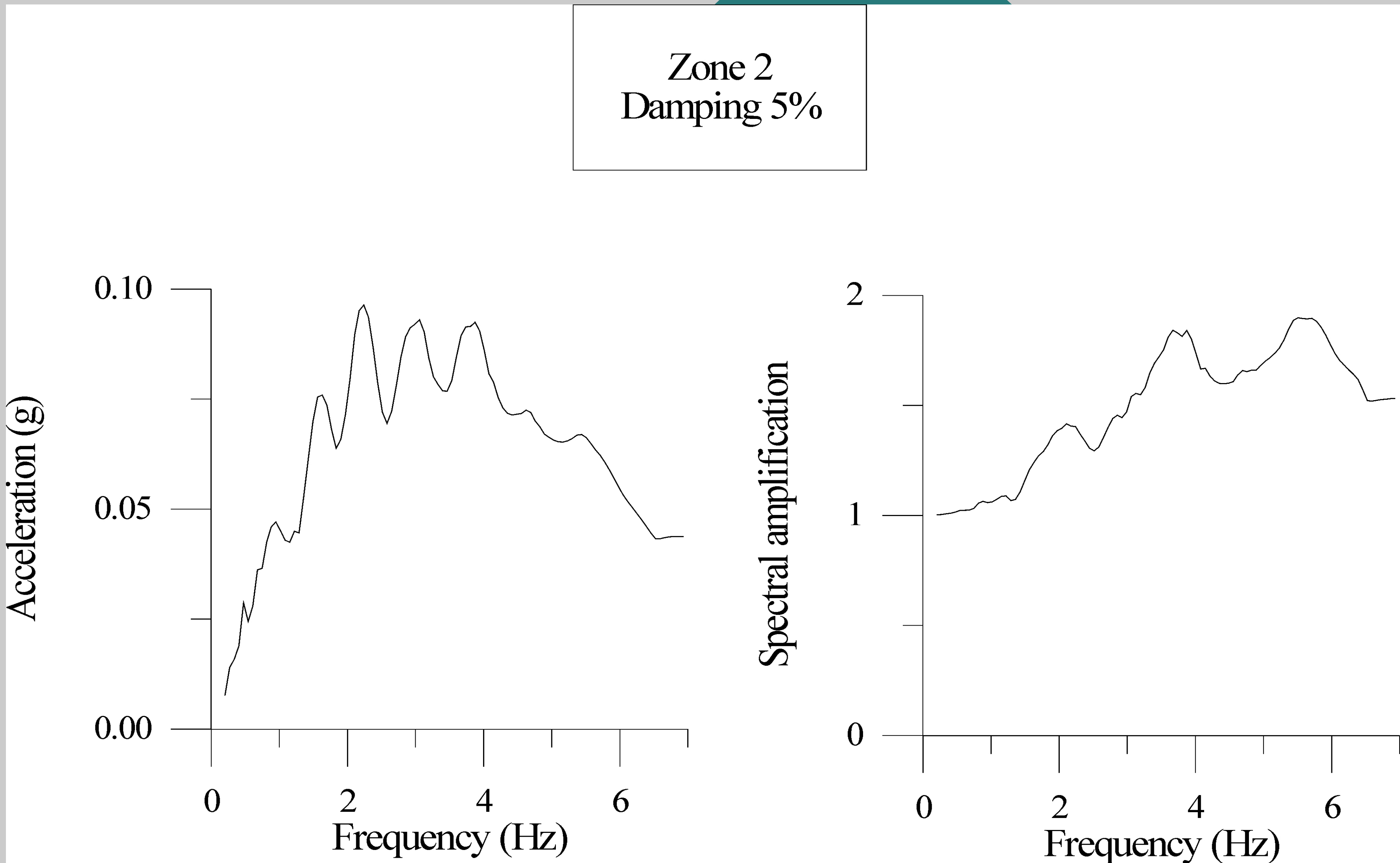
Zone 2
Damping 5%
0.10
0.05
0.00
Acceleration (g)
0
2
4
6
Frequency (Hz)
2
1
0
Spectral amplification
0
2
4
6
Frequency (Hz)

Zone 3

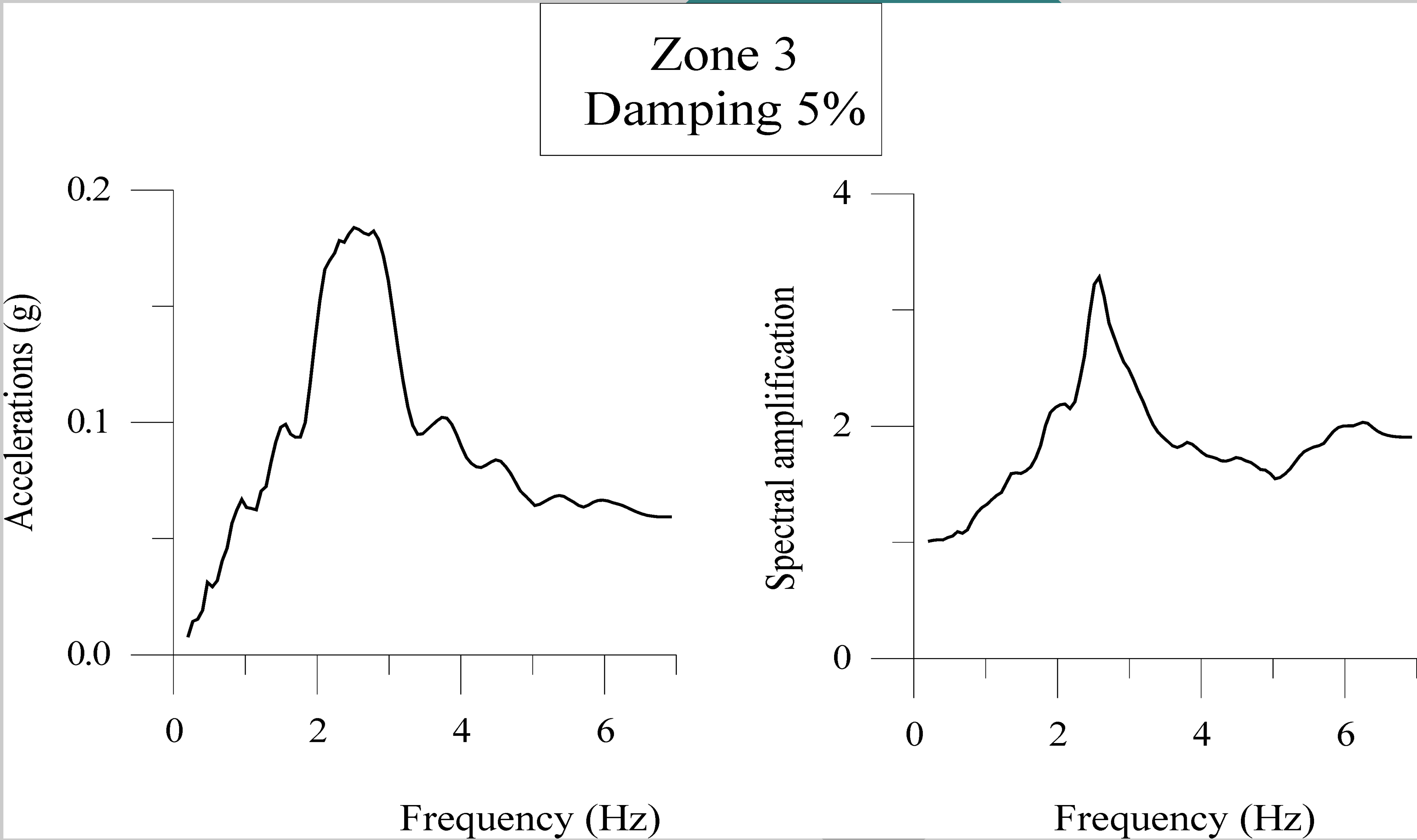
Zone 3
Damping 5%
0.2
0.1
0.0
Accelerations (g)
0
2
4
6
Frequency (Hz)
4
2
0
Spectral amplification
0
2
4
6
Frequency (Hz)

Zone 4

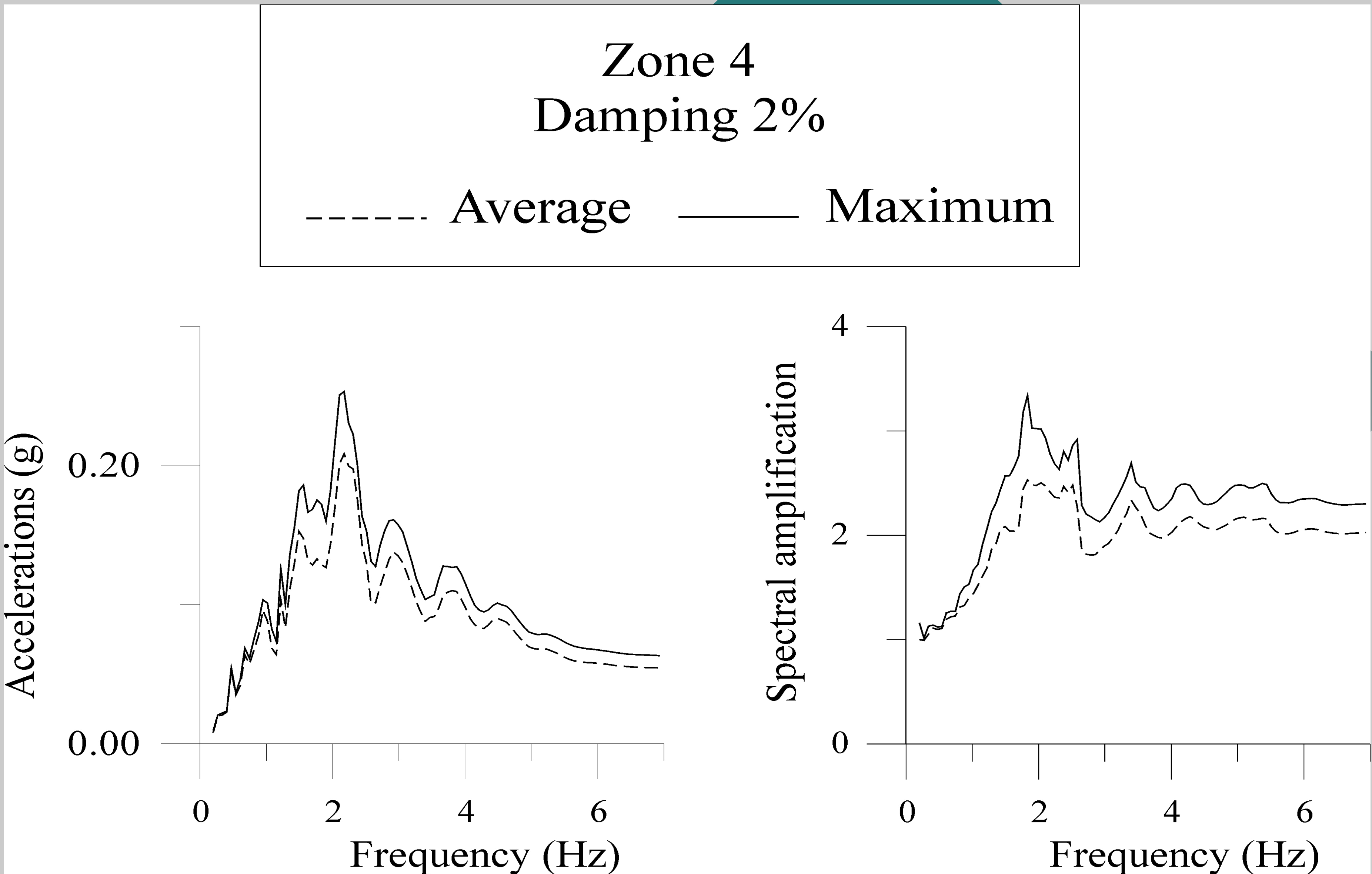

Zone 4
Damping 2%
Average
Maximum
Accelerations (g)
0.20
0.00
0
2
4
6
Frequency (Hz)
Spectral amplification
4
2
0
0
2
4
6
Frequency (Hz)

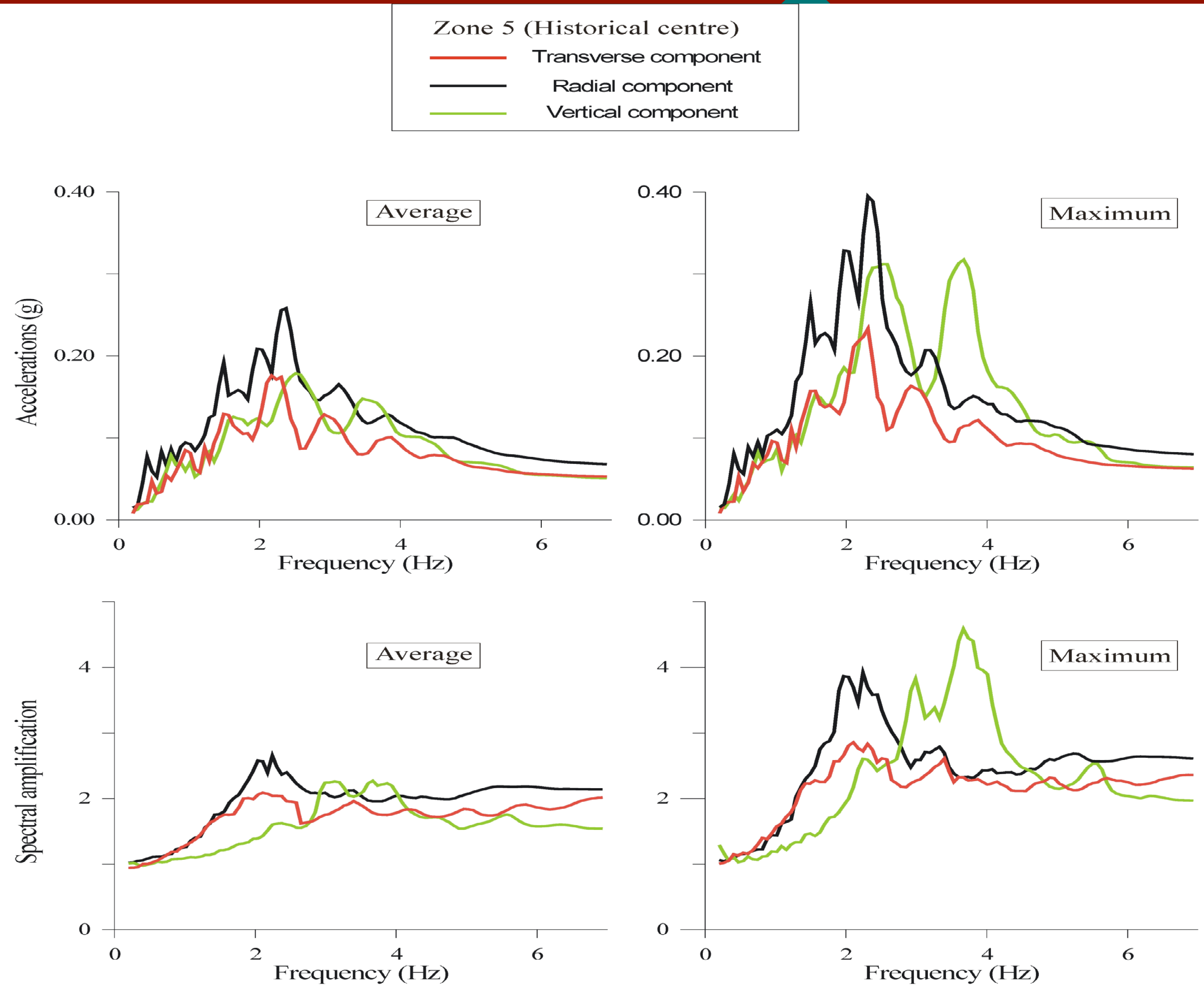

Zone 5 (Historical centre)
Transverse component
Radial component
Vertical component
Average
Maximum
Accelerations (g)
0.40
0.20
0.00
0
2
4
6
Frequency (Hz)
Spectral amplification

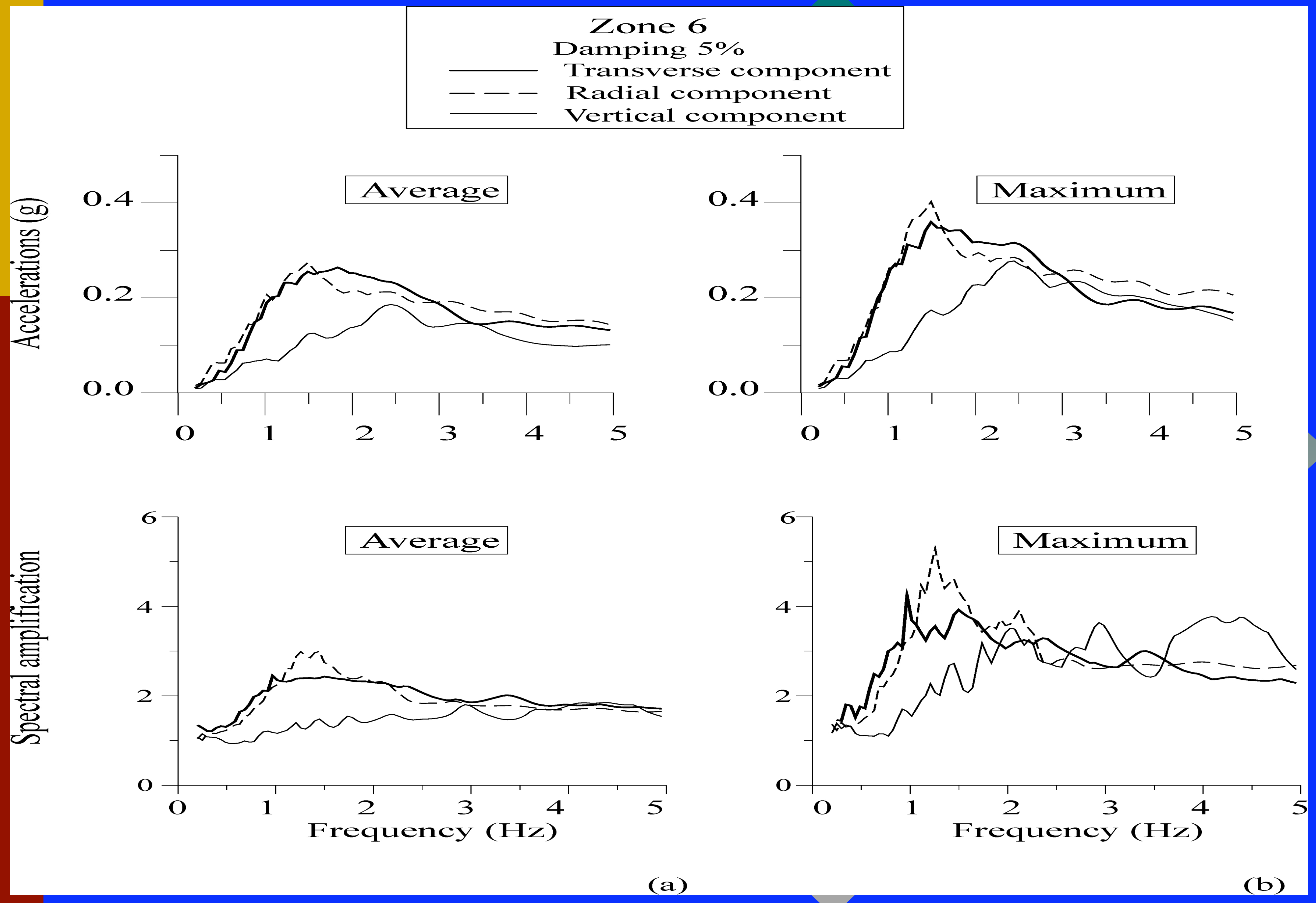

Zone 6
Damping 5%
Transverse component
Radial component
Vertical component
Accelerations (g)
Average
Maximum
0.0
0.2
0.4
0
1
2
3
4
5
Spectral amplification
6
Frequency (Hz)
(a)
(b)

Modelling of seismic input

- Several activities are presently in progress in many urban areas around the World.

- The realistic definition of hazard in scenario like format should be accompanied by the determination of advanced hazard indicators as, for instance, damaging potential. This can be achieved from a joint use of synthetic signals and available observations.

- A selection of main results is given in “Seismic ground motion in Large Urban Areas”, Pageoph Topical Volume, 161, 2004, pp342, edited by Panza, Paskaleva and Nunziata

IUGS
UNESCO
IGCP

END

OF

PART 4

Characterization of local soil mechanical properties

Characterization of local soil mechanical properties

- Complementary to the definition of earthquake scenarios is a good knowledge of the geotechnical properties of the main constituents of the subsoil.
- The velocity models obtained from the inversion of refraction data, when used as input in waveform modelling, may cause a significant underestimate of the ground motion.

Characterization of local soil mechanical properties

- Refraction of waves is a critical phenomenon. As such refracted waves carry very little energy, therefore they cannot be responsible of real damage.
- Damage is caused by reflected or surface waves, especially in soft soils.

Characterization of local soil mechanical properties

- For microzonation purposes, the information obtainable from the inversion of surface waves dispersion is therefore preferable.

Characterization of local soil mechanical properties

- S-wave velocities can be inferred from the inversion of Rayleigh and Love phase and group velocities determined with different techniques, like f(frequency)-k(wavenumber), SASW and FTAN methods.

FTAN - MAP

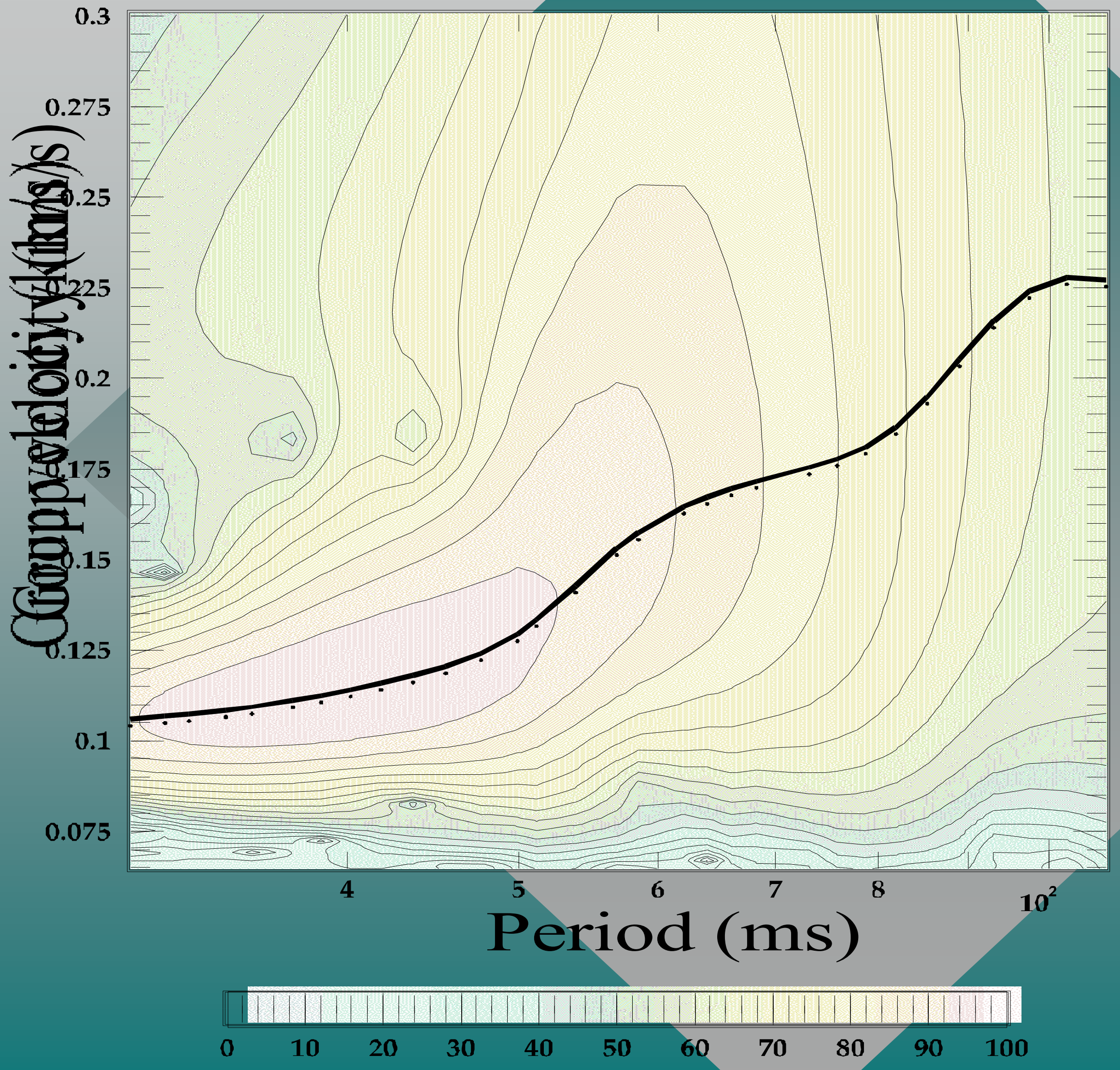
0.3
0.275
0.25
0.225
0.2
0.175
0.15
0.125
0.1
0.075
4
5
6
7
8
10^2
Period (ms)
0
10
20
30
40
50
60
70
80
90
100

Inverted Models

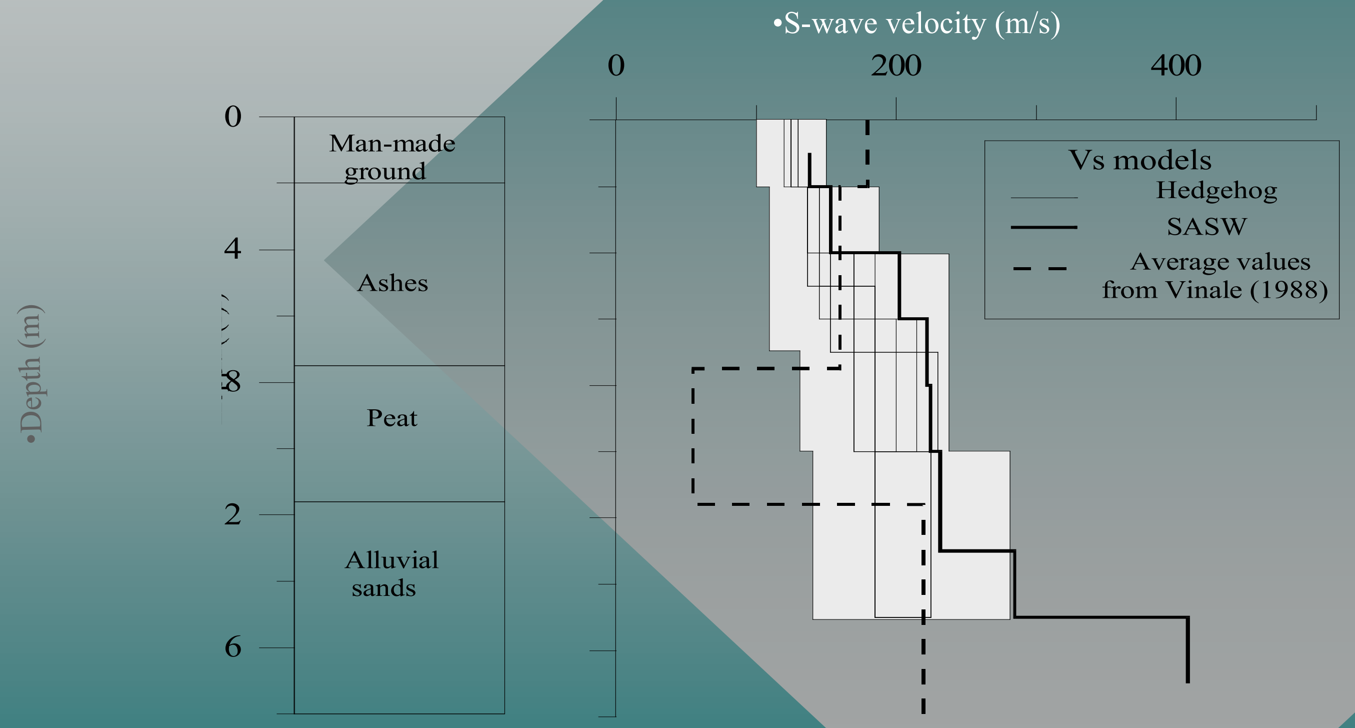

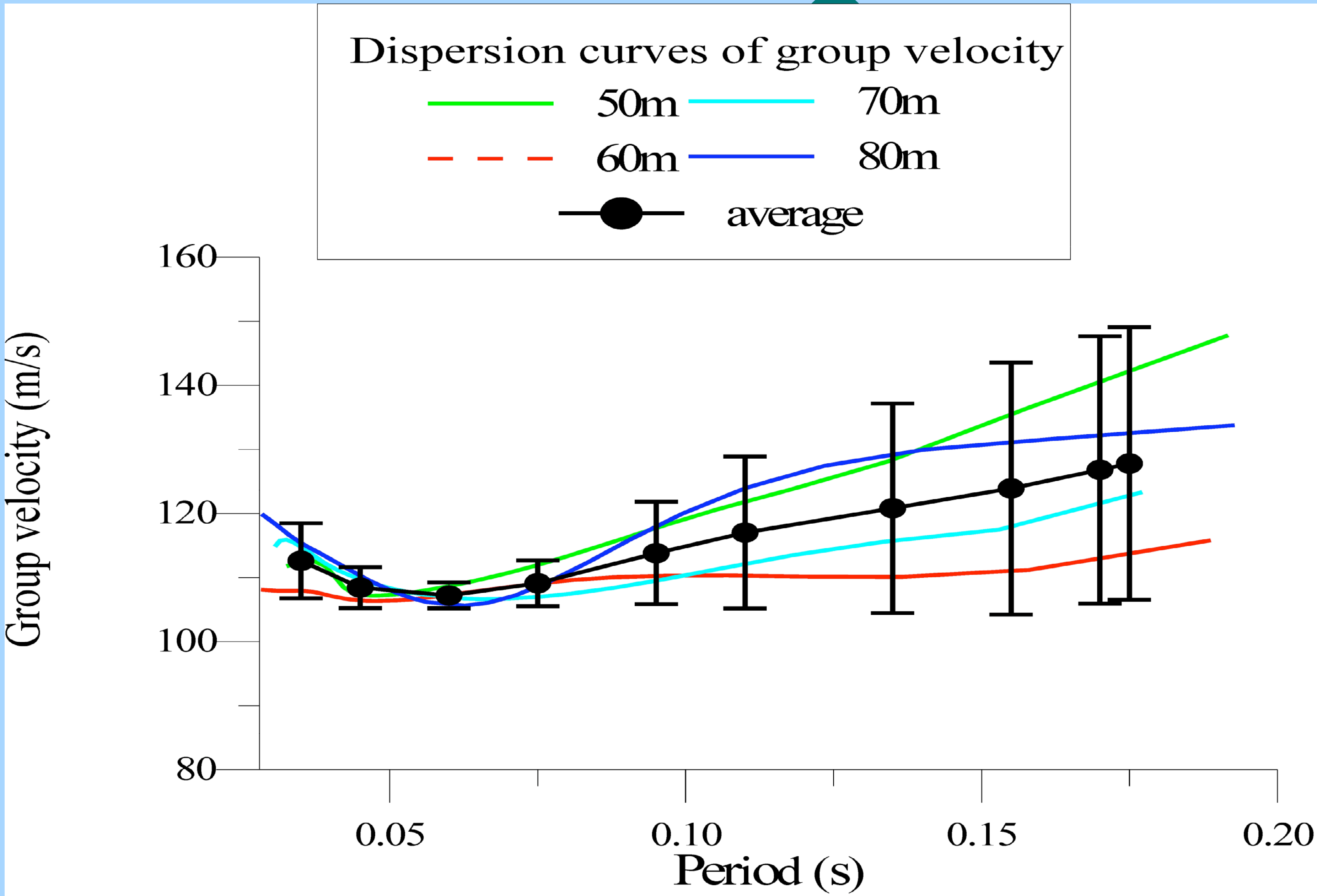

Dispersion curves of group velocity
50m
70m
60m
80m
average
160
140
120
100
80
Group velocity (m/s)
0.05
0.10
0.15
0.20
Period (s)

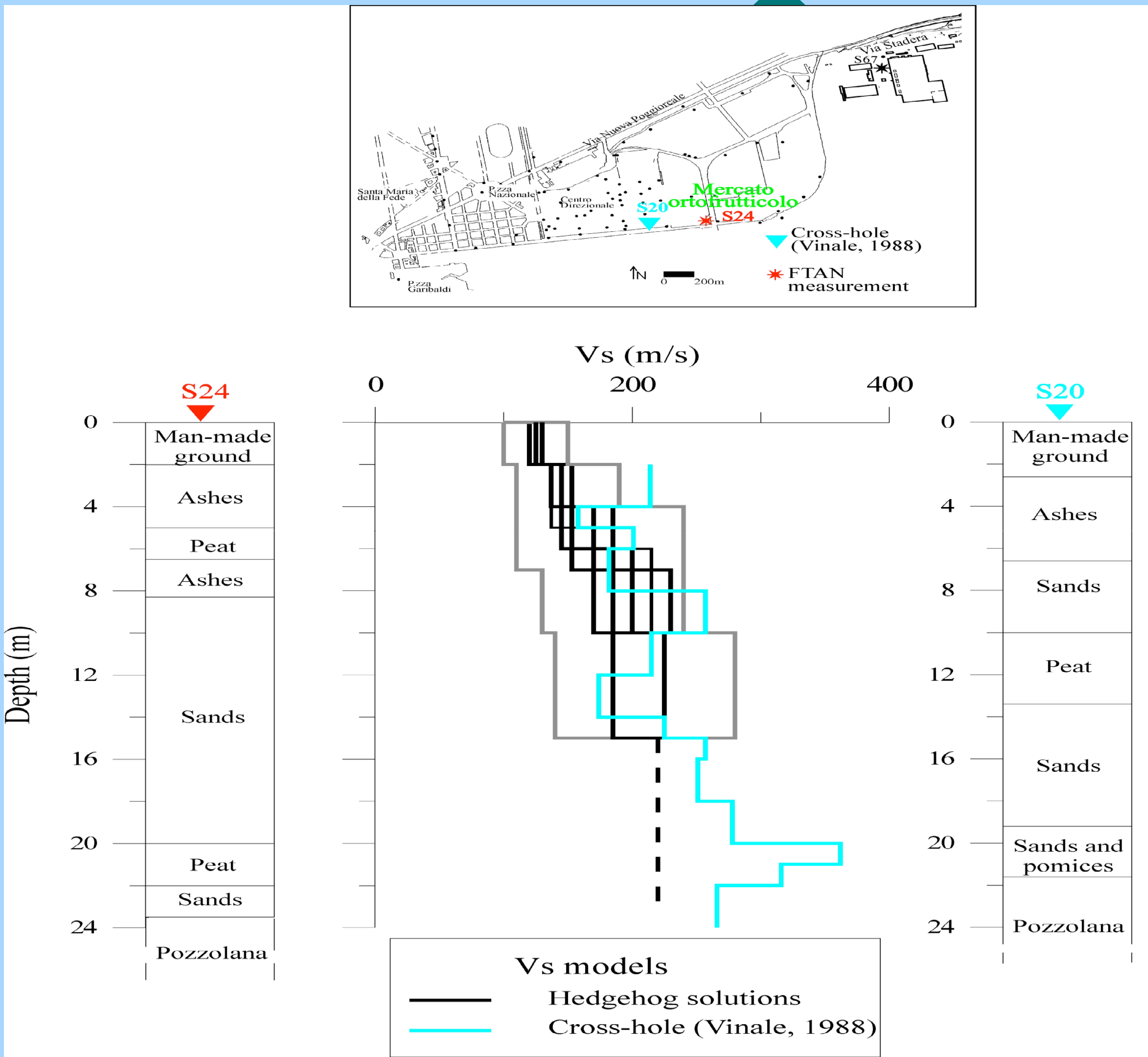

Via Stadera
S67
Via Nuova Poggioreale
Santa Maria della Fede
P.zza Nazionale
Centro Direzionale
Mercato ortofrutticolo
S20
S24
Cross-hole (Vinale, 1988)
FTAN measurement
P.zza Garibaldi
N
0
200m
Vs (m/s)
0
200
400
S24
S20
Depth (m)
0
4
8
12
16
20
24
Man-made ground
Ashes
Peat
Ashes
Sands
Peat
Sands
Pozzolana
Man-made ground
Ashes
Sands
Peat
Sands
Sands and pomices
Pozzolana
Vs models
Hedgehog solutions
Cross-hole (Vinale, 1988)

(a)

(a)

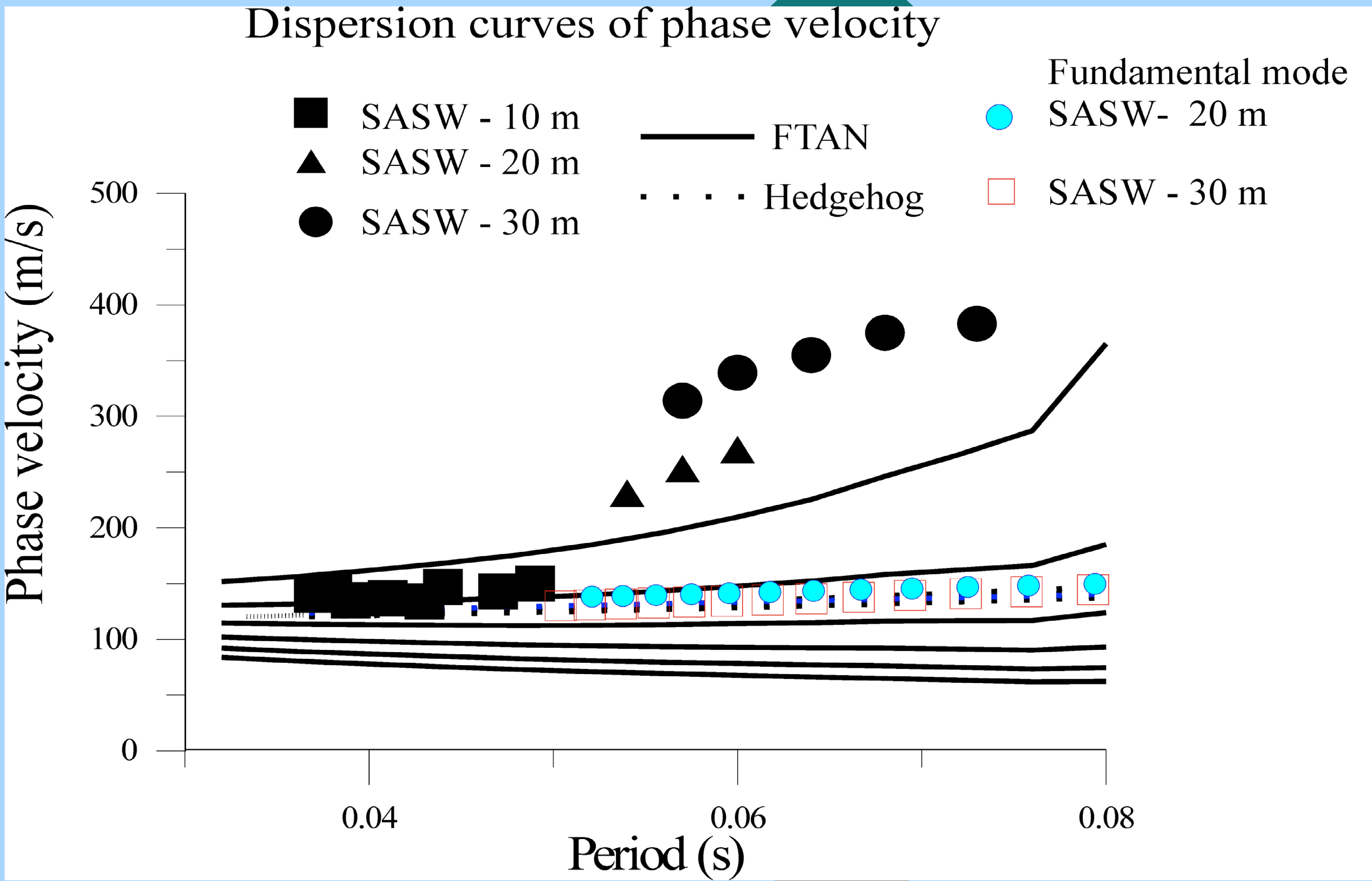
Dispersion curves of phase velocity
SASW - 10 m
SASW - 20 m
SASW - 30 m
FTAN
Hedgehog
Fundamental mode
SASW- 20 m
SASW - 30 m
Phase velocity (m/s)
500
400
300
200
100
0
0.04
0.06
0.08
Period (s)

Characterization of local soil mechanical properties

- For engineering geophysics FTAN method is particularly suitable and provides accurate group velocity measurements.

Characterization of local soil mechanical properties

- When the elastic properties along the path are known, as well as the location and depth of the source, and fundamental and higher modes are excited, it is possible to determine the gross Q values along the path, by using the synthetic seismograms approach.

Q estimate

a), c) and e) fundamental, first higher mode and their sum extracted with FTAN;
b), d) and f) synthetic signals

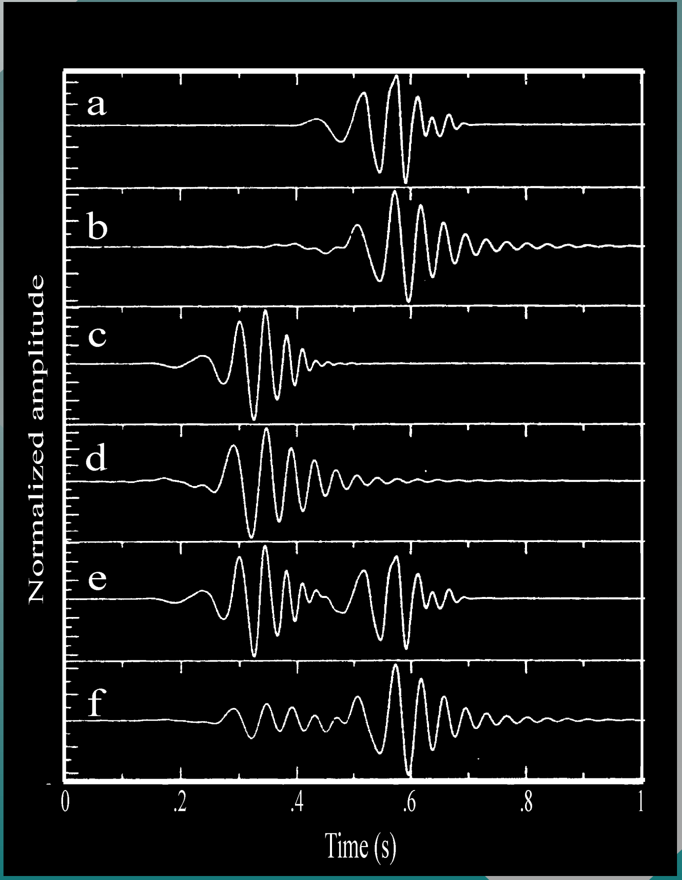

WHY

GROUP VELOCITY SHOULD BE PREFERRED TO

PHASE VELOCITY MEASUREMENTS?

Group and phase velocity can be defined as follows

$$U(\omega) = x/[t_o + d\phi_H(\omega)/d\omega - d\phi(\omega)/d\omega] \qquad (1)$$

$$c = x/\{t_o + [f_H(\omega) - f(\omega) \pm 2\pi N]/\omega\} \qquad (2)$$

where x is the distance source receiver, t_o the difference between the origin time and the starting time of the analysed signal, ϕ_H and ϕ are respectively the phase of the recorded signal and the source apparent initial phase, at the frequency ω, and N is an integer that can only be determined empirically.

As a rule **φ(ω) is a weak function of ω**, thus **dφ(ω)/dω** can be considered **negligible** for practical purposes.
On the other side, especially **at short periods, the determination of N can be very problematic**.

To eliminate the dependence of the phase velocity from the apparent initial phase of the source, $\phi(\omega)$, the so called two-station method can be applied:

$$c = \delta x / [\delta t_o + (\delta\phi_H(\omega) \pm 2\pi\delta N)/\omega] \quad (3)$$

where δx, δt_o, $\delta\phi_H(\omega)$ and δN indicate the difference between the quantities appearing in (2) as measured at the two stations. For more details see e.g. Panza (1976).

THE END

THANK YOU FOR YOUR ATTENTION